Saph Pani

Enhancement of natural water systems and treatment methods for safe and sustainable water supply in India

Project supported by the European Commission within the Seventh Framework Programme Grant agreement No. 282911

Deliverable D2.3

Report on field investigations on the performance of MAR techniques under the conditions in India

SAPHPANI

Work package	WP2 Managed aquifer recharge and soil aquifer treatment
Deliverable number	D 2.3
Deliverable title	Report on field investigations on the performance of MAR techniques under the conditions in India
Due date	Month 33
Actual submission date	Month 36
Start date of project	01.10.2011
Participants (Partner short names)	Anna, BRGM, KWB, NGRI, NIH, SPT
Review and introduction	Christoph Sprenger (KWB)
Authors in alphabetic order	Alexandre Boisson (BRGM) Dhanamadhavan S (Anna) Elango Lakshmanan (Anna) Farooq Ahmad Dar (NGRI) Mahesh Sonkusare (CGWB-NCCR) Marina Alazard (BRGM) Md. Wajihuddin (NGRI) Narayan C. Ghosh (NIH) Parimala Renganayaki Sundaram (Anna) R. P. Singh (NIH) R. Rangarajan (NGRI) Raicy Mani Christy (Anna) S. Sarah (NGRI) Shakeel Ahmed (NGRI) Sumant Kumar (NIH) Surjeet Singh (NIH) Tanvi Arora (NGRI) Taufique Warsi (NGRI) Thirunavukkarasu M (SPT)
Contact for queries	Christoph Sprenger christoph.sprenger@kompetenz-wasser.de
Dissemination level: (**PU**blic, Restricted to other **P**rogrammes **P**articipants, **RE**stricted to a group specified by the consortium, **CO**nfidential- only for members of the consortium)	PU
Deliverable Status:	Final version

Content

List of figures

List of tables

1 Introduction

Artificial recharge of groundwater has a long tradition in India and is realized by structures such as percolation ponds, check dams, nala bunds or well injection. The Central Groundwater Board (CGWB) estimates in the “Master Plan for Artificial Recharge” that about 29% (941 541 km^2) of India´s surface is suitable for artificial recharge in terms of availability of surplus water and storage capacity in aquifers (CGWB, 2013). From 2007 to 2012 about 99.9 Crores INR (about 14 Mill. €, 1€ ~ 70 INR) have been invested in demonstrative artificial recharge structures in 21 Indian states (CGWB, 2013). Within the Saph Pani project some of these Indian recharge structures have been investigated in Chennai, Raipur and Maheshwaram (Figure 1-1).

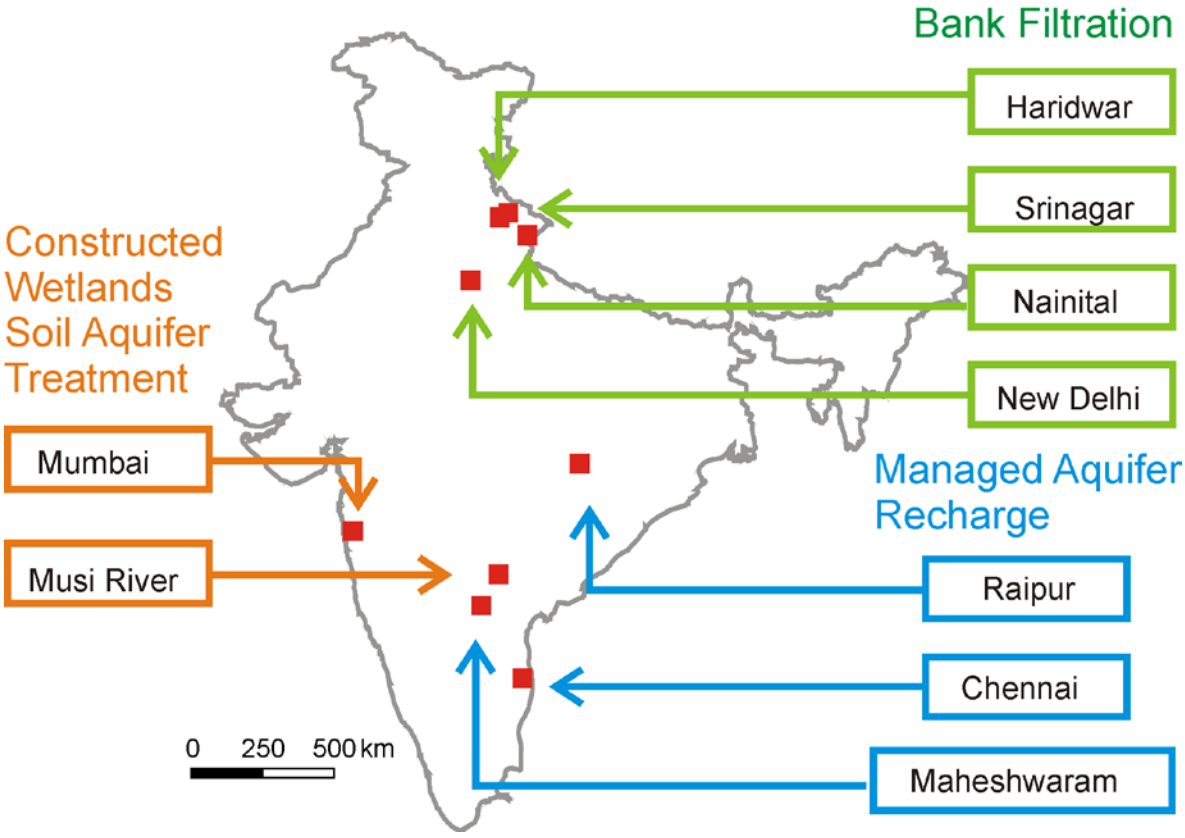

Figure 1-1: Location of field sites investigated within the Saph Pani project.

In a coastal aquifer close to Chennai the role of check dams and small-scale percolation ponds has been investigated in the context of salinity ingress (chapter 2). The role of traditional temple tanks as recharge structures was investigated in the city of Chennai (chapter 3). Percolation in hard rock aquifer by pond recharge was investigated in Maheshwaram close to Hyderabad (chapter 4). In the city of Hyderabad the function of dug wells as recharge structures was investigated (chapter 5). In Raipur the role of urban lakes or talabs was investigated for their potential in urban stormwater management and recharge structures (chapter 6).

An overview of the existing practice of man-made groundwater recharge in India is given by the Saph Pani deliverable 2.1 (Nättorp et al., 2012). The Saph Pani deliverable 2.2 documents the acquired data and outlines conceptual models for the investigated case studies (Boisson et al., 2013). This report is the third deliverable within WP 2 on Managed Aquifer Recharge. It focuses on the final assessment of the role and technical function of the investigated MAR structures. For each of the above-named case studies, the objective was to:

- describe the local setting and problem statement, under which the investigations have been carried out;
- give a description of applied field methods;
- establish a water balance for the investigated MAR structure(s);
- investigate the local effect on water quality by assessing the quality of ambient groundwater and the quality of infiltrated water in the subsurface.

An overview of the applied field methods for each of the case studies is given in Annex 1. The overall goal was to evaluate the transferability of the studied MAR concepts including a possible up-scaling of results regarding the role of MAR on catchment/aquifer scale. The context, in which artificial recharge takes place, is described for each case study separately in the following sections.

1.1 References

Boisson, A., Sprenger, C., Lakshmanan, E., Picot-Colbeaux, G., Ghosh, N.C., Ahmed, S., Kumar, S., Singh, S., Thirunavukkarasu 2013. Documentation of acquired data and conceptual model of MAR impact as input for WP5 modelling, Saph Pani deliverable 2.2, p. 117, http://www.saphpani.eu/downloads.html (accessed Sept. 2014)

CGWB, 2013. Master plan for artificial recharge to ground water in India, Central Ground Water Board, Government of India, New Delhi.

Nättorp, A., Ahmed, S., Boisson, A., Brand, J., Chadha, D.K., Ghosh, N.C., Grützmacher, G., Kumar, S., Lakshmanan, E., Sprenger, C., Wintgens, T., 2012. Report on existing MAR practice and experience in India, especially in Chennai, Maheshwaram, Raipur, p. 85, http://www.saphpani.eu/downloads.html (accessed Sept. 2014)

2 Mitigation of sea-water intrusion in the AK aquifer

2.1 Problem statement and objectives

Groundwater depletion and saline water encroachment are two major threats to most of the coastal aquifers of India. A detailed research work was carried out in the Arani-Koratalaiyar (A-K) River basins, North of Chennai to investigate the extent of seawater intrusion and possible remedial measures to mitigate seawater intrusion in the area.

In Chennai, seawater intrusion, the leaching of aquifer materials into the groundwater and salt pan activities caused high salinity of groundwater even at shallow depths. Therefore, groundwater is not suitable for irrigation and domestic use. The Government of Tamil Nadu has initiated several managed aquifer recharge structures including check dams and percolation ponds in the area to enhance the groundwater potential and to improve the groundwater quality of the area.

The objective of the study is to quantify the impact of managed aquifer recharge (MAR) structures in improving the groundwater availability. This is made by undertaking a assessment of MAR for coping with seawater intrusion and groundwater overexploitation and to develop recommendations and a management plan for implementing MAR systems that utilize excess monsoon water to counteract seawater intrusion in Chennai.

2.2 Site description

The check dam site is located north of Chennai in Thiruvallur district (Figure 2-1). It was constructed in the year 2010 across the Arani River, near Paleshwaram village at a distance of about 35 km from the sea. This check dam is of 260 m length with the crest height of 3.5 m from the river bed and has a storage capacity of 0.8 million cubic meter of water.

The percolation pond site is located at Andarmadam, Thiruvallur district of Tamil Nadu (Figure 2-1). It falls within latitudes 13º 10' N to 13º 25' N and longitudes 79º 55' E to 80º 20' E. The eastern and southern part of the location is bounded by the Arani River. It lies nearly 4 km west of Bay of Bengal and 2 km south of Pulikat lake. The Buckingham canal flows parallel to the Bay of Bengal on the eastern side of the pond. The details of the sites are given in the Saph Pani deliverable 2.2 (Boisson et al. 2013).

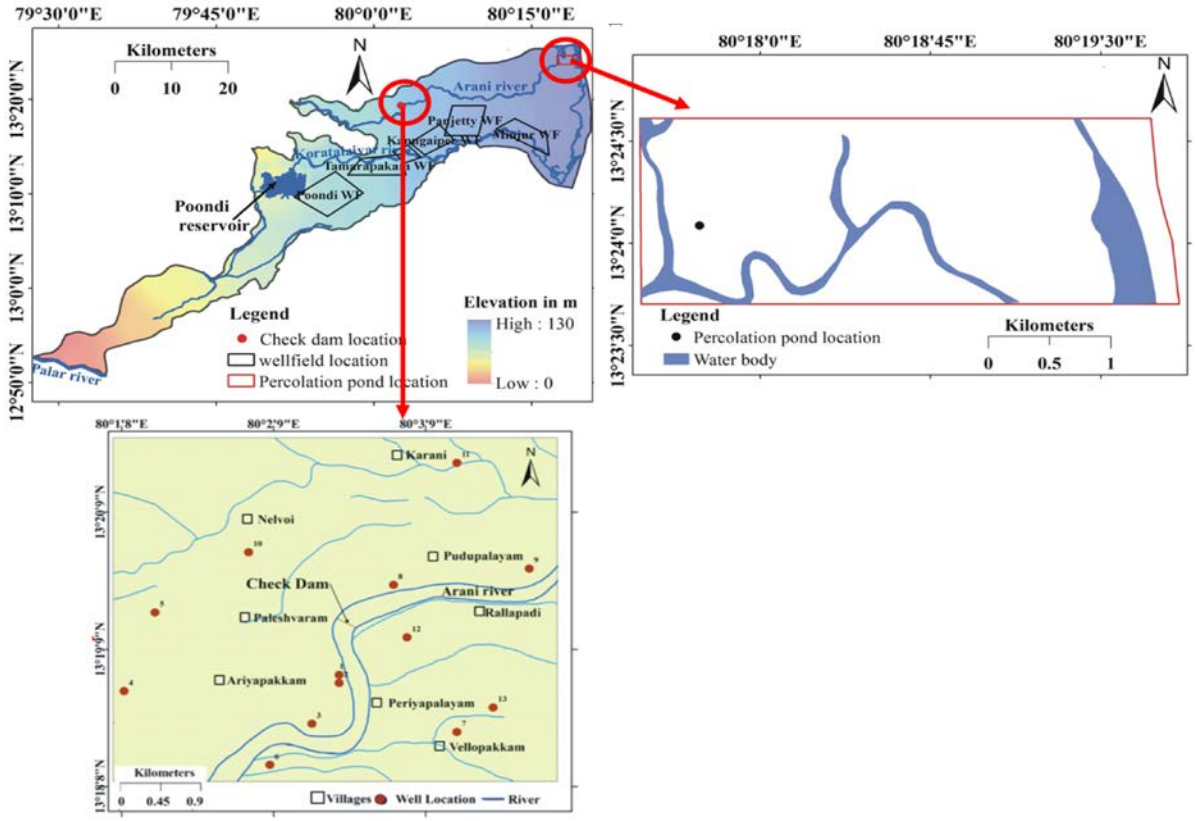

Figure 2-1: Location of the study area with the check dam and percolation pond

2.3 Results and interpretation

2.3.1 Check dam in the AK-aquifer

2.3.1.1 Percentage of recharge from the check dam

Variations in the water level of the check dam were measured through the manual staff gauge installed at the structure from November 2011 to June 2012. The maximum water level in the check dam was observed during monsoon season (November to December), where for a few weeks the check dam was overflowing. The check dam became dry during May /June. The surface water level variation in the check dam is shown in Figure 2-2.

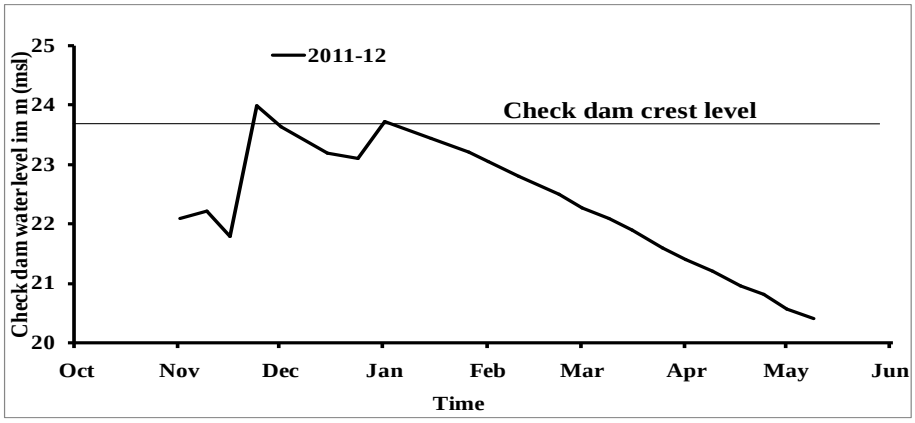

Figure 2-2: Water level fluctuation in the check dam

The water surface area and volume of water stored at various water levels in the check dam was estimated using three dimensional capabilities of Arc Gis 9.2 software. The elevations of the river bed were measured using the Differential global positioning system (Leica GS09). Based on the height of the check dam and the river bed topography, it was estimated that this check dam is capable of storing 0.8 Million m^3 of water. Figure 2-3 shows the storage volume corresponding to various water levels in the check dam. The R^2 value of 0.89 indicates a good accuracy of the storage volume derived from ArcGIS.

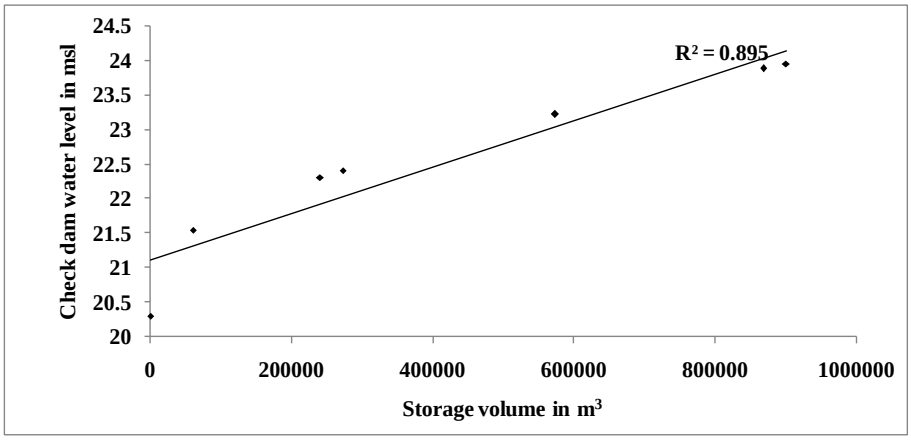

Figure 2-3: Storage volume corresponding to water level in the check dam

The volume of water recharged and evaporated was then calculated using the water balance method with

Recharge [m^3] = Change in storage volume [m^3] – Water loss due to evaporation [m^3] (Equation 2.1)

The obtained values were used for the estimation of groundwater recharge. Based on the variation in daily water level and surface area, the estimated cumulative volume of water stored by the check dam was about 1.7 Million m^3 during the year 2011-2012.

As no water stored in the check dam was used directly for domestic and irrigation purpose, the water lost from the check dam was mainly due to groundwater recharge and evaporation. Evaporation data were obtained from the Indian Meteorological Department, Chennai. Figure 2-4 gives the monthly recharge from check dam using the water balance method. During the period from November 2011 to May 2012 about 1.12 Million m^3 (66%) of the water stored by the check dam was recharged into the aquifer (Parimalarenganayaki and Elango 2013) and about 0.56 Million m^3 (34%) of water stored by the check dam was lost as evaporation.

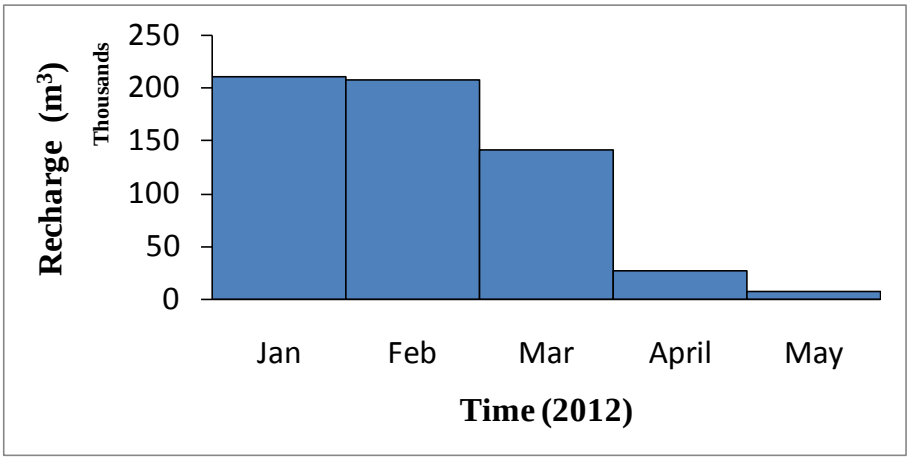

Figure 2-4: Volume of water recharged from the check dam

2.3.1.2 Impact on groundwater level development

The efficiency of the check dam in augmenting the groundwater recharge was assessed by comparing the temporal variation between the water level in the check dam and groundwater level in some of the nearby wells (Figure 2-1) monitored by Parimala Renganayaki (2014) used for drinking water supply/ irrigation. Based on the similarity between the water level fluctuation in the check dam and groundwater levels measured in the wells, the latter could be classified into two groups. Exemplarily, the plot of water level data for four wells (Wells no. 1, 11, 12, 13) is shown in Figure 2-5 (Parimalarenganayaki and Elango 2014).

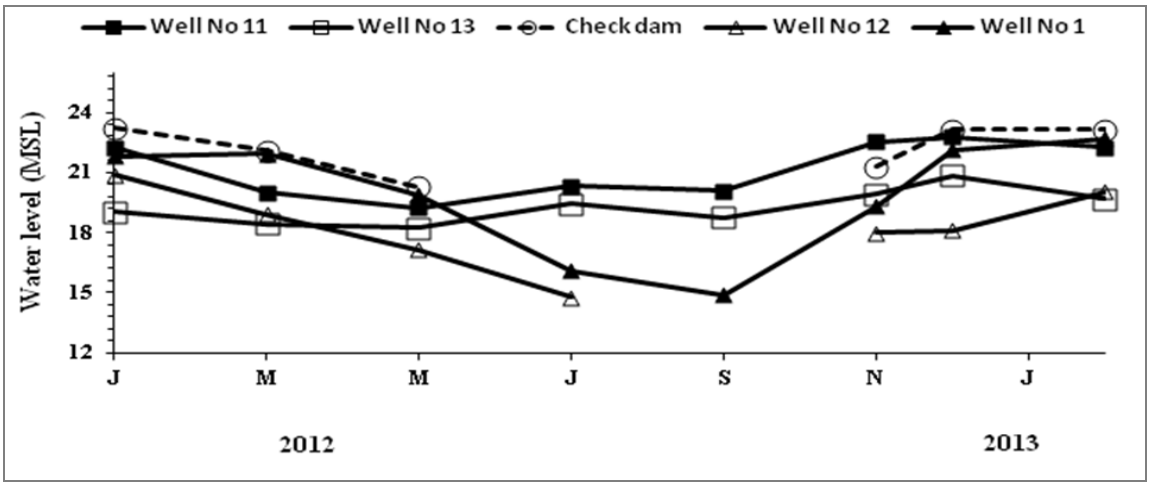

Figure 2-5: Water levels in the check dam and monitoring wells

In the first group of wells (Wells no. 11 and 13), groundwater level rises twice a year coinciding with the northeast and southwest monsoon. This indicates that rainfall is the major source of recharge at these locations. In the other group of wells (Wells no. 1 and 12), the fluctuation in groundwater levels is very similar to the water level fluctuation in the check dam. This similarity indicates that surface water stored by the check dam is the major source of recharge at these locations.

Taking into account additional wells up to a distance of 1.5 km from the check dam towards the eastern direction, an increase of groundwater levels between 1 m and 2.5 m could be observed (Well nos 1 and 12) after the construction of the check dam.

Improvement in groundwater quality due to recharge:

Figure 2-6 shows a plot of chloride, a dominant conservative anion, versus the electrical conductivity, which is a function of total dissolved solids, for water samples collected during January, March and May 2012 from the check dam and nearby wells. The water samples from the check dam had the lowest chloride concentration and electric conductivity. The concentrations of the groundwater samples collected from the sampling wells (Figure 2-1) increased with distance to the check dam. Hence, the wells recharged from the check dam had less salinity and thus the quality of groundwater in the region has improved by constructing the check dam (Parimalarenganayaki and Elango 2014).

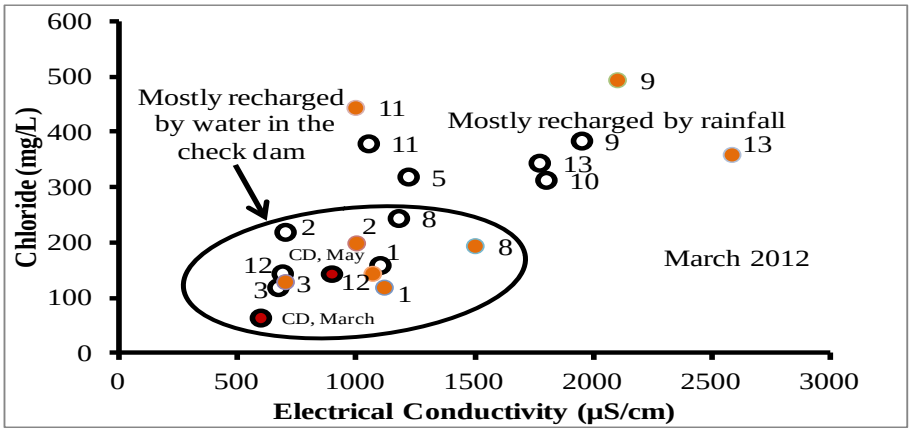

Figure 2-6: Electrical conductivity and chloride concentration of groundwater and surface water

2.3.2 Percolation pond

2.3.2.1 Water table rise

The water level in the pond and in three nearby observation wells namely P1 (0.5 m from the pond), P2 (1.0 m from the pond) and P3 (1.5 m from the pond) (Raicy et al. 2014) was measured once in 15 days. In P3, the groundwater level was measured using a digital automatic water level indicator once in every 3 minutes from September 2012 to May 2013 and September 2013 to January 2014 (Figure 2-7). The figure shows that the water level in the pond was high from September 2012 to February 2013. Afterwards, the water level gradually decreased and it became empty during May 2013 (Raicy et al. 2014). During the same period, the groundwater level in the observation well P3 gradually increased and almost sustained at more than 30 cm above the mean static water level of the area. This confirms that this recharge structure enhances the groundwater level in the nearby area.

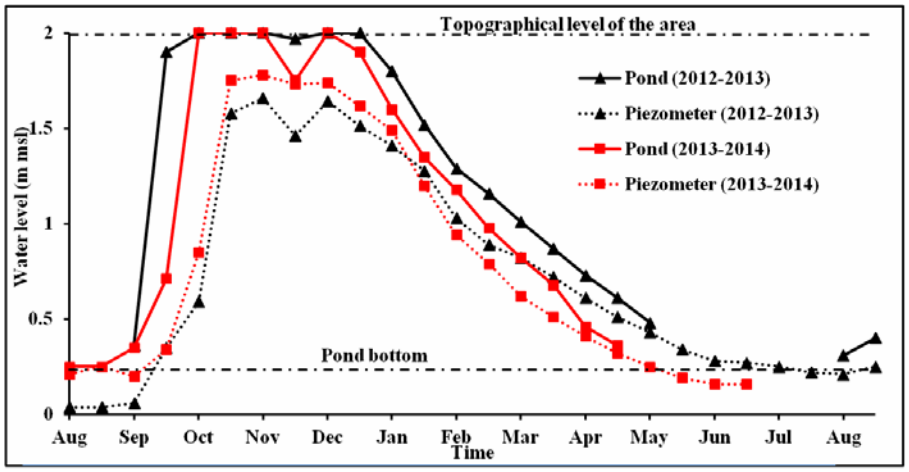

Figure 2-7: Water level in the pond and groundwater level in nearby piezometer (Raicy and Elango, 2014 c)

2.3.2.2 Estimation of recharge

The amount of water recharged from the pond into the aquifer was estimated considering

- the water level in the pond and the observation wells
- the surface area of the pond at different time periods
- pan evaporation of the area and
- rainfall of the area monitored by the automatic weather station in the area.

The total volume of water recharged by the pond into the aquifer was calculated to be approximately 250 to 300 m^3 for the period from August 2012 to June 2013. Figure 2-8 shows the distribution over the year.

The recharge rates were very high up to December and gradually decreased after that. Even though the water level in the pond was almost constant until February 2013 (Figure 2-7), the recharge volume showed a decreasing trend after September 2012 (Figure 2-8). This was mainly attributed to clogging by suspended particles carried into the pond with the surface run-off from the surrounding area.

These suspended particles settle at the pond surface and occupy the voids in the soil at the pond bottom reducing the rate of infiltration of pond water into the aquifer. Clogging can be controlled by the periodical removal of clogged layers, once the pond gets dry after each monsoon. Further enhancement of groundwater recharge could be reached by constructing a recharge shaft at the centre of the pond bottom in order to directly recharge the aquifer.

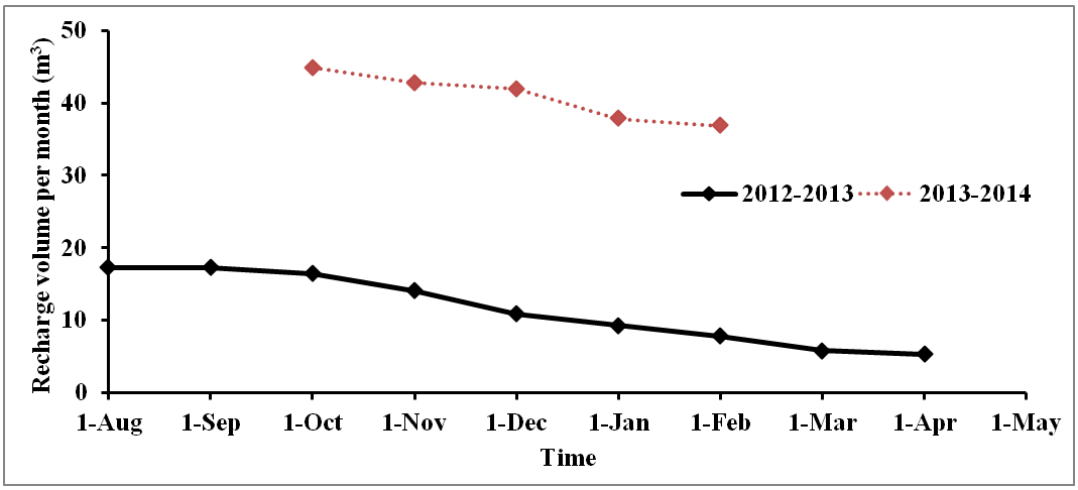

Figure 2-8: Volume of water recharged from the pond from August 2012 to June 2013 (Raicy and Elango 2014b)

Figure 2-8 further shows that from August 2012 to May 2013, the volume of recharged water has been significantly less compared to the time period of October 2013 to January 2014. Again, this was attributed to clogging. From August 2012 to February 2013, recharge had been done only by infiltration through the pond bottom. Immediately after rain events, the recharge rate was very high, but gradually decreasing to a constant level. Given as volume per month, this led to significantly different recharge volumes.

2.3.2.3 Estimation of physical clogging

The effect of clogging inside the pond bottom was additionally studied in a laboratory experiment using pond soil and pond water in a simple experimental setup to calculate both, the clogging potential of the recharge structure and the rate of infiltration (Figure 2-9).

For this purpose, an undisturbed soil column from the pond bottom and suspended pond water were collected. A jar (Figure 2-9) was filled with compacted soil collected from the pond, with top and bottom of the jar fitted with permeable porous plates after removing the excess soil. The pond water was allowed to pass through the soil maintaining a constant source water head by means of an outlet pipe, through which excess water could flow off and be reused. After saturation of the soil with pond water by upward flow, flow direction was from top to bottom and the discharge volume was measured at the bottom at definite intervals of 8 minutes.

Figure 2-9: Photographs showing soil collection from the field and the experimental set up for clogging at the laboratory

The variation of the discharge volume with respect to time was then plotted (Figure 2-10). Results showed an increase of discharge for the first 8 minutes of the experiment, followed by a drastic decrease for the next 8 minutes. After these 16 minutes, the discharge volume of the soil decreased gradually due to a change in the entropy of the whole system indicating the movement of fine-grained particles to the bottom of the system, which reduced the interconnection of pore spaces in the soil. After 0.25 days, the discharge rate had stabilized (Raicy and Elango, 2014a). The discharge volume varied from 5×10^{-5} m^3 to 2.2×10^{-4} m^3. The same phenomenon occurred under field conditions as described above.

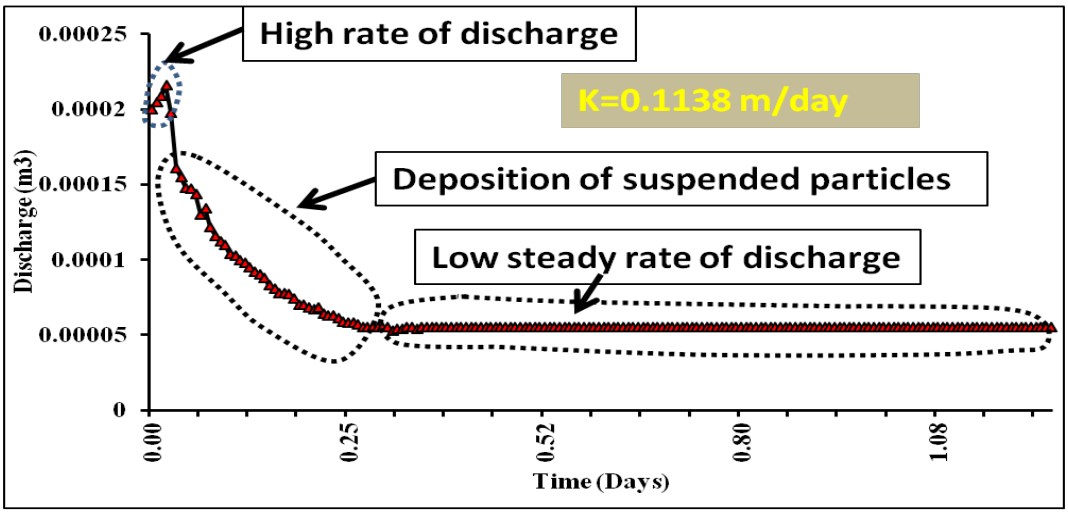

Figure 2-10: Discharge rates in laboratory clogging experiment (Raicy and Elango 2014b)

2.3.2.4 Groundwater quality

Groundwater collected from the observation wells and pond water was collected once every two weeks and the major and minor ions were analysed at the laboratory. The major hydrochemical facies identified were Na-Cl, Ca-Mg-Cl and Ca-Cl type of water. Alkalis exceeded alkaline earth metals and strong acids exceeded weak acids. The type of water changed with the depth of the sample. The water from shallow depths was comparably fresh and thus of recent infiltration.

The different water quality parameters are plotted along with their concentrations (mg/l) in Schoeller diagrams as shown in Figure 2-11. The pond and the observation wells P1, P2 and P3 showed different orders of dominance of chemical ions with Cl>Mg>Na>K>SO4> HCO3 in the pond, Cl>Mg>Na>K>SO4>HCO3 in P1, Na>Cl>Mg>SO4>K>HCO3 in P2, and Cl>Na>SO4>Mg>K>HCO3 in P3.

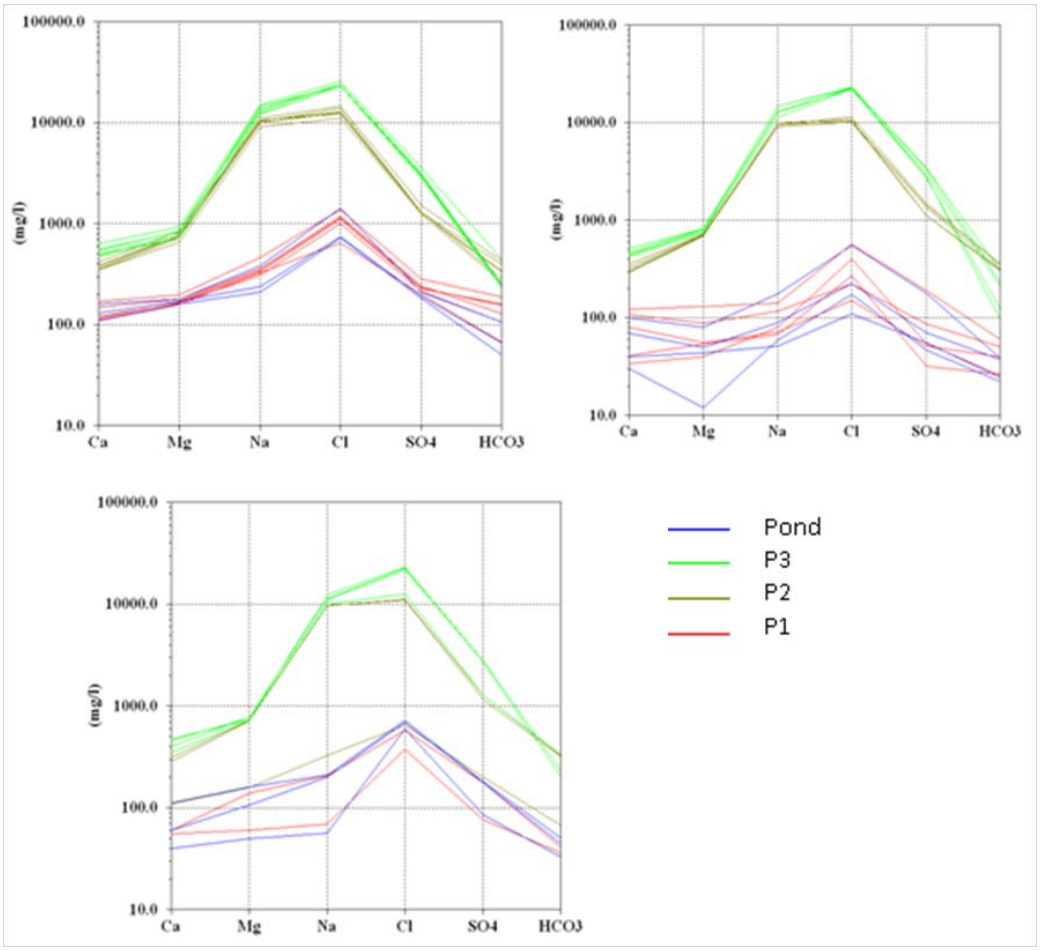

Figure 2-11: Schoeller diagram of samples collected before rainfall (top left), during (top right) and after rainfall (bottom left) to compare the ionic concentrations of different sets of samples

Na and Cl concentrations were elevated in all facies of waters in the area. During rainfall, the ionic concentrations initially increased. After continuous rainfall, ions decreased tremendously. Total dissolved solvents increased with depth (P1 to P3).

The samples from P3 indicated the point of intrusion of high chloride water. The groundwater changes its composition within short distances down-slope through processes such as cation exchange and mixing with fresh water forming other water types. As mixing is negligible at the investigated site because of the low permeability of the upper soil layer, the source process of higher Na and Cl concentrations in deep water must be cation exchange processes.

2.4 Conclusions

The efficiency of the check dam at the AK aquifer to improve the groundwater quality and usability was assessed using electrical conductivity and groundwater level measurements. Based on these measurements, the region positively influenced by this recharge structure could be delineated.

Groundwater in an area of 3 km^2 around the check dam is having electrical conductivity similar to that of the water in the check dam and groundwater level in this region has raised by about 1.5 m after construction of the check dam. Recharge from check dam was estimated to be about 1.12 Million cubic meters during 2011-to 12. Thus, the availability of water for irrigation purpose in this region has increased after the construction of the check dam. The percolation pond showed to be effective in augmenting groundwater recharge during the rainy season. The pond was almost completely filled from September 2012 to February 2013. Afterwards, the water level gradually decreased from February 2013 until it was emptied in May 2013.

Clogging was a major problem encountered and investigated in an experimental set-up in the laboratory. The discharge was found to be greatest immediately after the commencement of the test and then it gradually decreased until reaching a constant rate.

The groundwater quality in the area surrounding the pond was improved by recharge from the percolation pond. On a regional scale, the groundwater potential of the area could thus be improved by the implementation of several such ponds. As this region has very poor quality groundwater, the recharge resulting from constructing percolation ponds will improve the quality. Hence the water recharged may also be utilized at a later stage.

If such percolation ponds are planned in other locations facing saline groundwater, the quality of groundwater will improve and the local community may benefit by taping the freshly recharged groundwater at least by hand pumps.

In areas where the soil particles are fine, the clogging of finer suspended particles in the runoff water will be a cause of reduced infiltration. But this can be managed by conventional scraping of the bottom of the pond after drying it up. Even though infiltration rate decreases in due time, a considerable quantity of water will be recharged into the aquifer. This can further be improved by the construction of recharge shafts at the pond bottom, so that the pond water will be directly recharged into the deeper aquifer.

Overall, the construction of percolation ponds is most feasible in areas where the depth to the water table is more than 3 m, the aquifer is confined and the soil is characterized by high permeability.

2.5 References

BIS (1991) Bureau of Indian Standards IS: 10500, Manak Bhavan, The New Delhi, India.

Boisson, A., Sprenger, C., Lakshmanan, E., Picot-Colbeaux, G., Ghosh, N.C., Ahmed, S.,

Kumar, S., Singh, S., Thirunavukkarasu (2013) Documentation of acquired data and conceptual model of MAR impact as input for WP5 modelling, Saph Pani deliverable 2.2, p. 117, http://www.saphpani.eu/downloads.html (accessed Sept. 2014)

Parimalarenganayaki, S (2014) Managed Aquifer Recharge: An integrated approach to assess the impact of check dam, PhD Thesis, Anna University

Parimalarenganayaki, S.,Elango, L. (2014) Impact of recharge from a check dam on groundwater quality and assessment of suitability for drinking and irrigation purposes, Arabian Journal of Geosciences,7(8):3119-3129

Raicy M.C, Elango L. (2014a). Percolation pond as an aquifer recharge method in a saline aquifer, north of Chennai: a perspective on the site selection criteria, implementation and its effects, Water

Raicy M.C., L. Elango, (2014b) Experimental determination of clogging potential and infiltration rates in percolation ponds: A case study from Andarmadam, Thiruvallur district of Tamil Nadu. 2014, Environmental Monitoring assessment (submitted)

Raicy M.C., Parimalarenganayaki S., Dhanamadhavan S., Elango L., (2014) Understanding the surface water-ground water interactions by geochemical measurements in three different groundwater recharge structures, Journal of environmental science and management, (submitted)

Rajaveni S.P, Indu S. Nair and Elango L. (2014) Application of remote sensing and GIS techniques for estimation of seasonal groundwater abstraction at Arani-Koratalaiyar river basin, Chennai, Tamil Nadu, India. International journal of earth sciences and engineering, Vol 07 (1), ISSN: 0974-5904

3 Temple Tanks in urban Chennai

3.1 Problem statement and objectives

Temple tanks are very common in every temple of India. Normally, they are constructed for performing religious activities, but at the same time they also act as an example for managed aquifer recharge. The temple tanks maintain the ecosystems and act as rainwater harvesting, storage structures and infiltration ponds. Thus, they can play a major role in recharging groundwater.

The objective of this study was therefore to investigate the impact of temple tanks on groundwater quality. Four of altogether 64 temple tanks in the Chennai city and its suburbs (Times of India, Chennai, June 18, 2011) were selected to study the recharge impact by evaluating the quality of surface water and groundwater.

3.2 Site description

The tanks chosen for this study were (Figure 3-1 and Table 3-1):

- Adipuriswarar-Adikesava Perumal Temple Tank (Chindadripet).
- Agatheeswarar-Prasanna Venkatesa Perumal Temple Tank (Nungambakkam).
- Kurungaleeswarar-Vaikundavasa Perumal Temple Tank (Koyambedu) and
- Suriyamman Temple Tank (Pammal, Pallavaram)

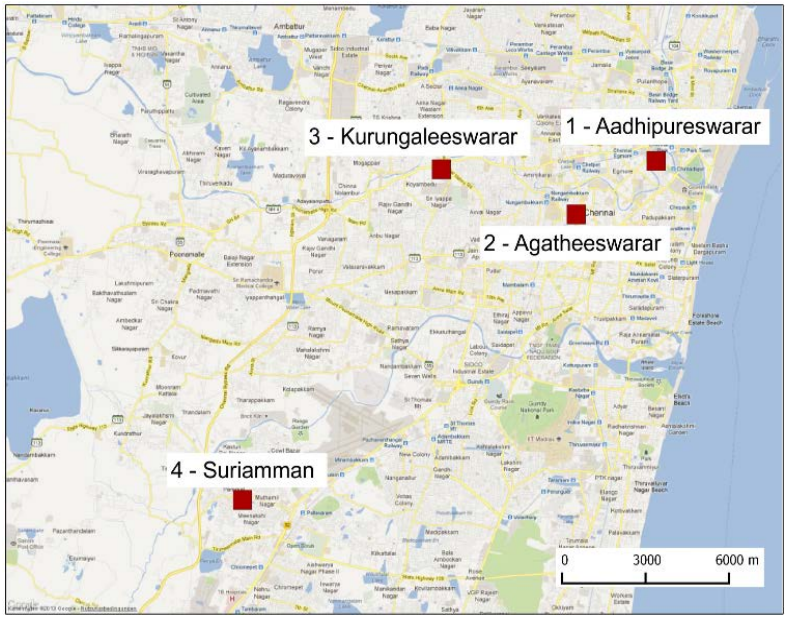

Figure 3-1: Study area with location of the temple tanks

Temple tanks are constructed in different sizes (Table 3-1) and different geometry near major temples with other elements such as entrance, rainwater inlets etc. In some of the large tanks, a central Mandapam in contemporary architecture has been incorporated

while many others are plain rectangular water storage structures with simple steps and protection at the sides. But the unique feature has been that the tank bed has always been just left as unpaved earth indicating that it is designed to permit percolation to enable recharging the wells around the tank.

There is always an arrangement to collect rainwater in to the tank from the sprawling temple complex as well as streets around and an outlet to drain any surplus exceeding the storage capacity. The stored water is usually lasting to the next rainy season as there is no large-scale direct extraction from the tank. The loss of water in the tank is mainly due to evaporation and percolation of stored water into the aquifer. Thus, the temple tanks may serve as a natural recharge structure.

Table 3-1: Name, temple tank size and location

Temple Name	Age/ Time of construction	Temple Tank Size (m)	Location	Total depth of well (m)	Distance of well from the temple tank (m)
Aadhipureeswarar	Constructed in 1734 by Adhiappa Naicker	35×33×3.45	13°4'34.90"N 80°16'4.73"E Chindadripet	9.5	35
Agatheswarar	About 500 years old constructed by Bommaraja of Bommarajapuram	45.72×30.48×3.01	13°3'36.13"N 80°14'30.82"E Nungambakkam	9	25
Kurungaleeswarar	About 1000 years old, constructed by King Raja Raja Cholan I of Chola dynasty	54.9×53×3	13° 4'25.41"N 80°11'52.26"E Koyambedu	9.5	32
Suriyamman	About 750 years old	180×100×3	12° 58'21.69"N 80°07'58.29"E Pammal	8.5	15

In the scope of the project, the lithology of the first three tanks has been ascertained by drilling boreholes using a hand bore set. Soil samples were collected at different strata for analysis. The fourth tank is known to fall in hard rock terrain.

Based on the drillings and previous work, the following lithological properties could be assigned:

- Adipuriswarar Temple Tank at Chindadripet is located in coastal alluvial sub stratum

- Agatheeswarar Temple Tank at Nungambakkam has sub stratum consisting of alluvium of fluvial origin
- Kurungaleeswarar Temple Tank at Koyambedu is in clayey sub stratum
- Suriamman Temple Tank falls in hard rock terrain consisting of weathered and fractured rock (Charnockite) as sub stratum

3.3 Results and interpretation

3.3.1 Adipuriswarar temple

At the Adipuriswarar temple, surface water and groundwater were sampled with the following results: the pH of surface water and groundwater varied between 7.0 and 9.5 indicating that the water is of neutral to alkaline nature. Total hardness and TDS of surface water and groundwater were within the permissible limit of BIS (2012). The major ion concentrations of surface water and groundwater are shown in Figure 3-2. It can be seen that the measured ions show large differences in surface and groundwater.

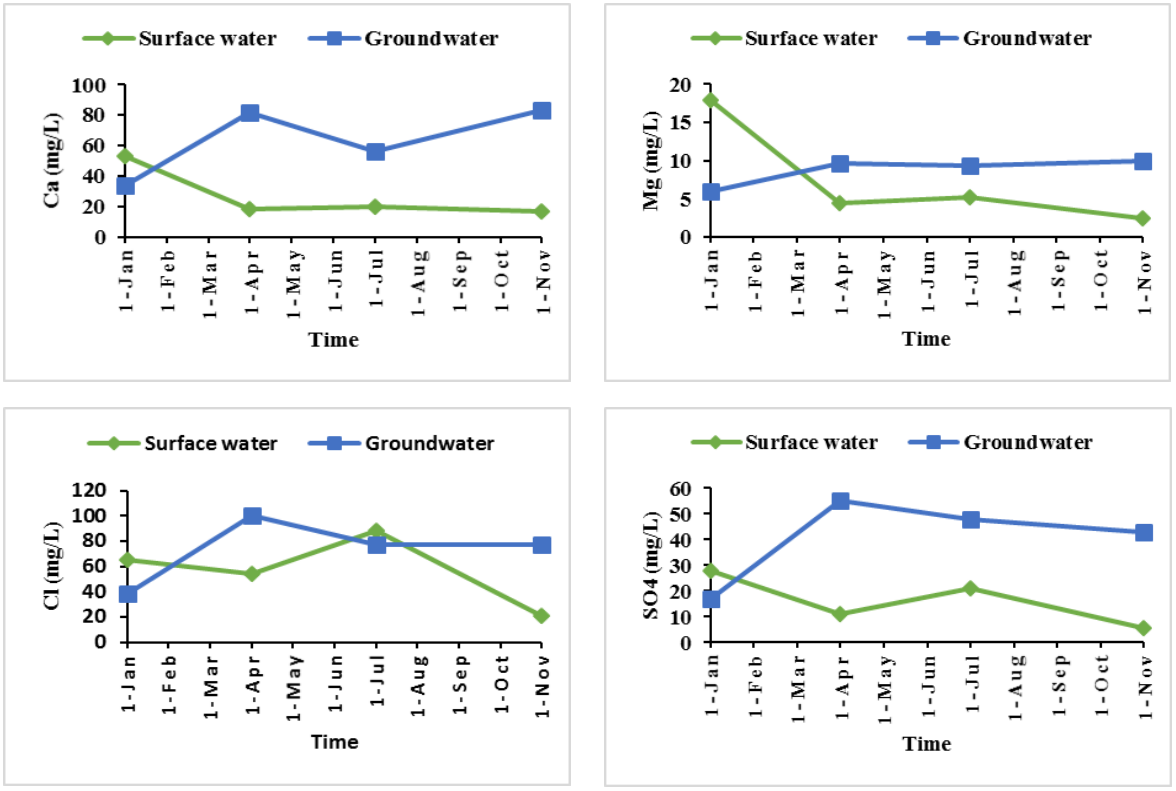

Figure 3-2: Selected parameters of surface and groundwater chemistry of Adipuriswarar Temple

3.3.2 Agatheeswarar temple

Mean values of the parameters measured in groundwater and surface water in Agatheeswarar temple are shown in Figure 3-3. The pH of surface water and groundwater

varied from 6.8 to 7.9. Total hardness and TDS were within the permissible limits suggested by BIS (2012) making the water suitable for drinking purposes. Major ion chemistry of surface water and groundwater represented by calcium, chloride and sulphate ions show large differences.

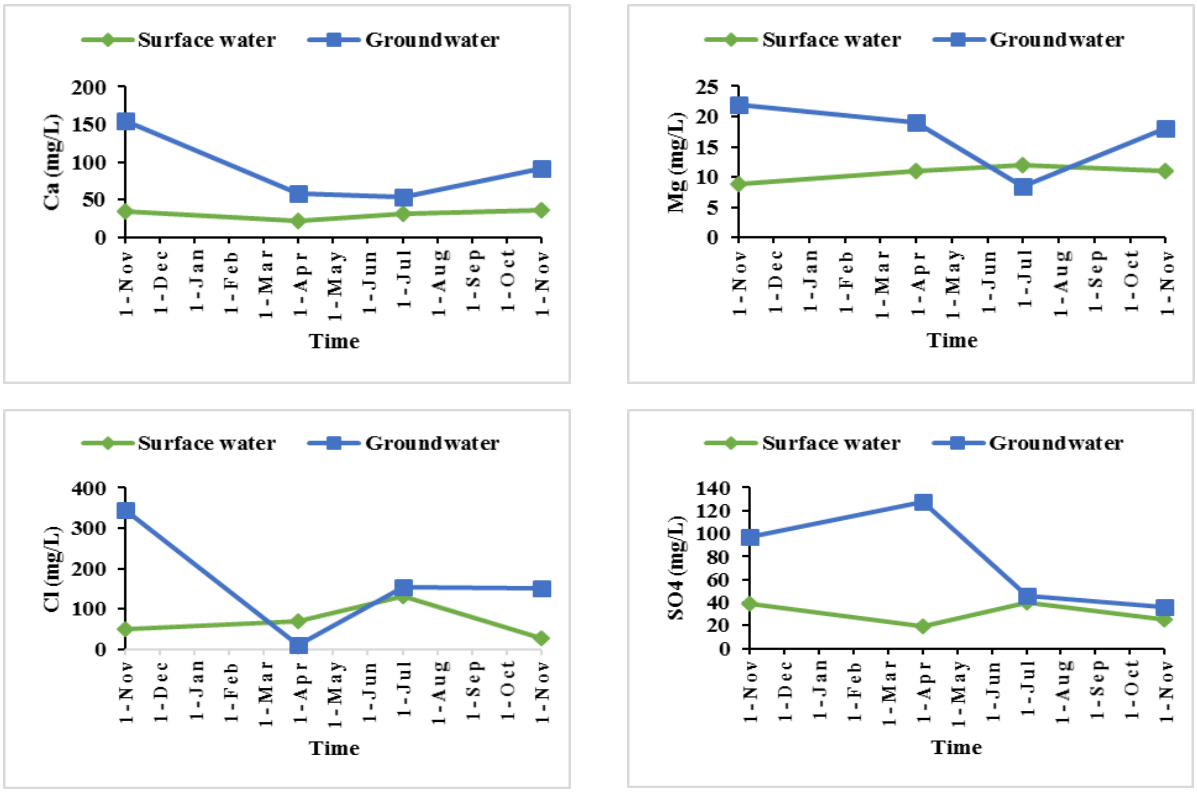

Figure 3-3: Selected parameters of surface and groundwater chemistry of Agatheeswarar temple

3.3.3 Kurungaleeswarar temple

The pH of surface water and groundwater from the Kurungaleeswarar temple showed to be alkaline with values ranging from 7.0 to 8.0. Total hardness and TDS of surface water and groundwater were within the permissible limit of BIS (2012). The concentration of major ions in surface water and groundwater is shown in Figure 3-4. Calcium, chloride and sulphate ion concentrations show large differences, but similar temporal trends.

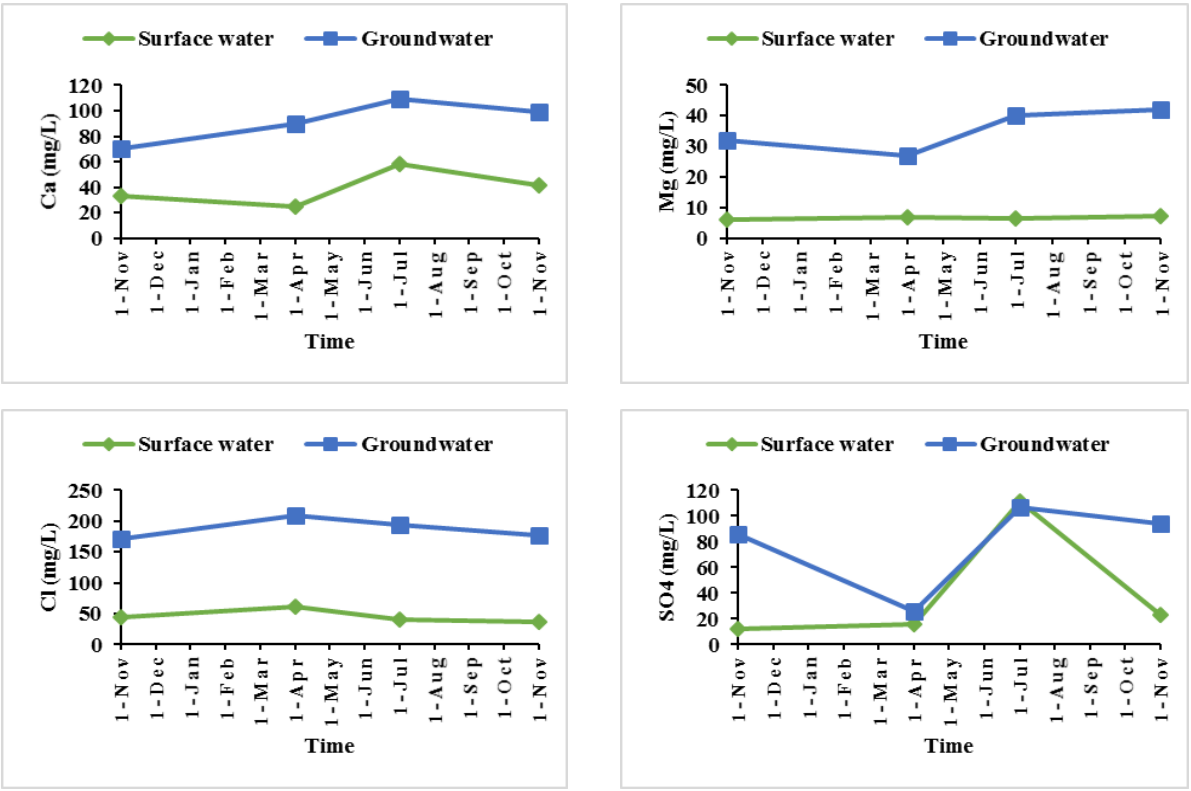

Figure 3-4: Selected parameters of surface and groundwater chemistry of Kurungaleeswarar temple

3.3.4 Suriyamman temple

In the Suriyamman temple, the pH of surface water and groundwater was alkaline in nature with values ranging from 7.0 to 8.0. Total hardness and TDS of surface water and groundwater were within the permissible limit of BIS (2012). The major ion chemistry of surface water and ground water (Figure 3-5) shows similar concentrations of magnesium, but large differences of calcium, chloride and sulphate.

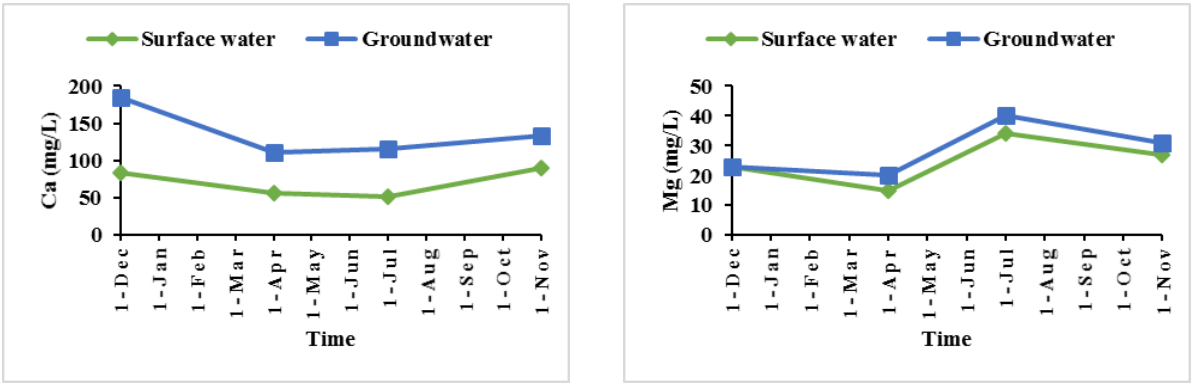

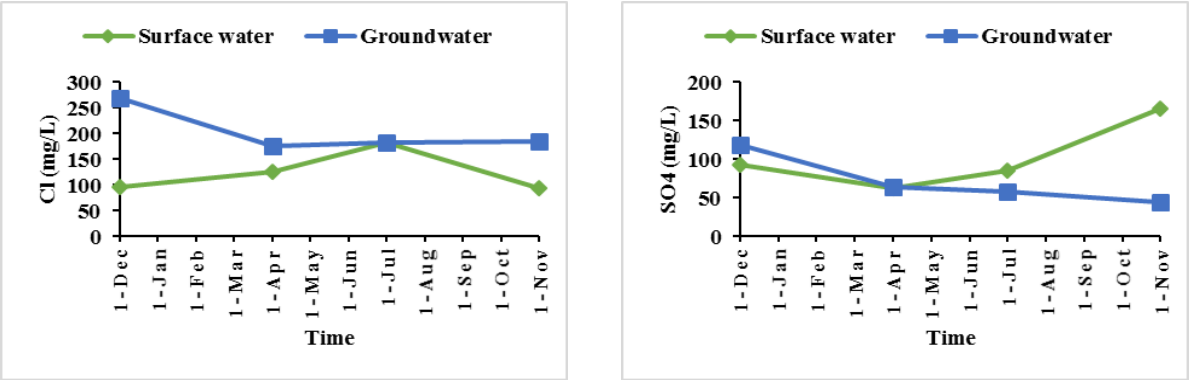

Figure 3-5: Selected parameters of surface and groundwater chemistry of Suriyamman temple

3.4 Discussion

The periodical study indicates from changes in the nature and chemistry that the water in the investigated temple tanks may interact with the groundwater on site. Especially at temples with, at least temporarily, similar chloride concentrations (Suriyamman, Agatheeswarar and Adipuriswarar temple) an infiltration of the temple tank water is likely. Even at the Kurungaleeswarar temple with differences of >100 mg/l in chloride concentration between surface- and groundwater an impact of tank infiltration cannot be excluded without knowing the chloride concentration in native groundwater. Anyhow, additional investigations are necessary to further characterise the tank infiltration potential. These investigations may include:

- Seasonal water table maps around temples
- Hydrochemical characterisation of native (not influenced by tank infiltration) groundwater upstream from tanks
- Water balance calculations of tanks

3.5 References

BIS (2012) Bureau of Indian Standards: 10500 – Drinking water specification, Manak Bhavan, New Delhi, India

4 Tummulur Tank in Maheshwaram

4.1 Problem statement and objectives

Managed aquifer recharge (MAR) through percolation tanks is a promising technique to increase local water availability. However, authors such as Dillon et al. (2009) point out the lack of data available for an accurate assessment and note that little evidence exists on the positive impact at local scale. Some authors even point out the possible negative impact at watershed scale due to the enhancement of local water extraction (Calder et al. 2008; Glendenning et al. 2012; Sakthivadivel 2007).

In the following study, a percolation tank located in the Maheshwaram watershed in Andhra Pradesh (India) is monitored to quantify the impact of the percolation tank on water availability and quality. The objectives of the present study are to assess the potential of percolation tanks as managed aquifer recharge structures by:

- quantifying the volume of water recharged to the aquifer by MAR structures
- developing simple methods for prediction of yearly tank recharge
- defining the hydrodynamic and hydrochemical characteristics of percolation tanks in crystalline aquifers
- assessing the impact of those structures on groundwater quality

For synthesis reason, only major results are presented in this report. More detailed information on methodologies and detailed results can be found in related publications (Boisson et al. 2014 (a, b), Pettenati et al. submitted; Picot-Colbeaux et al. submitted).

4.2 Site description

4.2.1 Maheshwaram watershed

The study was carried out in Maheshwaram watershed, located 35 km south of Hyderabad (Andhra Pradesh State, India). This typical watershed is a good example of south Indian context with semi-arid climate and crystalline aquifers. Moreover, previous hydrogeological studies in the watershed provided good data (Dewandel et al. 2006; Maréchal et al. 2004a, b, 2006; Wyns et al. 2004; Perrin et al. 2011). It covers an area of 53 km^2 (Fig. 4.2) and has a relatively flat topography ranging from 590 to 670 m above mean sea level. The climate is semi-arid with annual monsoon rains (rainy or ‘‘Kharif’’ season from June to October). Mean annual precipitation (P) is about 750 mm, of which more than 90 % falls during the monsoon season (Maréchal et al. 2006). The mean annual temperature is about 26 °C although during the summer (‘‘Rabi’’ season from October to May), maximum temperature can reach 45 °C (Maréchal et al. 2006).

The resulting potential evapotranspiration is 1,800 mm/year. Due to the rapid growth of the Hyderabad city, this watershed is now in transition from rural to suburban area.

The aquifer is overexploited with more than 700 boreholes used for agriculture dominated by rice paddy fields (Dewandel et al. 2010). Currently, the water table is 15–25 m below surface and there is no surface water except for a few days subsequent to very heavy rain falls (> 40 mm). Thus, no regular infiltration under streambeds is observable in the watershed during most of the year.

4.2.2 Main characteristics of the crystalline rock aquifer

Crystalline rock aquifers, which represent most of South India and about 66% of Andhra Pradesh state (GSI, 2005), show hydraulic characteristics which may limit the potential of MAR. As described by various authors (Acworth 1987; Chilton and Foster 1995, Dewandel et al. 2006) the typical geological profile is described by (Figure 4-1): the first zone is the saprolite (or alterite or regolith) on top consisting of clay-rich material, derived from bedrock decomposition with a thickness of approx. ten meters.

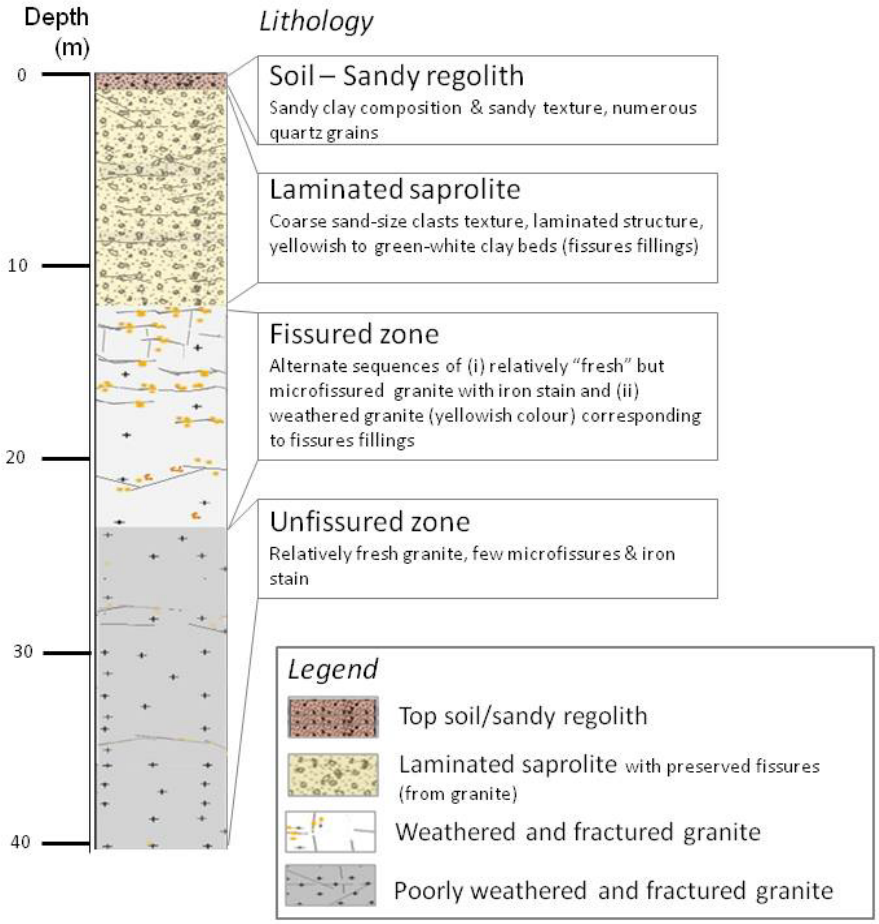

Figure 4-1: Geological log characteristic for the study area

Because of its clayey–sandy composition, the saprolite zone has a high porosity, and a low permeability. This zone is the main storage capacity of the aquifer. The second zone is a fissured zone, generally characterized by dense horizontal fissuring in the first few meters and a depth-decreasing density of subhorizontal and subvertical fissures (Maréchal et al. 2003; 2004).

This zone mainly provides the transmissive function of the aquifer and is tapped by most of the wells drilled in hard-rock areas. The third zone is the fresh basement which is only permeable where tectonic fractures are present. Boisson et al. (submitted) showed that the storage potential of the deepest fractures is very limited.

4.2.3 Tummulur tank monitoring program

Currently, three main percolation tanks are located within the watershed. The monitored tank is close to Tummulur village, in the downstream part of the watershed (Figure 4-2) and has been used for more than 10 years for water storage.

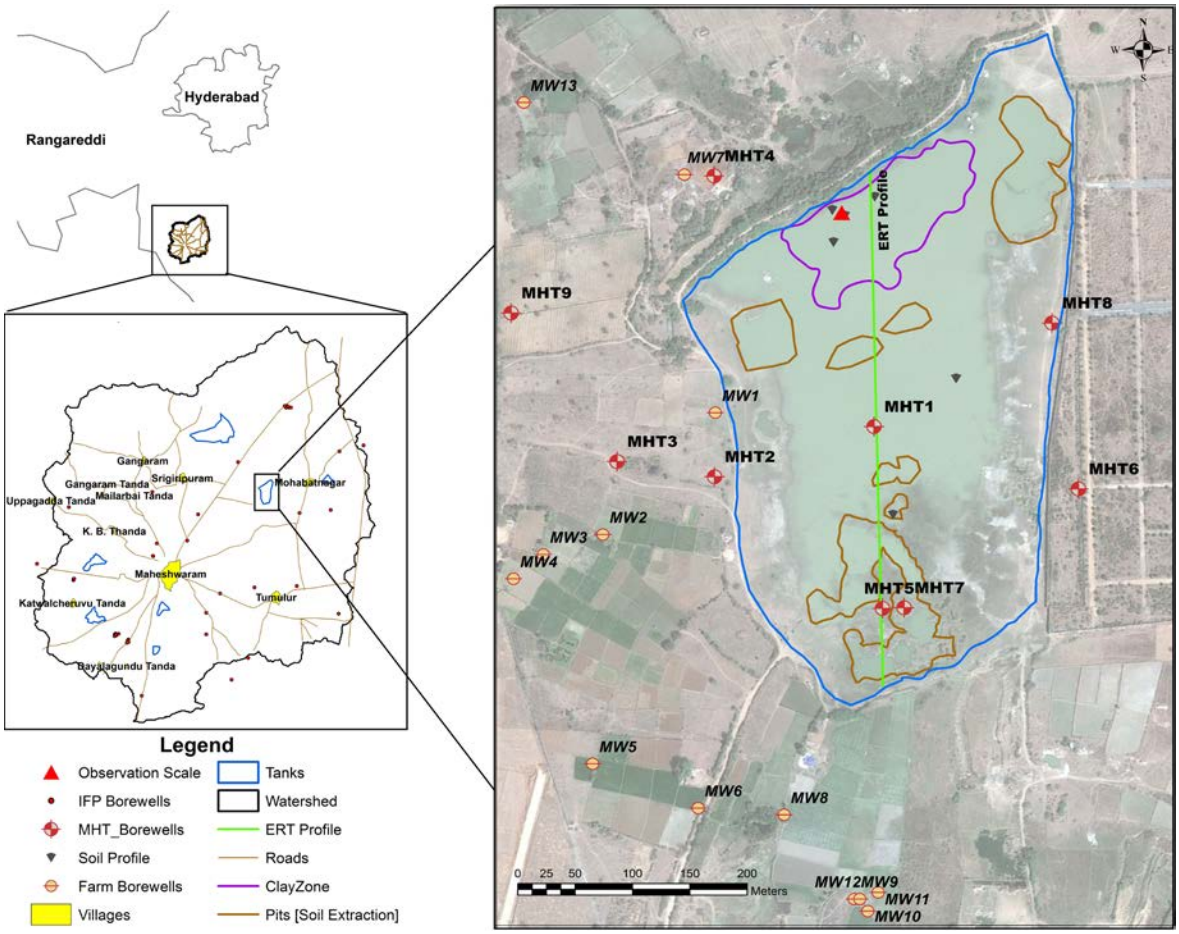

Figure 4-2: Study site map *(taken from Boisson et al. 2014 (b))*

An earth bund in its northern part dams the natural stream outlet, and consequently, runoff water can be stored over an estimated maximum area of 158 000 m^2 and a maximum water depth of 3.5 m.

Before the first significant rainfall events in 2012, the tank was dry over 7 months with temperature ranging from 30 to 45 °C which created shrinkage cracks at the entire tank area. The tank area is covered by silt loam soil on the surface underlain by sandy loam at a depth of 40–80 cm. Because of thin sedimentary deposits, there is an important clayey zone, at the foot of the bund, in the northern part of the tank. Clay pits are located on the southern part of the tank to feed the nearby brick industry.

Nine monitoring boreholes (labelled MHT's) were implemented in 2012 and one staff gauge records the surface water level within the tank. Temperature and water electrical conductivity logging are regularly performed in the boreholes, in addition with the long-term piezometer temperature and electrical conductivity records. Slugs tests were also performed (Boisson et al. 2014 (b)). Topography of the tank area was measured by DGPS survey and regular GPS tracking of the water contour give the tank area evolution. Within a radius of 500 m, at least 15 irrigation boreholes are in use (rice paddy and maize). Irrigation duration and times are controlled by the availability of electricity (7 h a day). The percolation tank constitutes a drinking water supply source for livestock (few goats and buffaloes). No significant direct tank water extraction for irrigation purposes occurs. This tank system is representative of MAR practice in semi-arid southern India.

Eight sampling campaigns for major ions analyses and two campaigns for stables isotopes ($\delta^{18}O$ and $\delta^{2}H$) analyses were performed in 2013 and 2014 corresponding to different hydrological conditions (Figure 4-3).

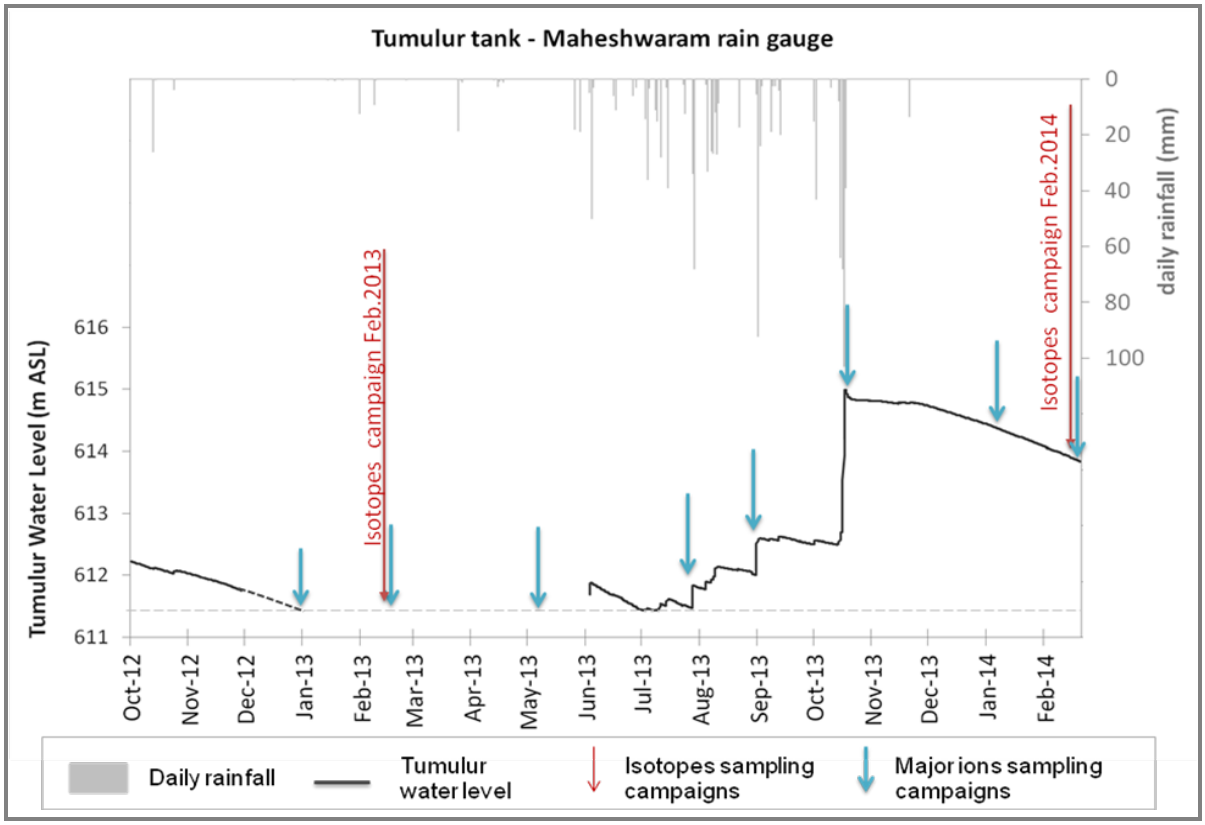

Figure 4-3: Corresponding hydrological conditions on the Tummulur site for the sampling campaigns in 2013 and 2014

Groundwater was sampled in 7 MHT boreholes and 3 farmer bore wells as well as the Tummulur tank water (see Figure 4-1). In situ electrical conductivity, temperature and pH were measured for each sample. Water was collected in clean polyethylene bottles according to each analysis requirement (i.e. filtration, acidification, air tightness) and analysed in BRGM's laboratory in Orléans. More details on sampling and analyses are given in annex 3.

4.3 Results and interpretation

4.3.1 Field results and observation

The Tummulur tank was monitored from 01/01/2012 to 11/04/2014. Variability of the monsoon (700 mm in 2012; 1 110 mm in 2013) has a large impact on water level and tank area evolution (Figure 4-4).

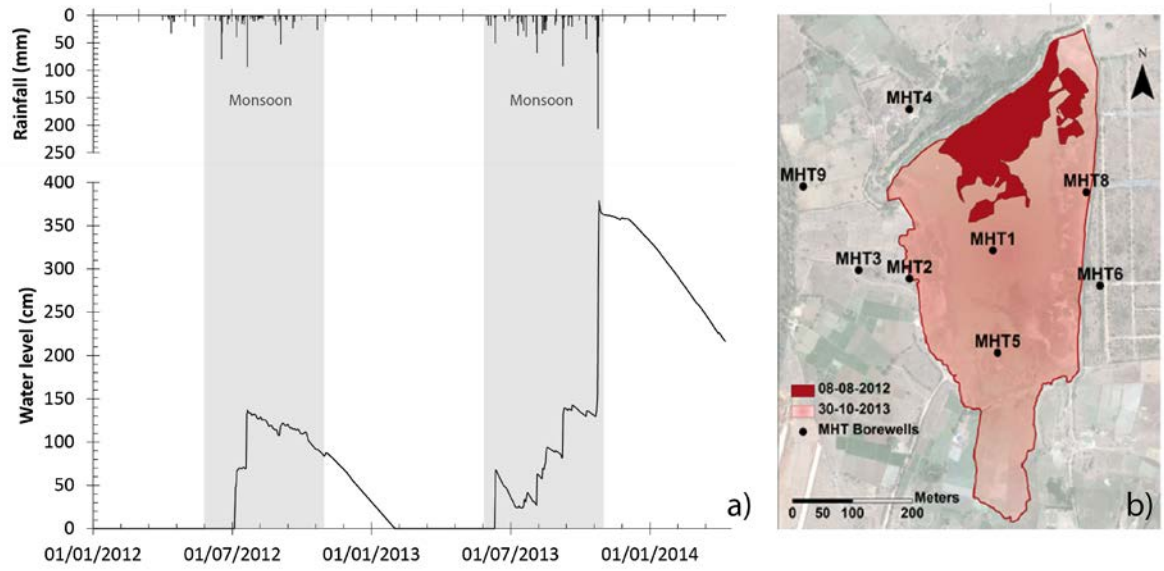

Figure 4-4: a) Evolution of water levels in the tank versus rainfall; b) Maximum water extent in tank area after 2012 monsoon (08/08/2012, dark red) and 2013 monsoon (30/10/2013, light red)

From the water levels coupled with the DGPS topographic survey the maximum tank volume after the 2012 monsoon is estimated to be 8 100 m^3 and above 90 000 m^3 after the 2013 monsoon. During the monsoon, few extreme events appear to have a major impact on the tank replenishment.

4.3.2 Tummulur tank water budget

The water budget of the Tummulur tank has been performed following the methodology developed in Massuel et al. (2014) computed on a daily basis. To sum up, the balance is based on the following equation:

$$\Delta V = F_{net} + R_{rain} - I_{rf} - E - L_v - S_{eep} - P \qquad \text{(eq.4.1)}$$

where

ΔV = change in tank water storage

F_{net} = net inflow to the tank i.e runoff

R_{rain} = direct rainfall collected on the surface of the water tank

I_{rf} = irrigation return flow

E = evaporation from the tank surface (estimated from class-A pan data with a pan coefficient of 0.8)

L_v = water consumption by livestock

S_{eep} = seepage across the dam

P = percolation

From the local condition, i.e. limited cattle and limited paddy the terms I_{rf} and L_v can be neglected. This assumption is justified since Massuel et al. (2014) show that in a similar context with a more developed rice paddy agriculture and goats breeding those elements represent a minor part of the water budget (<5%).

To limit the number of unknown in equation 4.1, a relation between tank water level and percolation is developed on the days without rainfall, runoff or seepage through the dam when the percolation can be defined as:

$$P = \Delta V - E \qquad \text{(eq. 4.2)}$$

This relation (Figure 4-5) is then used to define percolation on every day basis depending of the water level.

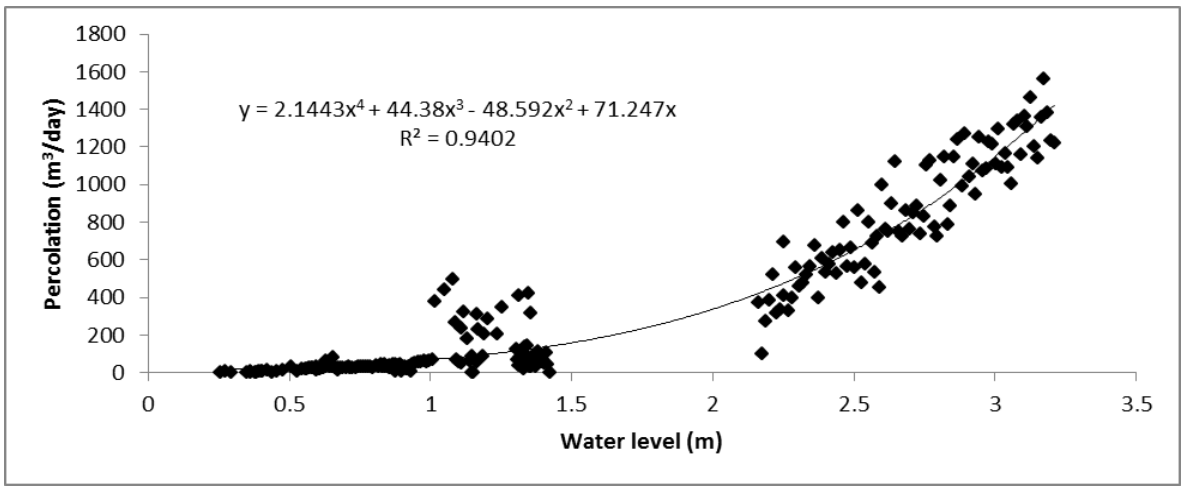

Figure 4-5: Relationship water level percolation rate

Using this relation in eq.4.1 a complete water budget at the tank scale can be drawn. Results are presented Figure 4-6 and Table 4-1. Note that the budget for the 2013 monsoon ends on 11/04/2014 while the percolation and evaporation will continue in the following months.

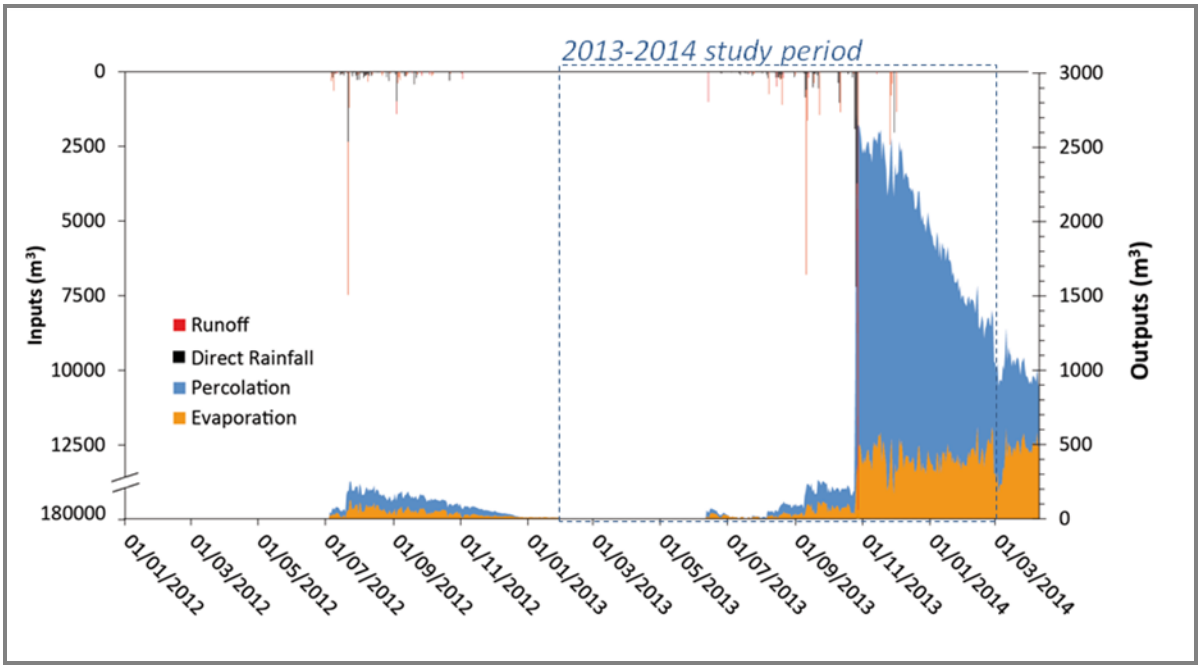

Figure 4-6: Temporal evolution of main components of water budget at Tummulur percolation tank

Table 4-1: Main components of water budget of Tummulur percolation tank

	2012 Monsoon		2013 Monsoon	
	m^3	%	m^3	%
Input	18 407	100	300 108	100
Runoff	10 612	58	278 442	92
Direct rainfall	7 795	42	21 666	8
Output	19 010	100	305 124*	100
Evaporation	7 281	38	75 970	25
Percolation	11 730	62	229 155	75
Balance in-out	-603		-5016	
Error		3.2		1.7

*Budget for the 2013 monsoon ends on 11/04/2014 and the evaporation and percolation will continue

Results of the water balance show a high variability in the tank infiltrated water from 11 730 m^3 in 2012 monsoon to 229 155 m^3 for the 2013 monsoon. Results are in

agreement with the predictive water balance performed in Boisson et al. (2014 (b)) for the 2012 monsoon, through a different approach. As well, the estimated infiltration rates and ratio percolation over inputs are on the same range than observed in Massuel et al. (2014) in a similar context. It is noteworthy that the refilling of the tank occurs mainly during a few intense events, through runoff (up to 92.8% in 2013). On the contrary, outputs are evolving slowly all along the flooded period.

Maréchal et al. (2006) estimate the mean annual groundwater abstraction at the watershed scale to be 8.8 million m^3/ year. Therefore, the percolated volume from the Tummulur tank represents 0.13% and 2.6% in 2012 and 2013 monsoons, respectively. Considering the 40% of return flow in average (Maréchal et al. 2006), the percolated water from the tank represent 0.24 and 4.2% of the groundwater abstraction at the watershed scale for the two monitored events.

Those calculations show that under low rainfall conditions, the impact of percolation tank is negligible at the watershed scale, and very limited at the local scale. On the contrary, in case of complete filling, the tank has a significant impact on the total water budget and can be very helpful for the surrounding farmers. However, it should be noted that following an important rainy season, farmers tend to increase the irrigated surface in the tanks surrounding and therefore increase the water abstraction at the watershed scale.

4.3.3 Flow characteristics in crystalline aquifer

In crystalline rock aquifers, flow is constrained by the fracture network (distribution of fracture length, orientation, density and connectivity (Bour and Davy 1998; de Dreuzy et al. 2001)). Studies in the Maheshwaram watershed have shown that the predominant water flow occurs horizontally (Maréchal et al. 2006) mostly in the fractures at the contact between the saprolite and the top of the granite (Dewandel et al. 2006; Mayo et al. 2003). Detailed investigations also show that the storage decreases drastically with depth and that the deepest fractures may have a semi-confined behaviour (Boisson et al. submitted). An example of a detailed log with pictures of fractures and fissures is shown in Figure 4-7.

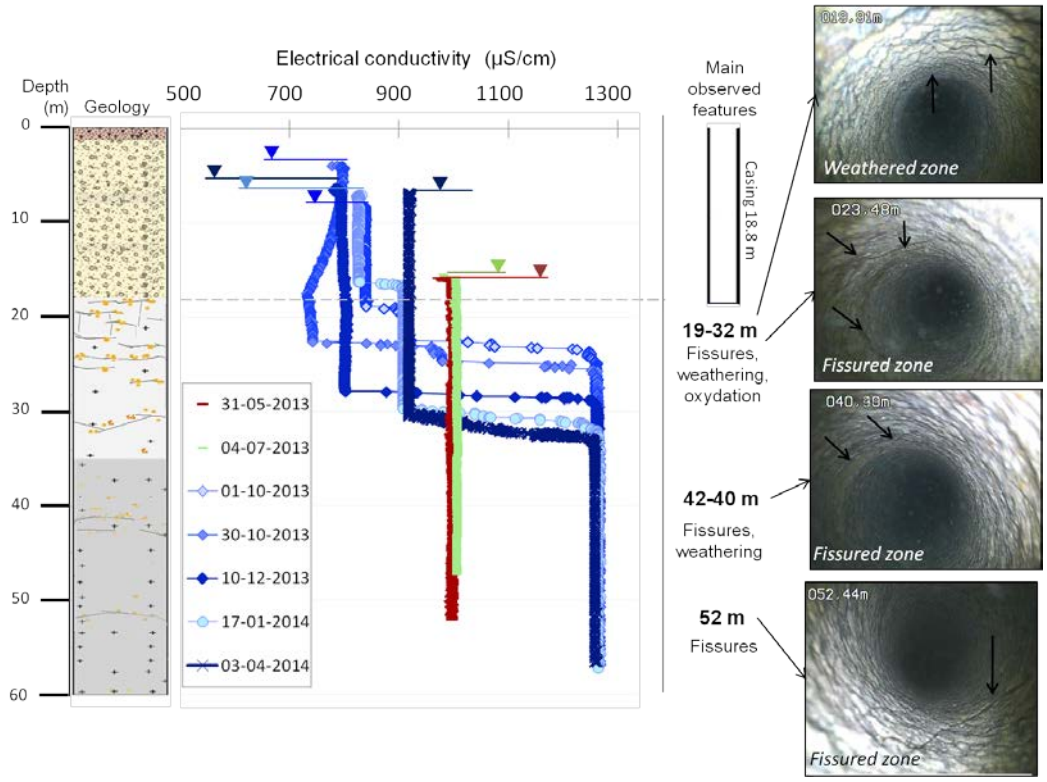

Figure 4-7: Geological profile of MHT9 borehole with electrical conductivity measured in groundwater and observed textures in the open borehole. Pre-monsoon campaign is shown in red, early stage of the monsoon (July 2013) is shown in green, and late stages of the monsoon and post-monsoon campaigns are shown in bluish colours. Water levels in the borehole for each campaign are shown as triangles

In this example, before monsoon (June) the conductivity profile is constant at a value of ~1 000 µS/cm. When the recharge starts (September-October), the borehole appears to cross two separate water bodies: the upper part of the profile appears to be diluted by rainfall and surface water (decrease of electrical conductivity); while in the deepest part, the conductivity is higher, as observed also in other borehole logs (not shown here). This water with high conductivity values should come from the deepest parts of the aquifer and/or zone of important salinization. Local or regional changes in pressure gradient may mobilise different productive zones or fractures.

The crystalline rock aquifer structure implies a strong variability of porosity with depth, ranging from 0.5 to 10% in the saprolite layer (Wyns et al. 1999) and from 1 to 2% in the fractured zone (Dewandel et al. 2012; Maréchal et al. 2004).

The higher storage capacity of the saprolite regarding the fractured zone can create strong discrepancies in the piezometric evolution. In MHT4 borehole, for example, two rain events of 18 and 19 mm (03/06 and 06/06/2013, when the water is in the fractured zone) induced water level rise of 8 m, while a rainfall event of 50 mm (12/06/2013, when the water table has reached the saprolite) induced a rise of 24 cm (Figure 4-8).

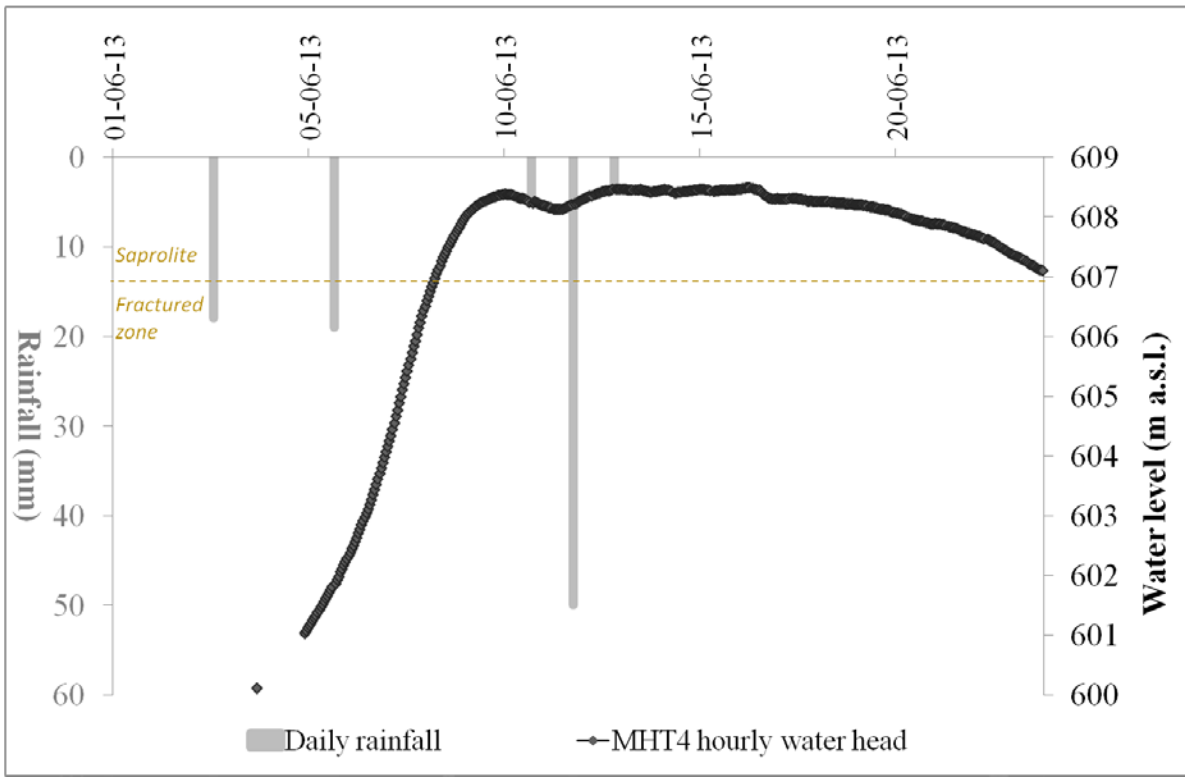

Figure 4-8: Evolution of groundwater levels following rainfall event of different intensity in MHT4 borehole. The limit between the saprolite and the fractured zone (about 607 m a.s.l.) is shown as a dotted line

This specificity should be taken into account while doing the monitoring of the bore wells, since a given rise of the water level can be done by different water volume depending of the local storage capacity.

Weathering maps made from ERT Electrical Resistivity Tomography profiles presented in Boisson et al. (2014 (a)) show that the storage potential of the tank is more important in the southern part of the tank due to a deeper weathering profile.

4.3.4 Impact of Tummulur tank recharge on groundwater quality

Groundwater on the Tummulur site is characterised by elevated salinity (electrical conductivities between 800 and 1 700 µS/cm). Chemical groundwater facies is dominated by Na-HCO_3^- water type (cf. Appendix I) mainly caused by cation exchange, silicate weathering and leaching of fluid inclusions (Siva Soumya et al. 2013). The abundance of major anions is as HCO_3^->SO_4^{2-}>(NO_3^- or Cl^-)>F^- and that of major cations is Na^+>Ca^{2+}>Mg^{2+}>K^+. The sampled groundwater shows concentrations of nitrate and fluoride above permissible limits for drinking water (50 mg/L and 1.5 mg/L, respectively according to the WHO guidelines or 50 mg/L and 1.2 mg/L respectively according to BIS (BIS 2012)).

In the Maheshwaram context (i.e. strong evaporation rates, mineral dissolution of primary F^--containing minerals such as fluorapatite, biotite and epidote, important irrigation return

flow) fluoride is accumulated in groundwater (Pettenati et al. 2013). This accumulation is enhanced by the reduction of Ca^{2+} activity due to calcite precipitation and by Ca^{2+}/Na^{+} exchange mechanism on clay minerals, thus impeding fluorite (CaF_2) precipitation, which is the only efficient mechanism controlling fluoride concentrations (Jacks et al, 2005). As a result of the strong cationic exchanges, most of the groundwater samples show a Na^{+} excess, as seen on a scatter plot comparing the Na+K excess vs Ca+Mg excess ((Na+K)-Cl vs. (Ca+Mg)-(SO4+HCO3) plot, Appendix I). In this geological context, HCO_3^- ions come from the silicate weathering process (Rajesh et al. 2012), and organic matter mineralization leading to high CO_2 content in the soils can significantly increase the HCO_3^- content. High sulphate, nitrate and chloride contents do not come from the water-rock interaction; they mainly have anthropogenic and/or meteorological origin, enhanced by evaporation processes in soils (Rajesh et al. 2012; Siva Soumya et al. 2013).

This incoming surface water has a wide range of effects on groundwater chemistry, depending on both time and space. Electrical conductivities between pre- and post-monsoon samples are quite constant, but have strongly varied during the monsoon (Figure 4-9 and annex 3).

a)

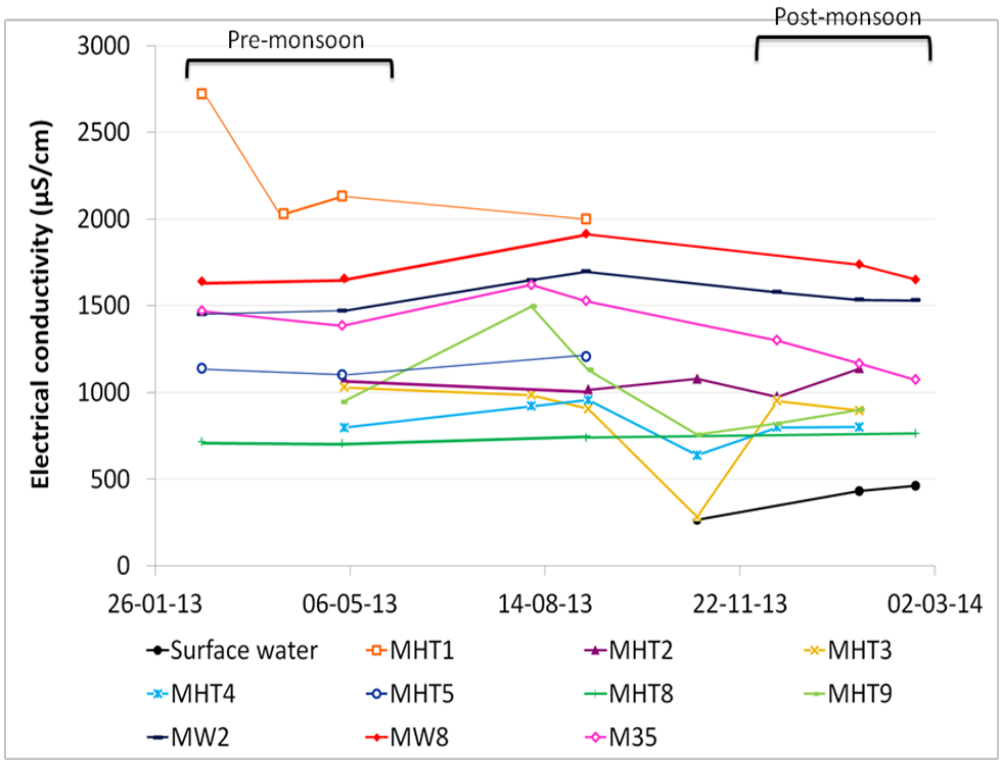

b)

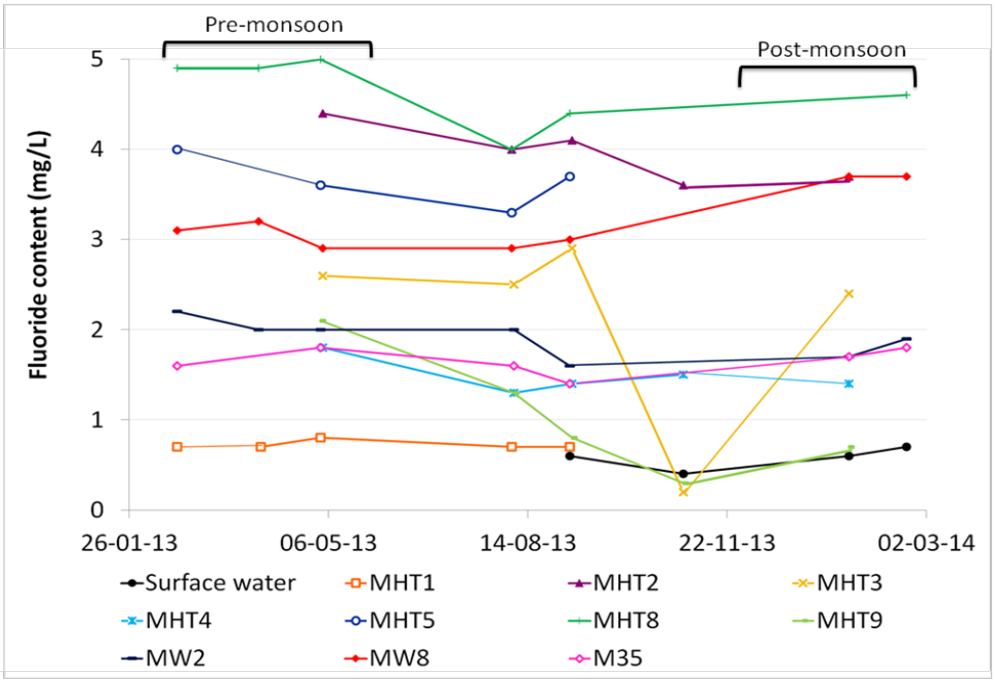

Figure 4-9: a) Electrical conductivities in 10 bore wells and surface water on Tummulur site between February 2013 (pre-monsoon) and February 2014 (post-monsoon). b) Fluoride content evolution in 10 bore wells and surface water on Tummulur site between February 2013 (pre-monsoon) and February 2014 (post-monsoon)

Nitrate, sulphate and chloride values tend to decrease after the monsoon due to dilution, but can significantly increase due to leaching of soil processes (i.e. the chloride content increase in MHT9 during the early stage of the monsoon and the important input of nitrates at the beginning of the monsoon for MHT4 and MHT9 and in the latest stage of the monsoon for MHT2 and MHT3 (see Annex 3, Figure A-3).

Except for MHT9, fluoride concentration do not decrease after the monsoon showing the fluoride content evolution complexity, i.e. an input of fresh water does not lead to its decrease (Figure 4.9b). Quite rapid chemical weathering of F^--bearing minerals and cationic exchanges within clay minerals can occur during the percolation time, in these highly eroded environments (Alazard et al. submitted).

4.3.5 Stable isotopes

Recharge from the Tummulur tank is highlighted by the change in isotopic content ($\delta^{18}O$ and $\delta^{2}H$) of surface- and groundwater between pre- and post-monsoon samples (Figure 4-10). Pre-monsoon groundwater samples (i.e. “dry conditions”) form a line which deviates from the local meteoric water line (LMWL) according to an evaporation line with the same slope value (=4.2) found by Négrel et al. (2011). The LMWL was defined by Kumar et al. (2010) for South India as $\delta^{2}H = 7.82 (\pm 0.17)^* \delta^{18}O + 10:23 (\pm 0.85)$ ‰ vs. VSMOW.

Surface water in February 2014 is much more depleted, because of a strong rain event in October 2013. The rain event of October 2013 was strongly depleted ($\delta^{18}O$ = -13.6 and $\delta^{2}H$ = -99.3 ‰ vs. VSMOW) and plot on the GMWL. Then, surface water in February 2014

strays from the GMWL as it has undergone evaporation. Some post-monsoon groundwater samples deviate from the pre-monsoon values under the influence of the surface water and show values between the “dry conditions” samples and the surface water sample, depending on the rate of surface water mixing.

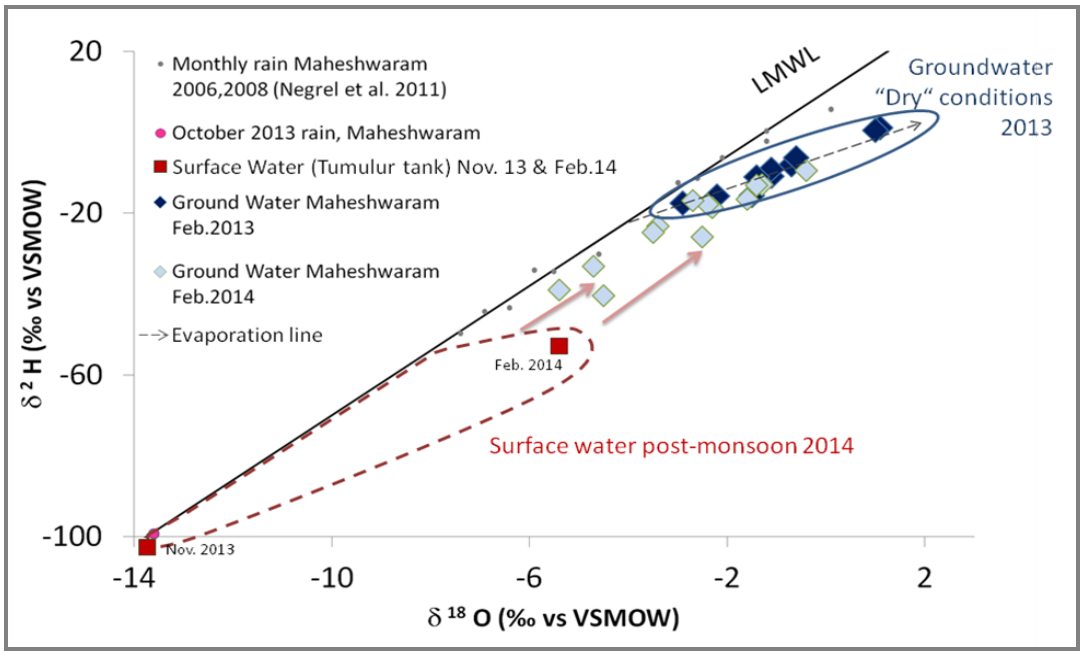

Figure 4-10: $\delta^{18}O$ vs $\delta^{2}H$ (‰ vs. VSMOW) plot of monthly rain in Maheshwaram (Negrel et al. 2011), groundwater (February 2013 and 2014) and Tummulur tank (November 2013 and February 2014). Evaporation line with a slope of 4.2 is shown as dashed lines

4.4 Discussion

This study is in agreement with the existing studies performed on percolation tanks in crystalline rocks aquifers performed in south India. It shows that during average monsoon conditions the ratio percolation/stored water range in general between 56-63 % (Massuel et al. 57 to 63%; Mehta et al. 1997: 57%; Perrin et al. 2009: 56%; Singh et al. 2004: 63%) and can be slightly higher in case of strong monsoon rainfall and high water levels (this study 75% for 2013 monsoon). On watershed scale tank recharge can be neglected (i.e. 2012 monsoon), but may reach 2.6% of the total watershed abstraction in case of strong monsoon (i.e. 2013 monsoon). Results of this study are in agreement with estimates from Perrin et al. (2012) stating that percolation tanks may contribute up to 33% of the total recharge on watershed scale (32 tanks on an 84 km^2 watershed near Gajwel in Andhra Pradesh).

It is important to note that the tank clearly enhances groundwater availability during rainy years (when rainfall and aquifer replenishment are naturally above average), but cannot be considered as a solution to bridge groundwater availability during dry years when aquifer replenishment is low. For this purpose, a careful management of the stored water

in the subsurface is recommended to be performed over several years. This management should include monitoring of water levels and regulation of groundwater abstraction. Moreover, this study shows that long term monitoring should be installed as well as methods for long term water budget calculation. By doing that percolation tanks may also enhance water abstraction at the watershed scale since the farmers adapt their crop to the water availability in crystalline rock aquifers (Fishman et al. 2011; Aulong et al. 2012).

The steep transition in EC logs between pre- and post-monsoon shows the complex flow pattern during recharge. It appears that the aquifer encompasses several water bodies with distinct chemical features, whose connectivity evolves during the recharge processes. This latter point is discussed more detailed in Alazard et al. submitted). It also highlights the existence of different flow paths and that the recharge is not occurring only vertically but has a strong horizontal flow component having an impact on water level fluctuations.

The hydraulic tests point out the strong contrast in storage capacitiy of the different geological layers in the aquifer. Deep fractures may respond rapidly but do not bear large water volumes despite of high increase in water levels. This characteristic may lead to confusion since, most of the time, as observed by Bachelor et al. (2003), the monitoring of percolation tank efficiency is based on the rise of water level in nearby boreholes, without taking into account the specific properties of the geological media.

In hard rock aquifers, it should also be noted that the geological structure might create inequity between farmers during recovery of water. The accessibility is constrained by the connectivity to productive fractures, leading in case of low water level to compartmentalisation of the aquifer (Guihéneuf et al. 2014). Boisson et al. (2014 (a)) show that in the Tummulur case in 2012 only 2 farmers appear to pump 53 to 88% of the stored water for years of low rainfall, while other farmers with boreholes at similar distances to the percolation tank do not benefit at all.

For large planning it is also important to take into account the downstream externalities for the downstream users since the water collected in a given watershed will not flow in the following (Calder et al. 2008).

The water budget presented herein is based on observation and cannot be used for prediction. Simple predictive modelling based on water budget i.e. Boisson et al. (2014 (b)) are efficient, easy to perform and require limited monitoring. However, as observed by Boisson et al. (2014 (a)), recharged volume estimates from surface water balances may tend to overestimate the real effective recharge to the aquifer due to possible storage in the unsaturated zone in comparison with groundwater balances. This may be especially important in case of low monsoon rainfall. More investigation should be carried out on this point to develop guidelines and management policies to help efficiency assessment.

The tank’s impact on water quality is usually considered positive, since it is supposed to dilute contaminants. However, in the case of the geogenic contaminant fluoride, the infiltration of water with a different chemistry may change equilibriums and may tend to release fluoride in the aquifer (Pettenati et al. 2014).

This percolation tank assessment shows that those structures may be, under certain conditions (i.e. above average monsoon) are a possible solution to enhance groundwater availability, but show limited impact during average monsoon years. However, percolation tanks should be carefully considered and guidelines should be defined for assessment and management.

4.5 Conclusions

This report synthesizes the investigations performed on the Tummulur tank through the Saph Pani project. Main conclusions of the investigations are:

- Percolation tanks can be efficient to recharge water in case of high rainfall but have negligible impact on groundwater replenishment in case of low to average monsoon years (i.e below ~750 mm/year).
- Tank replenishment occurs by runoff during few limited rainfall events per year (2-3) of short duration (1-2 days).
- Water recovery in a hard rock aquifer may create inequity between farmers depending to the borehole localisation and connectivity to conductive fractures due to the geological media heterogeneity (details in Boisson et al. submitted and Alazard et al. submitted).
- Percolation tank may locally and temporary enhance water extraction due to increase of paddy field cultivated area and, hence, can have a limited impact on the watershed water balance
- Hydrogeological studies and monitoring networks should be installed to ensure accurate monitoring taking geological heterogeneity (both horizontally and vertically) into account
- Simple guidelines for MAR implementation and monitoring should be developed taking in account the conceptual models presented here
- Infiltration does not systematically improve water quality by dilution (e.g. not for fluoride, see Pettenati et al. 2014). Therefore, careful monitoring on water quality with regard to fluoride should be performed regularly to ensure adequate water quality.

4.6 References

Acworth RI (1987) The development of crystalline basement aquifers in a tropical environment. Q J Eng Geol 20:265-272

Alazard M., Boisson, A., Pettenati M., Dewandel, B., Perrin, J., Picot-Colbeaux, G., Maréchal, JC., Kloppmann, W., Ahmed, S.. Recharge dynamics and flow path investigation through borehole logging in fractured crystalline aquifer in a semi-arid climate. . Implication on MAR and water quality. Submitted to Hydrogeology Journal.

Aulong, S., Chaudhuri, B., Farnier, L., Galab, S., Guerrin, J., Himanshu, H. and Reddy P.P., 2012. Are South Indian farmers adaptable to global change? A case in an Andhra Pradesh catchment basin. Regional Environmental Change, 12(3): 423-436.

Boisson, A., Baisset, M., Alazard, M., Perrin, J., Villesseche, D, Kloppmann, W., Chandra, S., Dewandel, B., Picot-Colbeaux, G., Ahmed, S., Maréchal, JC. 2014. Comparison of surface and groundwater balance approaches in the evaluation of managed aquifer recharge structure: Case of a percolation tank in hard rocks aquifer in India. Journal of Hydrology 519, 1620–1633. doi:10.1016/j.jhydrol.2014.09.022

Boisson, A., Villesseche, D., Baisset, M., Perrin, J., Viossanges, M., Kloppmann, W., Chandra, S., Dewandel, B., Picot-Colbeaux, G., Rangarajan, R., Maréchal, J.C., Ahmed, S., (2014). Questioning the impact and sustainability of percolation tanks as aquifer recharge structures in semi-arid crystalline context, Environmental Earth Sciences DOI 10.1007/s12665-014-3229-2

Boisson, A., N. Guihéneuf , J. Perrin, JC. Maréchal, O.Bour, B. Dewandel, A. Dausse, M. Viossanges, S. Chandra, Estimation of the vertical evolution of hydrodynamic parameters in weathered and fractured crystalline rock aquifers: insights from a detailed study on an instrumented site . Submitted to Hydrogeology Journal

Bour, O., Davy, P., 1998. On the connectivity of three-dimensional fault networks. WaterResources Research 34, 2611{2622.

Calder, I., Gosain, A., Rao, M.S.R.M., Batchelor, C., Snehalatha, M., Bishop, E., 2008. Watershed development in India. 1. Biophysical and societal impacts. Environment, Development and Sustainability 10, 537–557. doi:10.1007/s10668-006-9079-7

Chilton PJ, Foster SSD (1995) Hydrogeological characteristics and water-supply potential of basement aquifers in Tropical Africa. Hydrogeol J 3(1): 3-49

de Dreuzy, J., Davy, P., Bour, O., 2001. Hydraulic properties of two-dimensional random fracture networks following a power law length distribution 1. E_ective connectivity. Water Resources Research 37, 2065{2078.

Dewandel, B., Lachassagne, P., Wyns, R., Maréchal, J.C., Krishnamurthy, N.S., 2006. A generalized 3-D geological and hydrogeological conceptual model of granite aquifers controlled by single or multiphase weathering. J.Hydrol. 330, 260-284.

Dewandel, B., Perrin, J., Ahmed, S., Aulong, S., Hrkal, Z., Lachassagne, P., Samal, S., Massuel, S., 2010 Development of a tool for managing groundwater resources in semi-

arid hard rock regions: application to a rural watershed in South India. Hydrol. Process. 24:2784–2797. doi: 10.1002/hyp.7696

Dillon, P., Gale, I., Contreras, S., Pavelic, P., Evans, R., Ward, J., 2009. Managing aquifer recharge and discharge to sustain irrigation livelihoods under water scarcity and climate change. In: IAHS (Editor), Improving integrated surface and groundwater resources management in a vulnerable changing world. IAHS Publ, pp. 1-12.

Fishman RM, Siegfried T, Raj P, Modi V, Lall U (2011) Over-extraction from shallow bedrock versus deep alluvial aquifers: Reliability versus sustainability considerations for India's groundwater irrigation Water Resour Res 47

Glendenning, C.J., van Ogtrop, F.F., Mishra, A.K., Vervoort, R.W., 2012. Balancing watershed and local scale impacts of rain water harvesting in India - A review. Agric. Water Manage. 107, 1-13.

Guihéneuf, N., Boisson, A., Bour, O., Dewandel, B., Perrin, J., Dausse, A., Viossanges, M., Chandra, S., S. Ahmed, S., Maréchal, J.C. (2014). Groundwater flows in weathered crystalline rocks: impact of piezometric variations and depth-dependent fracture connectivity. J. Hydrol.511: 320-334.

Jacks G., Bhattacharya P., Chaudhary V., Singh K.P. 2005. Controls on the genesis of some high-fluoride groundwaters in India. Appl. Geochem. 20, 221-228.

Marechal, J.C., Dewandel, B., Subrahmanyam, K., 2004. Use of hydraulic tests at different scales to characterize fracture network properties in the weathered-fractured layer of a hard rock aquifer. Water Resour. Res. 40, 11.

Maréchal, J.C., Dewandel, B., Ahmed, S., Galeazzi, L., Zaidi, F.K., 2006. Combined estimation of specific yield and natural recharge in a semi-arid groundwater basin with irrigated agriculture. J. Hydrol. 329, 281-293.

Massuel, S., Perrin, J., Mascre, C., Mohamed, W., Boisson, A. and Ahmed, S. (2014) Managed aquifer recharge in South India: what to expect from small reservoirs in hard rock. J. Hydrol.512: 157-167.

Mayo AL, Morris TH, Peltier S, Petersen EC, Payne K, Holman LS, Tingey D, Fogel T, Black BJ, Gibbs TD (2003) Active and inactive groundwater flow systems: evidence from a stratified, mountainous terrain. GSA Bull 115(12):1456–1472

Négrel P, Pauwels H, Dewandel B, Gandolfi JM, Mascré C, Ahmed S (2011)Understanding groundwater systems and their functioning through the study of stable water isotopes in a hard-rock aquifer (Maheshwaram watershed, India). J. Hydrol. 397: 55–70.

Perrin J, Mascre C, Pauwels H, Ahmed S (2011) Solute recycling: An emerging threat to groundwater quality in southern India? J Hydrol 398(1-2): 144-154.

Perrin, J., Ferrant, S., Massuel, S., Dewandel, B., Maréchal, J.C., Aulong, S. and Ahmed, S., 2012. Assessing water availability in a semi-arid watershed of southern India using a semi-distributed model. Journal of Hydrology, 460: 143-155.

Pettenati M., Perrin J., Pauwels H., Ahmed S. 2013. Simulating fluoride evolution in groundwater using a reactive multicomponent transient transport model: Application to a crystalline aquifer of Southern India. Applied Geochemistry 29, 102–116.

Pettenati M., Picot-Colbeaux, G., Thiéry, D., Boisson, A., Alazard, M., Perrin, J., Dewandel, B., Maréchal, J.C., Ahmed, S., Kloppmann, W. 2014. Water quality evolution during managed aquifer recharge (MAR) in India crystalline basement aquifers: reactive transport modeling in critical zone. (2014) GES - Procedia: Earth and Planetary Science 10: 82-87. DOI: 10.1016/j.proeps.2014.08.016

Picot-Colbeaux, G., Thiéry, D., Pettenati M., Boisson, A., Perrin, J., Sarah, S., Dewandel, B., Maréchal J.C., Ahmed, S., Kloppmann, W. Modeling managed aquifer recharge capacity of crystalline aquifers in semi-arid context (South India): Implementing natural percolation tank dynamics into MARTHE code. Submitted to Hydrogeology Journal.

Rajesh R., Brindha K., Murugan R., Elango L. 2012. Influence of hydrogeochemical processes on temporal changes in groundwater quality in a part of Nalgonda district, Andhra Pradesh, India. Environ Earth Sci 65, 1203–1213.

Sakthivadivel, R., 2007. The groundwater recharge movement in India. In: M. Giordano and K.G. Villholth (Editors), The Agricultural Groundwater Revolution: Opportunities and Threats to Development. CAB International.

Siva Soumya B., Sekhar M., Riotte J., Banerjee A., Braun J.J. 2013. Characterization of groundwater chemistry under the influence of lithologic and anthropogenic factors along a climatic gradient in Upper Cauvery basin, South India. Environ Earth Sci 69, 2311–2335.

Wyns R, Baltassat JM, Lachassagne P, Legtchenko A, Vairon J (2004) Application of proton magnetic resonnace soundings to groundwater reserves mapping in weathered basement rocks (Brittany, France). Bull Soc Géol France 175: 21–34

5 Dug wells at NGRI campus in Hyderabad

5.1 Problem statement and objectives

The campus of the National Geophysical Research Institute (NGRI), India, has a number of functioning dug wells. Due to the development of the Institute and colony within NGRI campus and mushrooming growth of densely populated residential colonies and commercial establishments outside the institute campus, the groundwater extraction from the region has increased over the last two decades. In addition, the above development reduced groundwater recharge by sealing and increased surface run-off and inflow from rainfall events to surface water bodies. This had created stress in the groundwater regime and resulted in a reduction in yield of the wells, which are used for drinking water and gardening purposes, and caused a general reduction in the availability of sustained groundwater supply particularly during summer periods.

The site was chosen for the MAR study within the project amongst others because of the good availability of reliable information on the subsurface. This report is documenting the evaluation of hydrogeophysical and hydrogeological data generated at the NGRI campus with the aim to understand the subsurface regime of natural groundwater replenishment. The investigations had also the objective to define a suitable recharge site for constructing a rain garden in order to improve the sustainable groundwater supply. The dug wells were used to verify its recharge capacities. The investigations included rainfall analysis, determination of vadose zone hydraulic properties (infiltration tests, soil moisture measurements, soil sampling etc.), time lapse resistivity measurements, compilation of groundwater level, constructing water table maps and evaluation of existing data.

5.2 Site description

The watershed around NGRI campus has a surface area of 13 km^2 and includes a combination of rurally developed areas and urbanized parts. The chosen case study site is the NGRI campus which is a small part of the watershed (Figure 5-1). While north of the campus the city is highly urbanised, south from the campus still large open spaces exist.

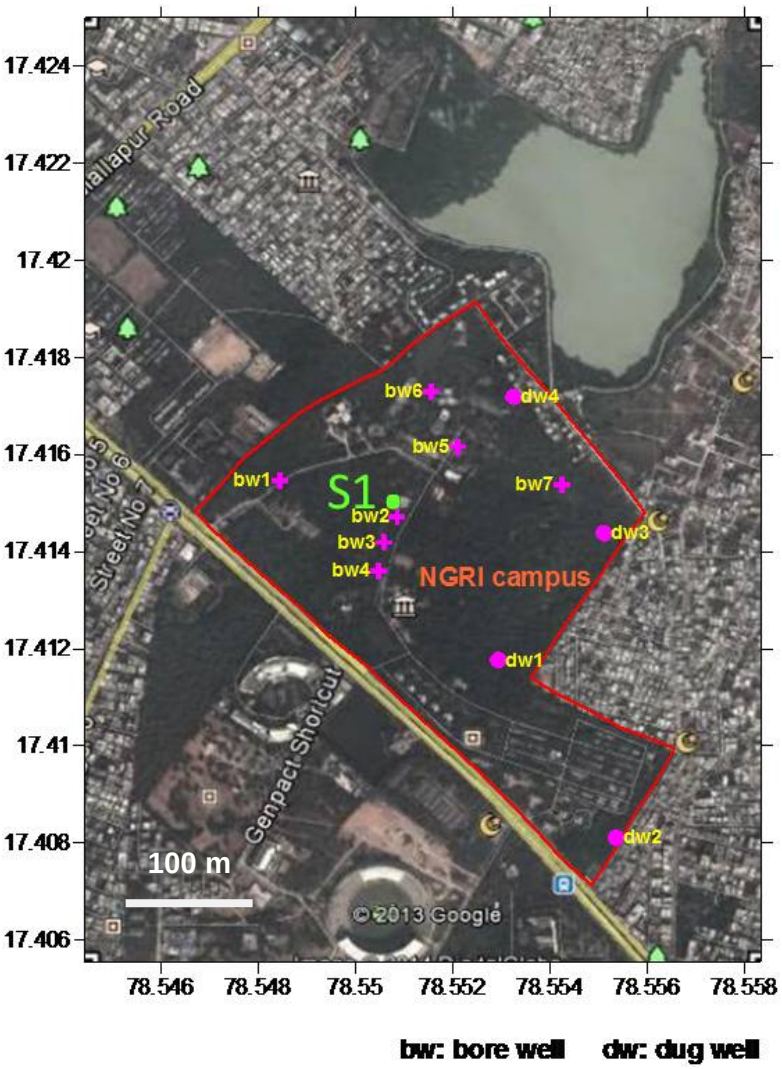

Figure 5-1: Map of the study area at NGRI campus and location of dug- and bore wells

Geologically, the study area is situated on a granitic formation of about 10 m thickness covered by a 0 to 30 m thick weathered rock layer. The soil thickness in the whole area varies between less than a meter to four meters (Figure 5-2).

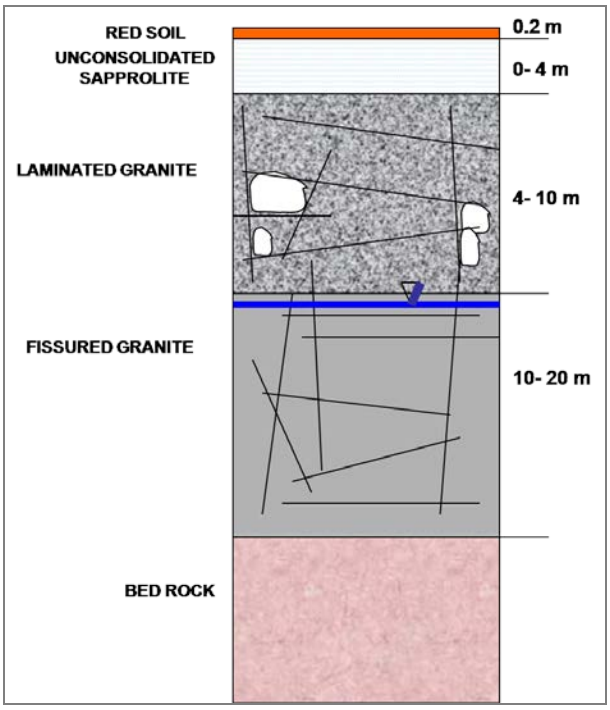

Figure 5-2: General lithology of the study area (modified after Arora (2008))

The natural hydrographical network has been considerably changed by the rapid urban development in recent years. All drains are perennial and feed the river Musi, situated two kilometres south of the study area. This river also transports the wastewater from the city of Hyderabad.

Groundwater occurs under phreatic conditions in the weathered zone and under semi-confined to confined conditions in the weathered-fractured and fractured zones. The pre- and post-monsoon groundwater level varies from 5-11 mbgl and 3-9 mbgl respectively with the water level fluctuation of 5-6 m. Its inhabitants, institutes and industries intensively exploit the groundwater in the watershed. Engerrand (2002) quantified the withdrawal rates for a 40-years period from 1961 to 2001. In spite of the heavy withdrawal of 11,000 m^3 per day, the water levels do not seem to be falling much in the watershed. Further groundwater level data were obtained from selected observation wells at the NGRI campus during 2012-13.

Average annual and seasonal rainfall (July to September) at the NGRI campus site is 746 mm and 707 mm, respectively. The seasonal rainfall contributes about 94 % of total rainfall and is characterized by several moderate rainfall events (> 20 mm/d) and few moderate to high-intensity rainfall events (>40 mm/d) occurring during monsoon months.

It was observed that during high intensity rainfall events in the neighbouring area, significant inflow occurred at a few places within the NGRI campus area. To improve the augmentation of groundwater resources, a check dam across a small stream to the northern side of the campus along BW 4 and three rain gardens near the site BW 3 were constructed within the campus area.

5.3 Results and interpretation

5.3.1 Rainfall and groundwater levels

The rainfall and water level data at the study site showed a correlation with 88 % concordance indicating that rainfall events are the major source of natural groundwater recharge. As Figure 5-3 shows, a high number of rainfall events results in an increasing water level (given in meter below ground level).

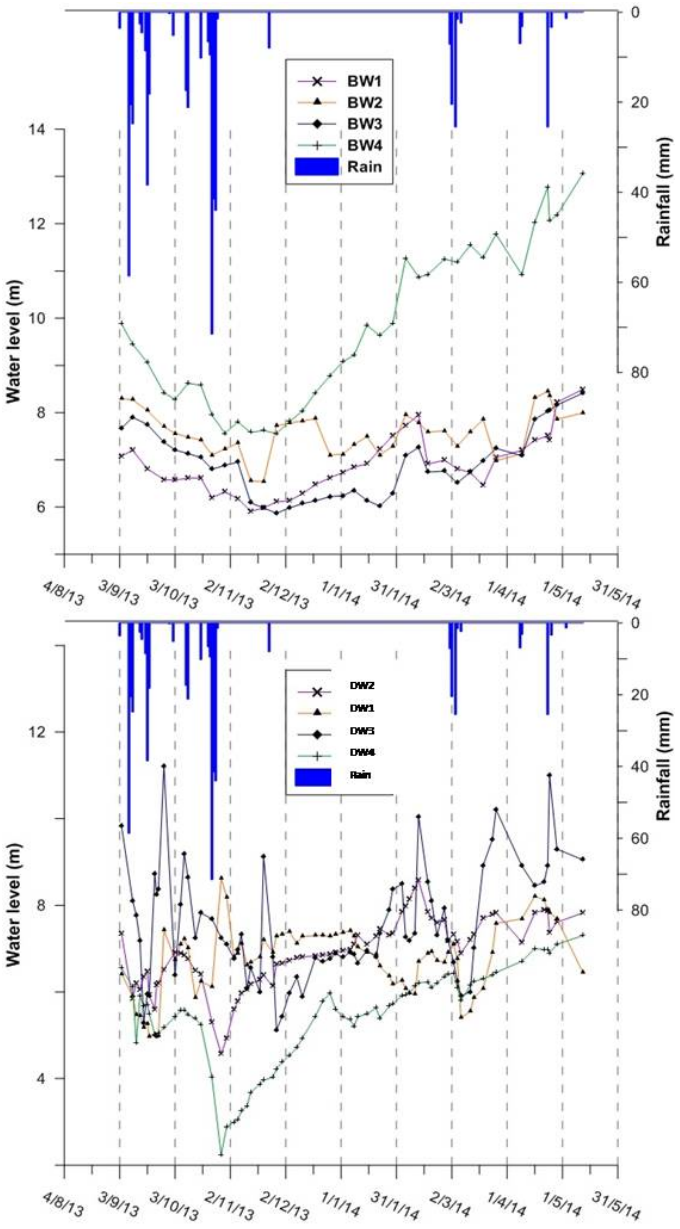

Figure 5-3: Hydrograph of the study area for the monsoonal cycle of 2013-2014; a) bore wells, b) dug wells

5.3.1 Water level maps

Seasonal water level measurements were taken to quantify the impact of the existing recharge structures for groundwater augmentation. The measurements involved 11 observation wells and four campaigns for a time period of November 2012 to August 2013. The data were used to draw contour maps of the groundwater table (Figure 5-4).

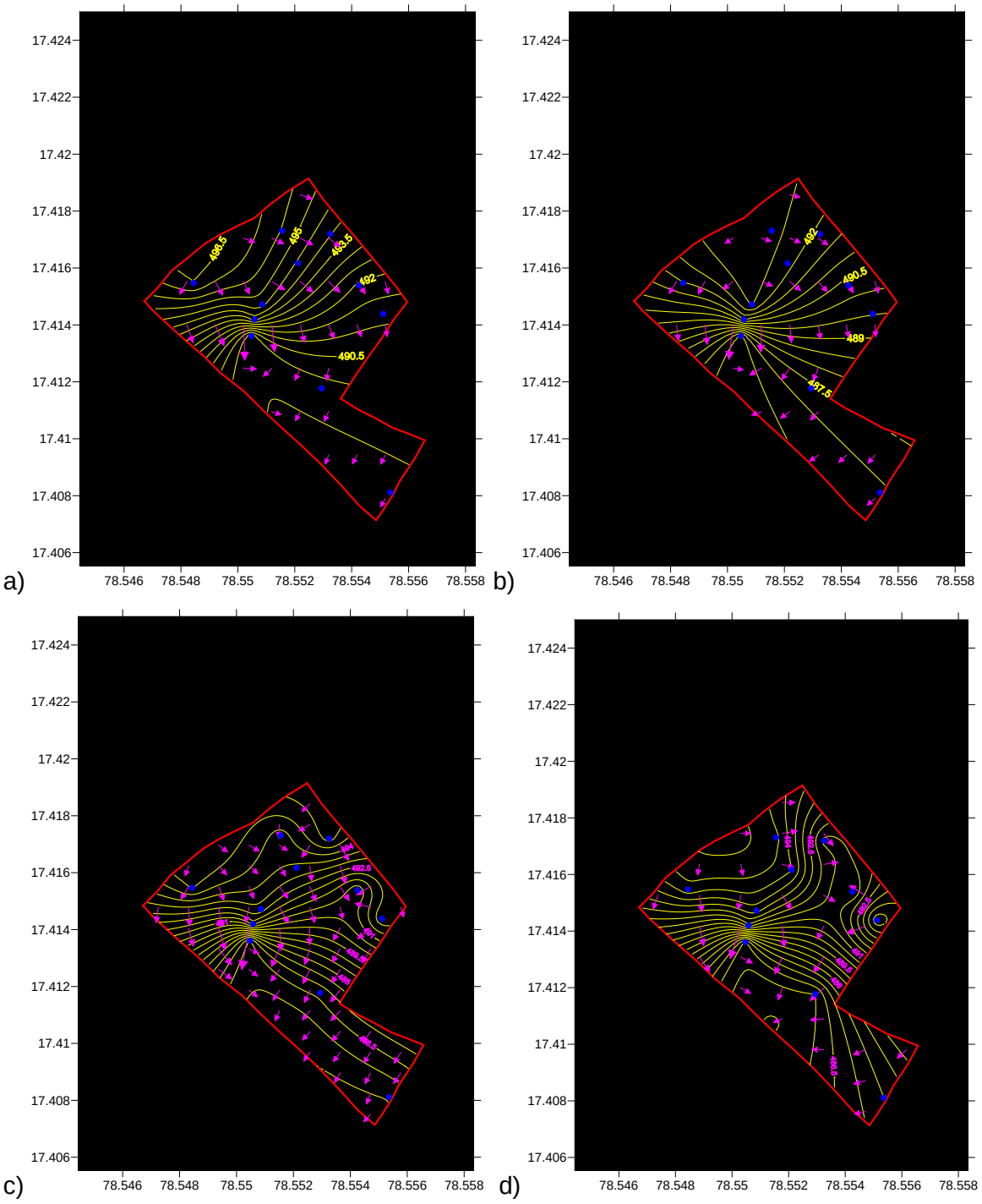

Figure 5-4: Groundwater level contour maps of a) November 2012, b) April 2013, c) July 2013, d) August 2013

The contour maps indicate that the pattern of groundwater flow is similar throughout the year: predominant groundwater flow from north to south in the northern part of the area and towards southwest and west in the southern part of the area.

5.3.2 Determination of soil infiltration rates

To determine the infiltration rate into the soil, repeated double-ring infiltrometer tests were carried out at three locations at the campus. A double ring infiltrometer with a diameter of 0.3 m for the outer ring and 0.2 m for the inner ring was pressed into the soil up to a depth of 10 cm. The rings were driven without tilt or undue disturbance of the soil surface and with constant annular space between the rings in all directions. Long-term infiltration rate measurements were carried out at four locations at the experimental site area along a line, each separated by a distance of about 20 meter.

Figure 5-5 shows the results of the measurements for the month of July 2013. The basic infiltration rate was calculated from the relationship between resistivity and soil moisture given by Arora (2008). From the obtained electrical resistivity and soil moisture data, recharge was calculated to be 92 mm/hr (Arora 2008).

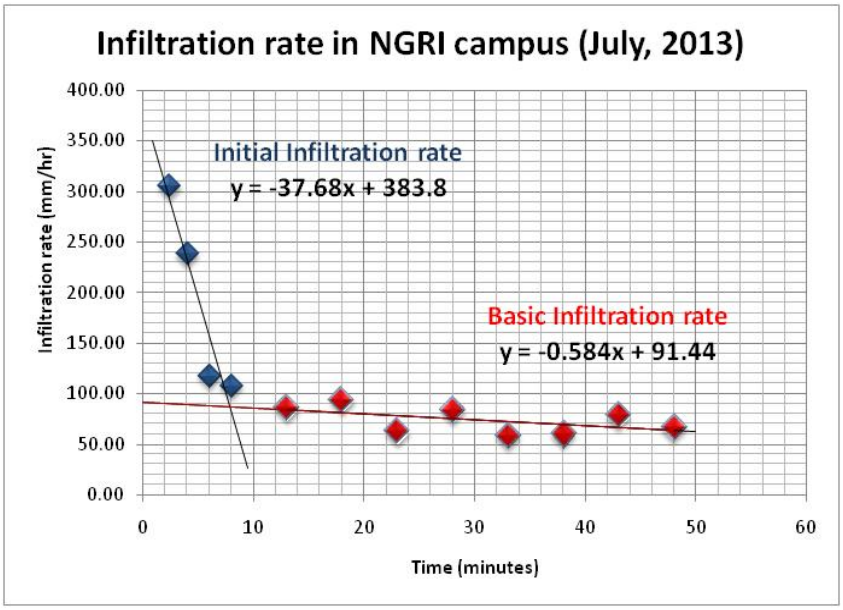

Figure 5-5: Initial and basic infiltration rates of the study area for July 2013

Results interpretation further showed that the infiltration rate varied from 2.1 to 6.3 m/d (Table 5-1).

Table 5-1: Summary of infiltration and percolation rate at infiltration test sites

Site no.	Location	Stabilized Infiltration rate (mm/hr)	Stabilized Infiltration rate (m/d)
1	Near magnetic obs1	263	6.3
2	Near magnetic obs2	169	4.1
3	Near magnetic obs3	85	2.1

5.3.3 Electrical Resistivity Tomography (ERT)

Because the electrical conductivity of a medium depends on its water saturation, the natural recharge due to infiltration can be monitored by measuring the electrical resistivity within the unsaturated zone. Time Lapse Electrical Resistivity Tomography (TLERT) measurement data were used to get information about subsurface flow and moisture movement in the unsaturated zone in order to evaluate zones of preferential natural groundwater recharge. The resistivity logs were further used to refine the lithology of the study area.

Published data from Arora and Ahmed (2010 and 2011) for the monsoon cycle of 2005 were taken and further improved for analysis. Their measurements covered the unsaturated zone up to a depth of 12 m at the two sites S1 and S2 (approximately 300 m apart) along two profiles of 96 m and 72 m length (P1 and P2) with an electrode spacing of 2 m and 1.5 m respectively. Resistivity measurements were carried out with the resistivity meter Syscal R1 Junior (IRIS Instruments, Orléans, France) equipped with 48 electrodes. The electrodes remained on the soil surface during all the experiment time to avoid any electrode polarization changes and to ensure a best quality of measurements.

The resistivity data were processed and interpreted with the help of RES2DINV software developed by Loke and Barker (1996) following an iterative optimization approach. The resulting tomograms of the data acquired between 15th October 2004 (post monsoon of 2004) and 15th October 2005 (during the monsoon period of 2005) at site S1 were further analyzed for the soil water content in the scope of this study and interpreted with regard to the movement of the water infiltration front. Figure 5-6 shows the tomograms of the time period 12th July 2005 (g) to 11th September 2005 (m). Thereby, low electrical resistivity corresponds to increased soil water content and the subsequent plots (g to m) show the change in resistivity from one time-step to another. The observed changes indicated both, a vertical and horizontal movement of infiltrating water.

Quantitatively the percent differences in electrical resistivity's associated with the arrival of the recharge match the recharge measurement fairly well both in time and space. Between 20 m and 42 m along profile S1P1 (Figure 5-6), a non-uniform distribution of moisture in the vertical profile following the infiltration after a rainfall event indicated a zone of preferential natural recharge. Between 68 m and 76 m along profile the passage

S1P2, the variation in resistivity is most presumably due to different geological materials exhibiting different porosities.

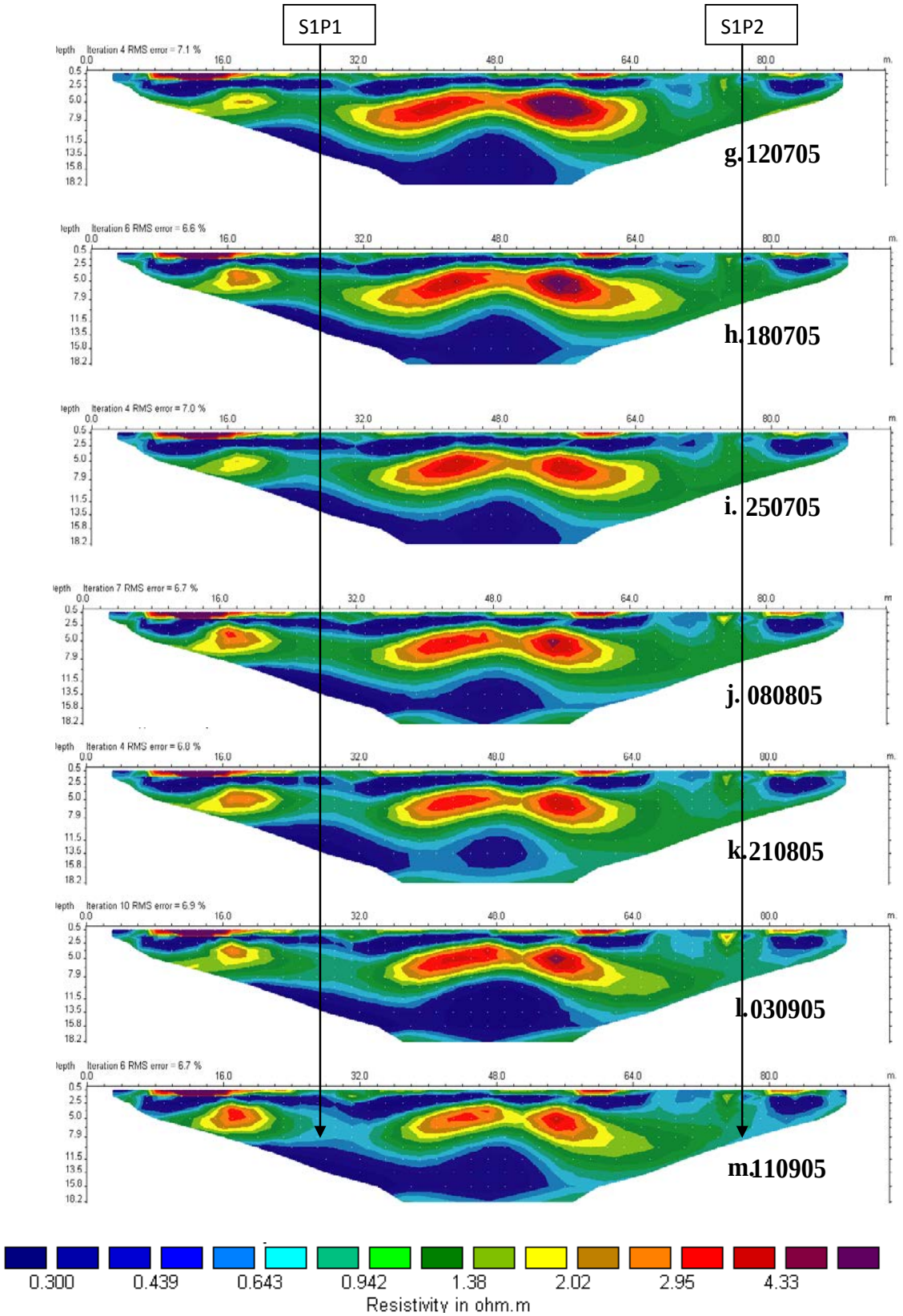

Figure 5-6: 2D inverted resistivity models for the time-lapse experiment carried out in the study area for the monsoon cycle of 2005 (labelled from g-m) (modified after Arora and Ahmed 2010)

After the time lapse experiment and observing the water level fluctuations in the well BW3, it was recommended to construct rain gardens. In total, three rain gardens (not shown in maps) were constructed up to a depth of 1.2 m from the surface in order to enhance groundwater recharge.

Figure 5-7: Rain gardens constructed in the upstream side of the NGRI Campus after the results of the time lapse experiment. The monitoring bore well BW3 is within this site, but outside the rain garden

TLERT showed that the resistivity was constant with time and that the method is reliable and sufficient to represent the depth profile. This also confirmed and justified the most common application of Electrical Resistivity methods for groundwater prospecting. The effect of rainfall recharge on the resistivity could be observed and the vertical and horizontal components of moisture movement through the unsaturated zone could be mapped.

5.4 Conclusions

The study area has a thick weathered / weathered-fractured zone up to the depth of 40 m followed by fresh granite rock with fracture zones. The deep fracture zones are moderately yielding compared to shallow weathered fractured zones.

The stabilized infiltration rate at three locations measured using double ring infiltrometer showed that the infiltration rate varied from 2.0 to 6.3 m/d. Laboratory permeability measurements carried out using constant head permeameter showed that the saturated permeability varied from 0.03 m/d to 0.39 m/d. A linear relation between infiltration rate and saturated permeability coefficient was observed with a correlation coefficient of 0.82. The unsaturated zone of the granitic terrain was investigated and analyzed using comparatively simple approaches such as geophysical analytical methods like TLERT and soil moisture measurements. Based on TLERT measurements and groundwater level monitoring within the dug wells a suitable site for construction of the rain gardens was recommended.

5.5 References

Arora, T (2013) Hydrogeophysical characterization of unsaturated zone, Lambert Academic Publications, ISBN 978-659-43870-7

Arora, T, Ahmed, S. (2011) Characterization of recharge through complex vadose zone of a granitic aquifer by time-lapse electrical resistivity tomography. Journal of Applied Geophysics, 73, 35-44

Arora, T, Ahmed, S. (2010) Electrical structure of an unsaturated zone related to hard rock aquifer, Current Science, 99 (2).

Arora, T (2008) Geophysics and Geostatistics: An integrated approach to characterize and monitor the unsaturated zone, Unpublished thesis.

Engerrand, C (2002) Hydrogéologie des socles cristallins fissurés à fort recouvrement d'altérites en régime de mousson: étude hydrogéologique de deux bassins versants situés en Andhra Pradesh (Inde). Thèse de doctorat, Université Paris VI

Loke, M.H., Barker, (1996) Practical Techniques For 3 D Resistivity Survey And Data Inversion, Geophysical Prospecting, 44, 499-523

Rangarajan R., Shankar, G.B.K., Rajeshwar, K., Venkatesam, V., Arora, T., Ahmed, S. (2014) Enhancement of natural water systems and treatment methods for safe and sustainable water supply in India, NGRI Technical Report (unpublished)

6 Urban storm water management in Raipur

6.1 Problem statement and objectives

Raipur city has a number of lakes of varying sizes, locally called *talab*, which encounter deteriorating water quality due to the dumping of municipal solid and liquid waste. Managed aquifer recharge (MAR) using existing *talabs* and proposed new MAR structures at the test sites of Raipur are expected to counteract decreasing groundwater levels caused by over-exploitation. As pilot cases, the Telibandha Lake located in the Raipur city area and Telibandha area located in the sprawling city area have been chosen for a MAR feasibility study. The Telibandha lake case envisaged the investigation of different aspects of utilization of the lake water for MAR, while studying of the Telibandha area envisaged the conservation of surface runoff for MAR.

The Central Ground Water Board (CGWB) in Raipur has shown a keen interest in the research and development of technological expertise for building MAR structures at an appropriate place and to develop the structure of appropriate sizes. Thereby, CGWB has undertaken extensive geophysical surveys in order to know the structures and the broad lithology of the area. In parallel, the National Geophysical Research Institute (NGRI) also undertook an extensive geophysical study to investigate the general geology of the area.

The case studies presented here include climatic, hydrologic, topographic, geologic, hydrogeological, and water quality data that have been analyzed thoroughly with the following objectives:

- to assess the storm water infiltration potential and its effect on groundwater quality
- to derive recommendation of measures to enhance lake water quality and improve the infiltration capacity of exisiting *talabs*

In addition, this case study provides recommendations for carrying out geophysical (ERT) studies to delineate the subsurface geology and groundwater potential zones.

6.2 Site description

Geologically, Raipur is situated in the southern part of the Chhattisgarh basin, which is of Proterozoic age. It is mainly underlain by sedimentary formations of the Chhattisgarh Supergroup and crystalline rocks of Archean age except along riverbanks, where recent alluvium deposits are found in isolated patches. The Raipur group is a Karst Aquifer system, represented by the Chandi Limestone and Deonagar Shale of the Chhattisgarh Super Group formation. The Raipur limestone is a grey, fine-grained, horizontally bedded, stromatolitic, massive limestone. While the primary porosity is negligible (Bodhankar and Chatterjee 1994), it has a distinct secondary porosity due to joints and karstification, which is supposed to occur in two horizons in Raipur city (Mukherjee et al. 2011).

Topographically, the relief is not very high with a slight slope towards northeast and towards the Kharun River in the west, thus forming a radial pattern drainage system emerging from elevated areas of the city (Figure 6-1). The elevation varies from 220 to 340 m. The land use pattern indicates that 42% of the area is occupied by agricultural land.

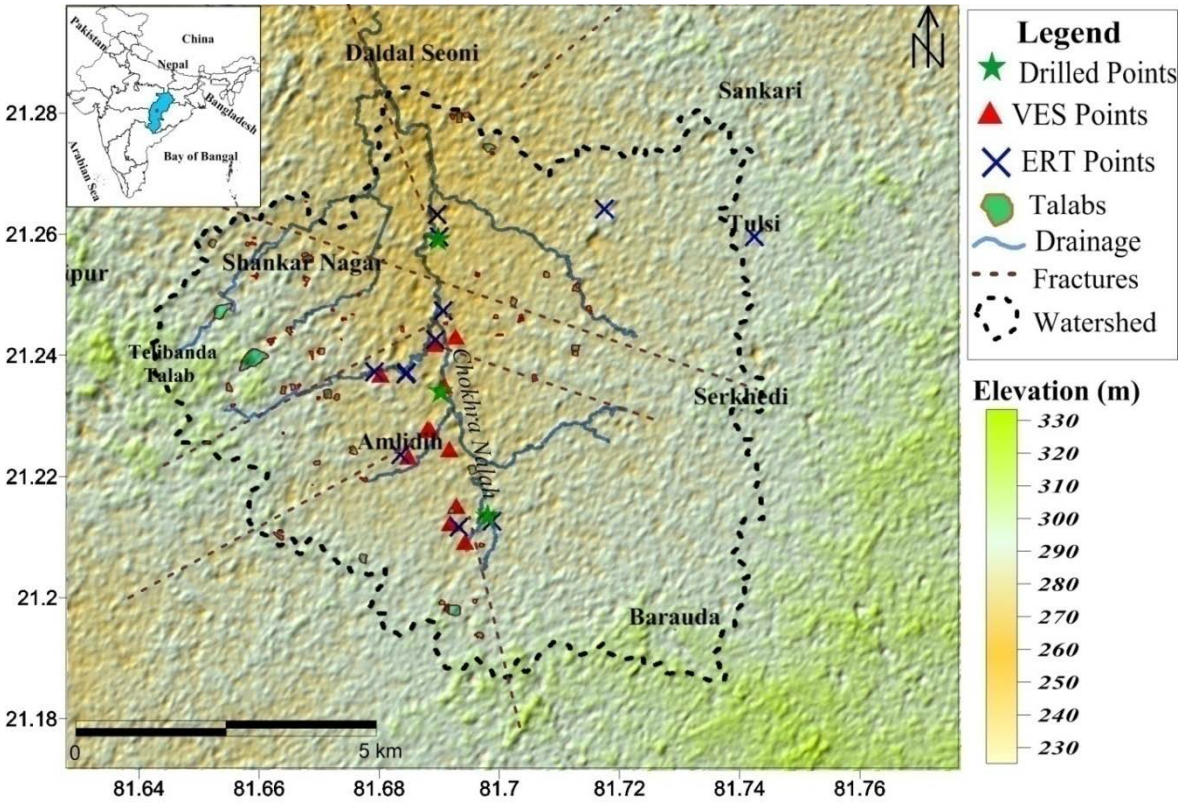

Figure 6-1: Drainage pattern of the Telibandha area and location of Electrical Resistivity Tomography (ERT) profiles and Vertical Electrical Soundings (VES) points

The only aquifer with sufficient volume is the limestone aquifer. Other aquifers consist mainly of deeply weathered shale and sandstone rocks, which are very thin and thus have a low spatial extent. Groundwater occurs in shallow aquifers and under semi-confined to confined conditions in the deeper fractured and cavernous aquifer of the Chhattisgarh succession. The depth of water level varies from 2 m to 13 m below ground surface (mbgs) during pre-monsoon and from 0.1 to 7 mbgs during post-monsoon period in the shallow aquifers. The long term (1995-2005) trend of water level development indicates that about 18% of the wells in the pre-monsoon and 2.6% of the wells in the post-monsoon period show a significant (20 cm/year) decrease in water level (CGWB, 2007).

6.3 Results and interpretation

6.3.1 Digital Elevation Model

A Digital Elevation Model (DEM) from ASTER (Advanced Spaceborne Thermal Emission and Reflection Radiometer) of 30 x 30 m resolution was used for topographic

interpretation. Watershed and drainage were delineated using the Spatial Analysis Toolbox of ArcGIS software. The lineaments were digitized from the shaded relief maps of DEM with different sun angle (see Figure 6-1).

6.3.2 Vertical Electrical Sounding

In a field survey, a total of 12 Vertical Electrical Sounding (VES) profiles were recorded (for methodology, please see Arora et al. 2013). Figure 6-2 shows the resistivity values for layers from different depths interpreted using 1X-1D software (www.interprix.com). There, blue colour indicates a low resistivity (5-200 ohm m) whereas the red colour indicates high resistivity of the order of 2000-3000 ohm m.

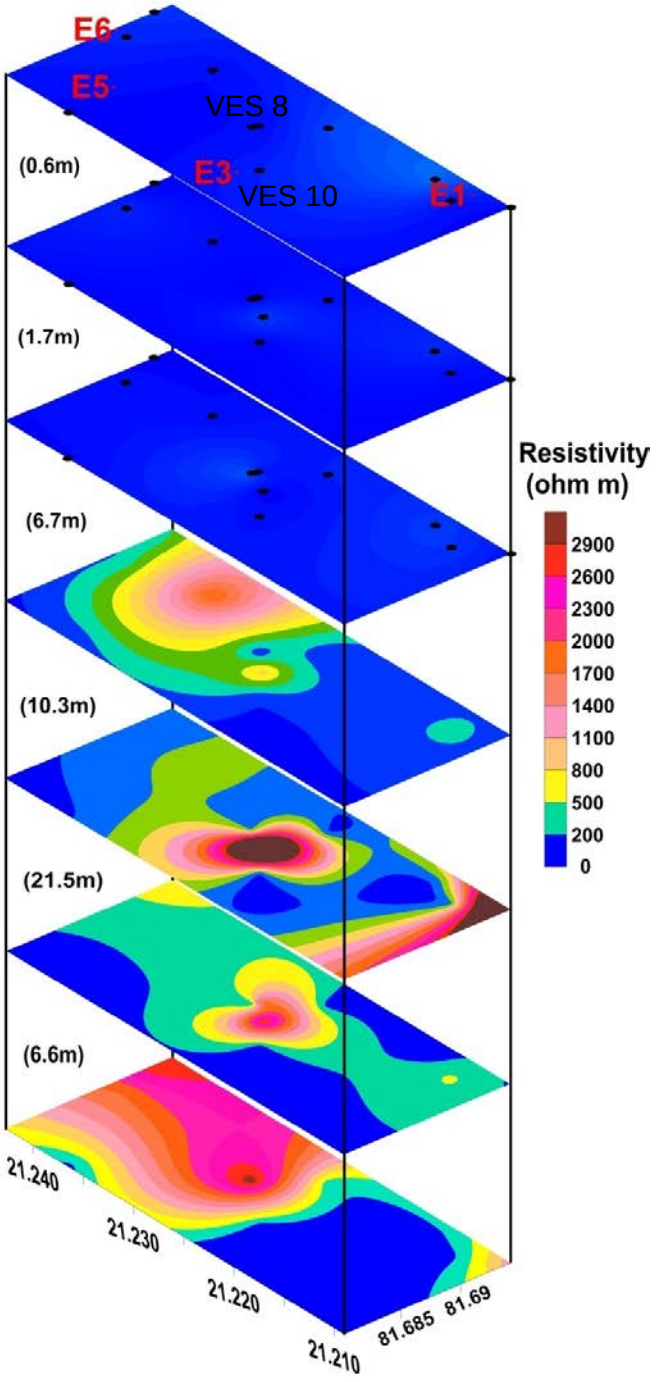

Figure 6-2: Results of Vertical Electrical Sounding(VES) at different depths. The black dots are the location point of the VES as shown in the base map

The profiles show a sharp transition zone at the depth of 2.3 m. The deeper layers show that the high resistivity value concentrates towards the VES 8 (which is in the centre of the upper graph). This shift gives an indication of some existing paleochannel between points VES8 and VES10 or some weak structure, as it would be typical for a Karst Aquifer system. Accordingly, the area around VES8 may be a suitable site for recharge.

6.3.3 Electrical Resistivity Tomography

Electrical Resistivity Tomography (ERT) was carried out along 12 selected areas in and around Telibandha lake region (see Figure 6-1). Methodology and procedure is described in Saph Pani Deliverable 2.2 (Boisson et al., 2013).

Exemplarily, the results for Station 1: AMLIDHI, (N 21° 12’ 49.9”, E 81°41’ 50.5”) are given. The profile was laid down in NNW-SSE direction along 480 m with electrode spacing of 10 m. The Wenner-Schlumberger array was used to survey the profile. A total number of 529 datum points were measured at 23 data levels, allowing to plot a pseudosection (Figure 6-3).The results clearly represents the layered structure of the limestone in the subsurface. Resistivity varied with the water content showing a thick layer of 15-20 m thickness of damp limestone with resistivity varying between 50-150 ohm-m at the depth of 5 m and up to 90 m with high resistivity of more than 300 ohm-m of dry limestone below.

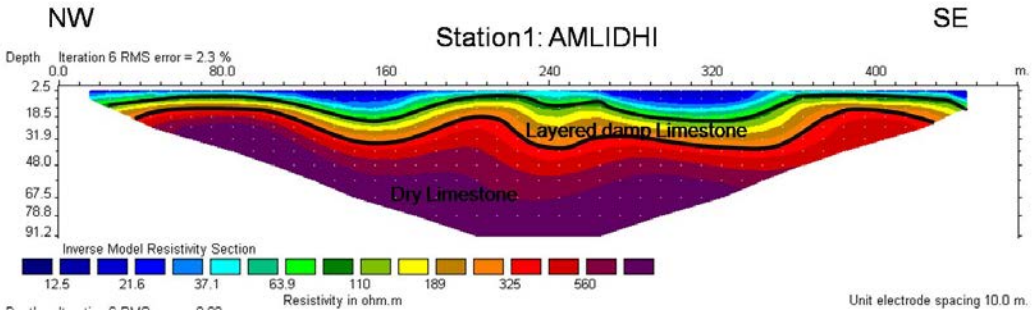

Figure 6-3: Electrical Resistivity Tomogram at station 1 at Amlidhi

6.3.4 Drilling of wells

The litholog data of three boreholes (Figure 6-4) gave a clear understanding of the subsurface geology of the limestone aquifer. The aquifer is overlain by a top black soil layer with 1-6 m thickness, high clay content, soil nodules (Kanker) and rich in iron. Below this layer is the flaggy limestone with high clay content reaching down to the fresh limestone. This weathering zone above the limestone is generally ~6 m thick. Below this zone, fresh limestone is encountered, where two fracture zones and solution activity is observed mostly in the central part of the watershed. The solution channels are mainly filled with sediments/soils and indicate their collapsed nature, which can also be related to the presence of solution-type features on the surface and presence of more surface ponds/ talabs. The fresh black limestone up to about 40 m depth has two fracture zones with high groundwater yield and two zones showing little solution activity indicating the effect of karstification processes in the limestone. The solution weathering in other layers was found to be insignificant. The results will be used to analyze the secondary porosity at a particular site to assess the quantity pore spaces available for recharging and storing water.

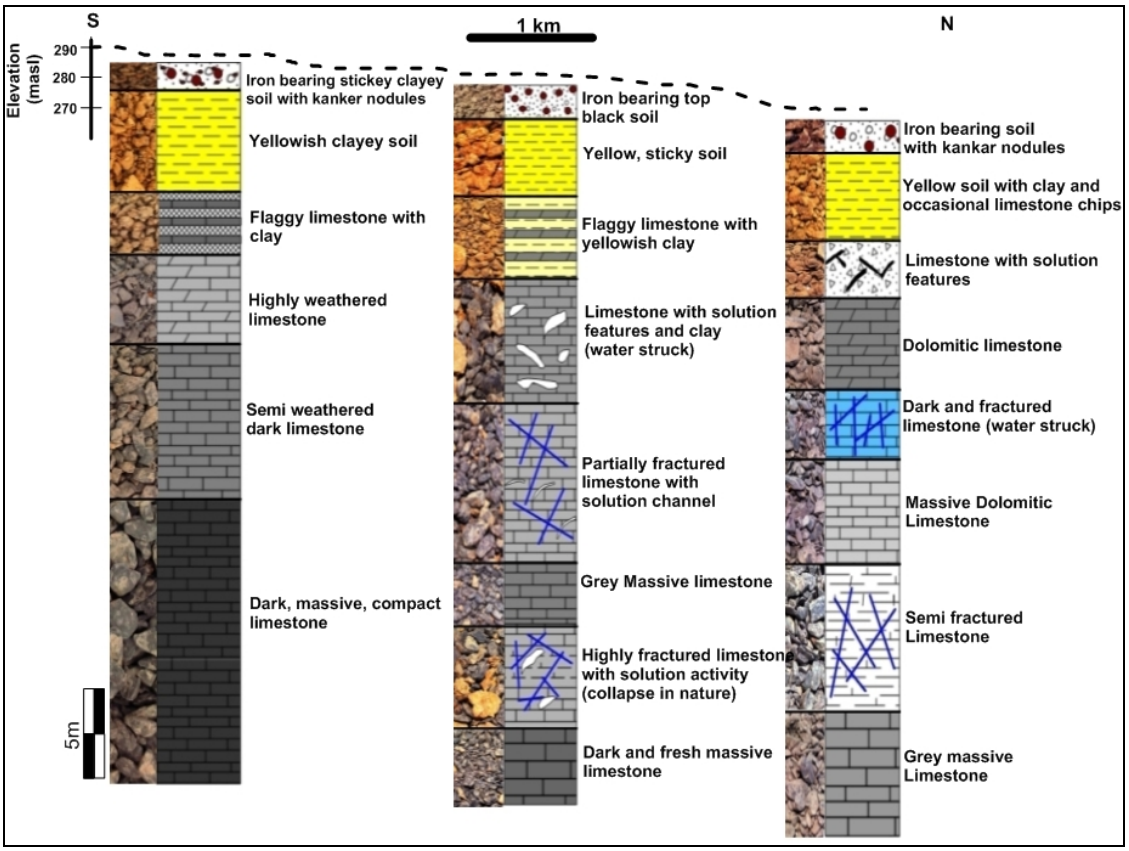

Figure 6-4: Lithologs of three bore wells drilled in the watershed. The location of drill points is shown in the base location map (Figure 6-1). Dashed line on top indicates the surface elevation in meters from well to well. Thick horizontal line at top of the figure is horizontal scale. S and N represent north and south directions

6.3.5 Water quality assessment

Raipur city has no planned treatment facilities for treating municipal effluents. Thus, the effluents are mainly drained into the depressed areas, surface water bodies and talabs through the local drainage systems. The lakes, which have limestone as underneath formation, pose a risk for the limestone aquifers as they are highly vulnerable to pollution because of their high storativity and hydraulic conductivity.

To ascertain the lake water quality, two sampling campaigns, one in the pre-monsoon and another in the post monsoon season, were carried out. Water sampling also included a number of dug and tube wells around the Telibandha Lake to assess the status of groundwater quality and the Kharun River that flows towards N-W direction and receives the city's effluents in many locations (Figure 6-5 and Figure 6-1).All samples were analyzed for: pH, EC, total dissolved solids (TDS), hardness, calcium, magnesium, sodium, potassium, iron, manganese, alkalinity, bi-carbonate, nitrate, sulphate, chloride, fluoride, DO, COD, BOD, faecal and total coliforms.

Results of the water quality analyses are given in annex 2. The parameters, which exceed the permissible limit of the BIS-standards (IS 10500:2012) for drinking water are highlighted.

Except bacteriological parameters (viz. Fecal coliform and Total coliform), turbidity and to a reasonable extent COD, Telibandha lake water meets the BIS drinking water quality standards. In case of drinking water, water constituents have to be free from any bacteriological contamination. The groundwater quality is also largely found to be safe except few water quality constituents in almost all wells excluding few dug wells and tube wells. The Kharun River water quality is seen to be satisfying the drinking water quality standards except turbidity and bacteriological contamination.

Table 6-1: ID and coordinates of water sampling sites

Sample ID	Name of location	Latitude	Longitude
DW 1	Jal Vihar	21°14'14.10"	81°39'21.20"
DW 2	Jal Vihar	21°14'13.84"	81°39'22.80"
DW 3	Anand Nagar	21°14'37.30"	81°39'33.50"
DW 4	Anand Nagar	21°14'32.10"	81°39'35.80"
DW 5	Anand Nagar	21°14'32.20"	81°39'35.70"
DW 6	Satnamimohalla	21°14'22.98"	81°40'1.92"
TW	Anand Nagar	21°14'36.90"	81°39'37.70"
HP	Jal Vihar	21°14'9.60"	81°39'25.40"
TL	Teliabandha Lake	21°14'19.06"	81°39'30.70"
KR	Kharun River	21°12'18.90"	81°36'14.70"

DW - Dug well; TW- Tube well; HP- Hand Pump; TL– Telibandha Lake; KR-Kharun River

Figure 6-5: Locations of the sampling sites in and around Telibandha Lake, Raipur

6.3.6 Lake water level analysis

In order to ascertain the variation of water level in the Telibandha Lake, its water level was monitored weekly for the period from 20th June 2013 to January 2014. The variation of water levels is shown in Figure 6-6. The maximum depth of water of 3.36 m was observed in September 2013 and the minimum depth of 2.83 m in January 2014. These data were used to verify the water balance components of the lake.

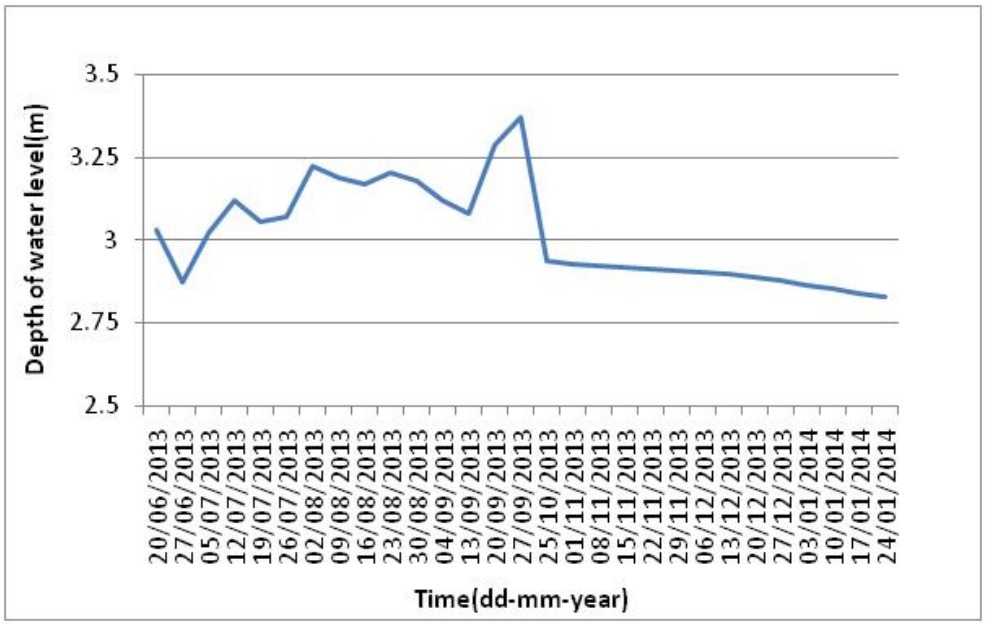

Figure 6-6: Variation of depth of water in the Telibandhalake measured during June, 2013 – January, 2014

6.3.7 Computation of groundwater recharge and lake water depth

To compute the unsteady groundwater recharge from variable inflows and outflows to/from the lake, the basic water balance equation as given below was used:

$$[Q_i(t) + A\,R(t)\,]\Delta t - [Q_o(t) + A_i(t)\,E_{vp}(t) + Q_{gw}(t)]\,\Delta t = \Delta V(t) \qquad \text{(Eq. 1)}$$

in which,

$Q_i(t)$ is the inflow rate from the lake catchment to the lake at time t [$L^3\ T^{-1}$]; A is the gross surface area of the lake [L^2]; R(t) is the rainfall rate at time t [LT^{-1}]; $Q_0(t)$ is the outflow rate from the lake at time t [L^3T^{-1}]; $A_i(t)$ is the water surface area of the lake at time t [L^2]; $E_{vp}(t)$ is the water surface evaporation rate at time t [LT^{-1}]; $Q_{gw}(t)$ is the groundwater recharge rate from the lake at time t [L^3T^{-1}]; $\Delta V(t)$ is the change in storage between time t and t +Δt [L^3]; Δt is the time step size, [T].

For deriving an expression of the groundwater recharge component, $Q_{gw}(t)$, as a function of hydraulic head, Hantush (1967) approximate analytical equation for the rise of water table due to uniform percolation of water from a spreading basin in a homogeneous and isotropic unconfined aquifer of infinite areal extent in absence of a pumping well is integrated into eq.(1).

The Hantush's expression is given by:

$$h(x,y,t) = \left(\frac{w\,t}{4\,S}\right) f(x,y,t) \qquad \textit{(Eq. 2)}$$

in which,

$h(x,y,t)$ is the rise in groundwater table below the rectangular spreading basin at location x, y [L]; w is the constant rate of percolation per unit area [LT^{-1}]; *S* is the storage coefficient of the aquifer [dimensionless]; t is the time since the percolated water joins the water table [T]; and f(x,y,t) is the analytical expression derived by Hantush (1967).

The average rise in water table, $\bar{h}(t)$, in terms of discrete time steps of Δt, from a train of pulse recharge is derived as:

$$\bar{h}(n\Delta t) = \sum_{\gamma=1}^{n} \frac{Q_{gw}(\gamma\Delta t)}{4\,a\,b}\ \delta_r(n-\gamma+1,\Delta t) \qquad \textit{(Eq. 3)}$$

in which

a is half of the length and b is half of the width of the rectangular basin.

Assuming a linear relationship between the influent seepage and potential difference, seepage during n^{th} unit time step is expressed using Darcy's equation, as:

$$Q_{gw}(n\Delta t) = \frac{4\,a\,b\,k_v\Delta t\left[H+\bar{D}(n\Delta t)-h_0-\sum_{\gamma=1}^{n-1}\frac{Q_{gw}(\gamma\Delta t)}{4\,a\,b}\delta_s(n-\gamma+1,\Delta t)\right]}{\left\{H-h_0+k_v\,\Delta t\,\delta_s(1,\Delta t)\right\}} \qquad \textit{(Eq. 4)}$$

in which

k_v is the vertical hydraulic conductivity [LT^{-1}]; $Q_{gw}(\gamma\Delta t)$ is the total recharge from the lake during γ^{th} period [L^3T^{-1}]; H is the height of the lakebed measured upward from the impervious stratum [L]; and $\bar{D}((n\Delta t)$ is the average water level in the lake measured from its bed [L] which is $(D(n\Delta t)+D(n-1)\Delta t)/2$.

From eq.(4), $Q_{gw}(n\Delta t)$ can be obtained by solving it in succession starting from time step 1.

Due to the fluctuation of water level in the lake caused by the variable inflows and outflows, the water-spread area changes with time. This is even more pronounced when the lake sides have low slopes. The algorithm presented in eqs (3) and (4) can be extended for variable recharge areas.

Let (2a(1), 2b(1)), (2a(2), 2b(2)) ……. (2a(n), 2b(n)) be the length and the width of the water-spread area during 1^{st} , 2^{nd} and n^{th} unit time period respectively and let δ_s(a(1), b(1), m), δ_s(a(2), b(2), m) ……δ_s(a(n), b(n) , m), m = 1, 2, ….n be the unit pulse response

coefficients, which can be generated using Hantush's equation. The water table rise at any point below the lakebed can then be expressed as:

$$\bar{h}(n\Delta t) = \sum_{\gamma=1}^{n} \frac{Q_{gw}(\gamma\Delta t)}{4\,a(\gamma)\,b(\gamma)}\ \delta_s(a(\gamma), b(\gamma), n-\gamma+1, \Delta t) \qquad \textit{(Eq. 5)}$$

and, the recharge rate is given by:

$$Q_{gw}(n\Delta t) = \frac{4\,a(n)\,b(n)\,k_v\,\Delta t\left[H + \bar{D}(n\Delta t) - h_0 - \sum_{\gamma=1}^{n-1} \frac{Q_{gw}(\gamma\Delta t)}{4\,a(\gamma)\,b(\gamma)}\,\delta_s(a(\gamma), b(\gamma), n-\gamma+1, \Delta t)\right]}{\left\{H - h_0 + k_v\,\Delta t\,\delta_s(a(n), b(n), 1, \Delta t)\right\}}$$

(Eq. 6)

When there are inflows to the lake from external sources (viz. from lake catchment or direct rainfall over the lake) and outflows from the lake (viz. losses due to evaporation and groundwater recharge), the depth of water in the lake will vary, which will lead to variable recharge rates and evaporation losses. The recharge rate and evaporation losses in such cases will depend on the water-spread area and the corresponding depth of water present in the lake at that time.

Substituting the recharge component, $Q_{gw}(n\Delta t)$ from eq.(6) in eq.(1); the expression for time varying depth of water in the lake, D(nΔt) is given by:

$$\begin{aligned} D(n\Delta t) = {} & D(n\Delta t - \Delta t)\,\frac{A_{ws}(n\Delta t - \Delta t)}{A_{ws}(n\Delta t)} \\ & + \frac{1}{A_{ws}(n\Delta t)}\left[Q_i(n\Delta t) + R(n\Delta t)A_s - E_{vp}(n\Delta t)\bar{A}_{ws} - Q_0(n\Delta t)\right]\Delta t \\ & - \frac{\bar{A}_{rs}}{A_{ws}(n\Delta t)}\left[\frac{K_v\left[H + \bar{D}(n\Delta t) - h_0 - \sum_{\gamma=1}^{n-1}\frac{Q_{gw}(\gamma\Delta t)}{[4\,a(\gamma)b(\gamma)]}\,\delta_s[a(\gamma), b(\gamma), n-\gamma+1, \Delta t]\right]}{\left[H - h_0 + K_v\,\Delta t\,\delta_s[a(n), b(n), 1, \Delta t]\right]}\right]\Delta t \end{aligned} \qquad \textit{(Eq. 7)}$$

in which

$\Delta V(n\Delta t) = [A_{ws}(n\Delta t)\,D(n\Delta t) - A_{ws}(n\Delta t - \Delta t)D(n\Delta t - \Delta t)]$; D(nΔt)) is the depth of water in the lake at time t = nΔt; $D(n\Delta t - \Delta t)$ is the depth of water in the lake at the preceding time step, i.e., (n-1)Δt; A_{ws}(n-1)Δt = water surface area of the lake at the preceding time step (n-1)Δt; $A_{ws}(n\Delta t)$ is the water surface area of the lake at time step (nΔt); A_s is the gross top surface area of the lake; $\bar{A}_{ws}$ = $(A_{ws}(n\Delta t) + A_{ws}(n-1)\Delta t)/2$; and $\bar{A}_{rs} = 2\,(a(n)b(n) + a(n-1)b(n-1)$.

For computing $D(n\Delta t)$ and $Q_{gw}(n\Delta t)$ corresponding to unsteady inflows and outflows using eqs.(7) and (6) respectively, the variables; $Q_i(n\Delta t)$, $R(n\Delta t)$, $Q_o(n\Delta t)$, $E_{vp}(n\Delta t)$, $A_{ws}(n\Delta t)$, A_s, $D(n\Delta t-\Delta t)$, and the parameters H, h_0, T, S, and K_v, are to be known. For ascertaining $R(n\Delta t)$ and $E_{vp}(n\Delta t)$, a 10 year (2001-2010) daily data of rainfall and climate variables from an observatory located 2.2 km away from the lake were used. For estimating $Q_i(n\Delta t)$ from rainfall-runoff analysis, an SCS-CN model together with land-use and soil maps were used. For $Q_o(n\Delta t)$, measured outlet levels of the lake were used. For ascertaining $A_{ws}(n\Delta t)$, A_s and $D(n\Delta t)$, bathymetric survey data of the lake together with the derived rating curves were used. The parameters H and h_0 were obtained from hydrogeological data and aquifer characterization. The aquifer hydraulic parameters T, S, and k_s were taken from a field recovery test in a large diameter well.

To assess the effectiveness of the derived model (eq.7), weekly measured depths of water in the lake for the period of June 2013 to January 2014 were compared with the corresponding computed values of D(t).

Eqs. (6) and (7) require the value of vertical hydraulic conductivity, K_v. For estimating k_v, and the corresponding groundwater recharge rate $Q_{gw}(n\Delta t)$, different values of, k_v as fraction of K_s were assumed to examine the sensitivity of k_v to $D(n\Delta t)$. The root mean square error (RMSE) was considered as the guiding criterion to determine k_v. The k_v corresponding to the minimum RMSE of the computed $D(n\Delta t)$ profile for each value of k_v, and the observed depth of water (Fig. 6-7) represented the optimum k_v. The k_v of approx.0.00147 m/day (0.005% of Ks) that showed minimum RSME, indicates a very low permeability of the subsurface formations below the lakebed.

For estimating the vertical hydraulic conductivity, kv, and the corresponding groundwater recharge rate Q_{gw} $(n\Delta t)$, different values of kv as fractions of Ks were assumed to examine the sensitivity of kv to $D(n\Delta t)$. The root mean square error (RMSE) was considered as the guiding criterion to determine kv.

the optimum kv indicating a very low permeability of the subsurface formations below the lakebed is corresponding to the minimum RMSE of the computed $D(n\Delta t)$ profile for each value of kv and observed depth of water. Figure 6-7 shows the resulting optimum at a kv of approx. 0.00147 m/day (0.005% of Ks).

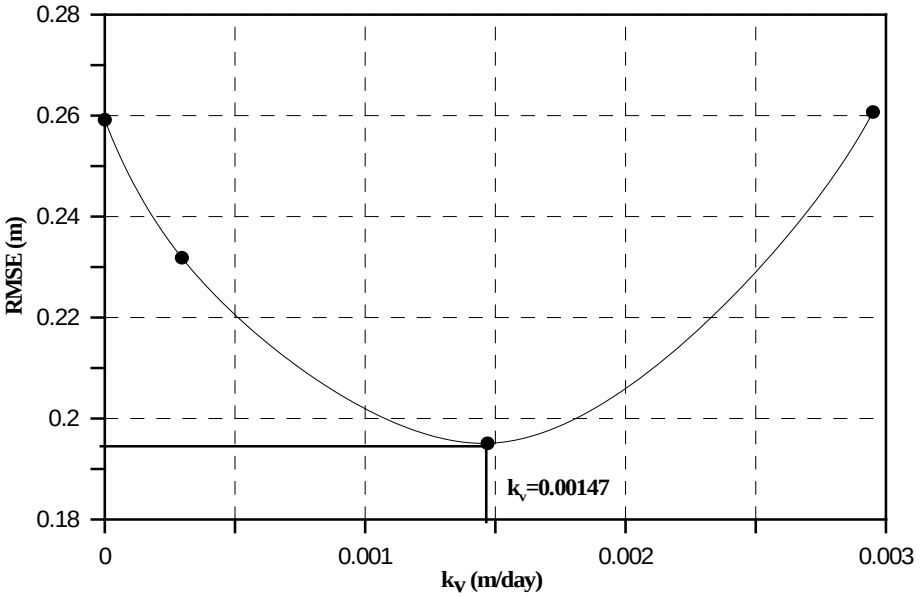

Figure 6-7: Root mean square errors (RMSE) of the computed, for different k_v, and observed depth of water in the lake

Figure 6-8 shows the comparison of the computed D(t) profile with the observed water depth in the lake and Figure 6-9 shows the resulting profiles of computed $Q_{gw}(t)$ for K_v =0.00147 m/day and S= 0.02. The recharge rate corresponding to these values for the Telibandha Lake ranges between 3.75 mm/day and 4.82 mm/day without any hydrogeological interventions.

The computed values of the water balance components shown in Figure 6-10 and Figure 6-11 respectively represent the daily variations of QI(t), $E_{vp}(t)$, $Q_{gw}(t)$, and $Q_o(t)$ (Figure 6-10) and the cumulative values (Figure 6-11 and Table 6-2) of these variables.

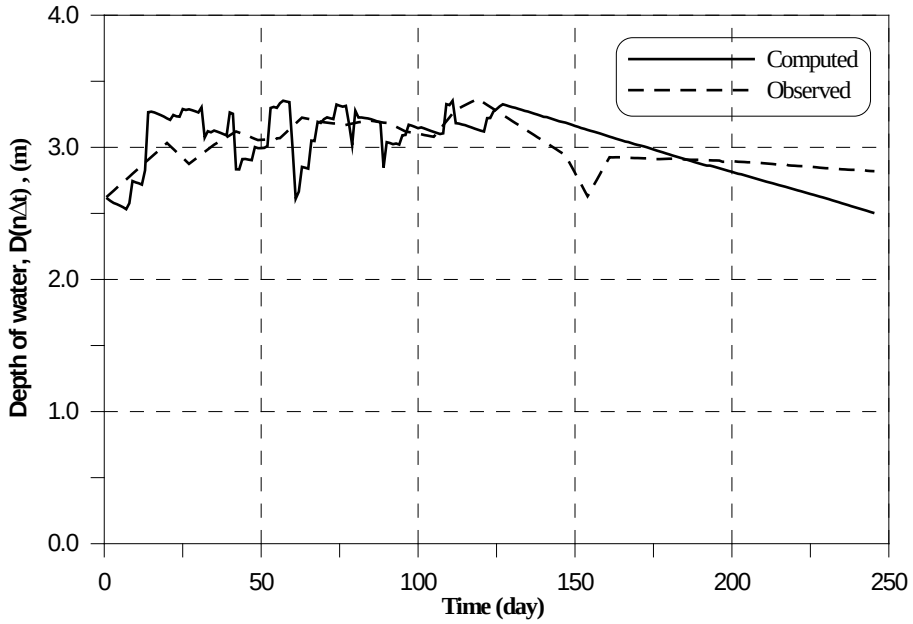

Figure 6-8: Comparison of profiles of computed depth, D(t) and observed depth of water in the lake

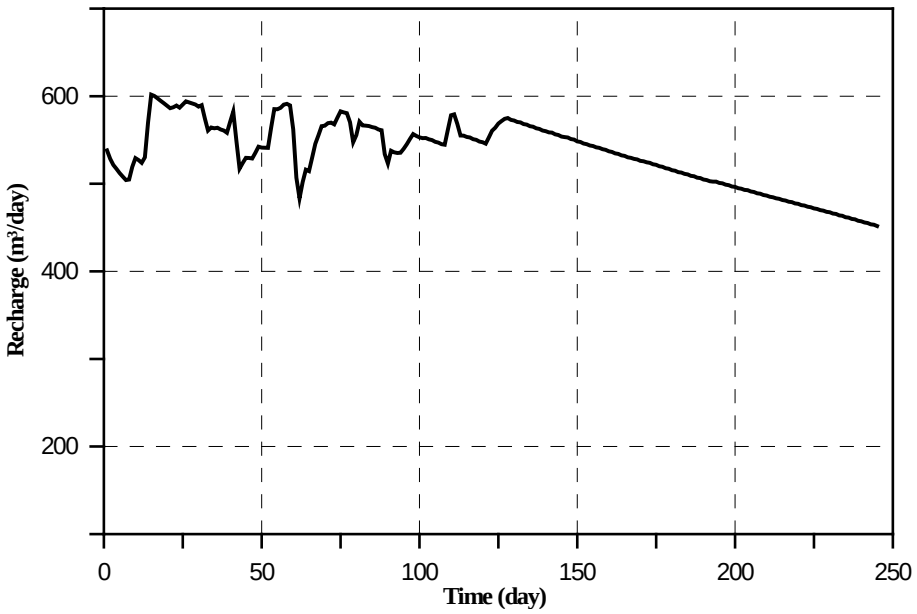

Figure 6-9: Computed profile of daily groundwater recharge, $Q_{gt}(t)$ from the Telibandha lake for different values of vertical hydraulic conductivity, K_v

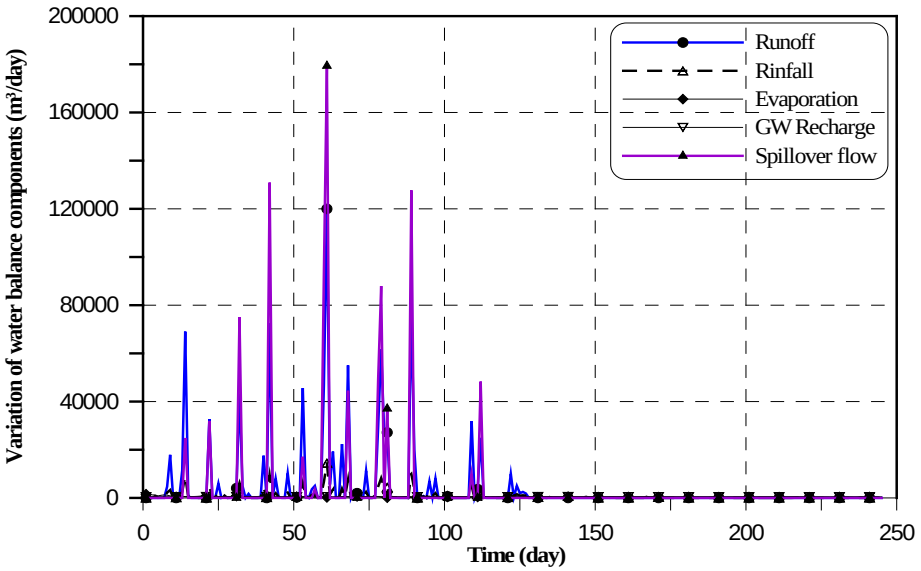

Figure 6-10: Plots of time varying daily inflow rate, $Q_i(t)$, total flow from direct rainfall over the lake, $R_i(t)$, total evaporation from the lake water surface, $E_{vp}(t)$, total groundwater recharge from lake, $Q_{gw}(t)$, and spill over flow from the lake, $Q_o(t)$.

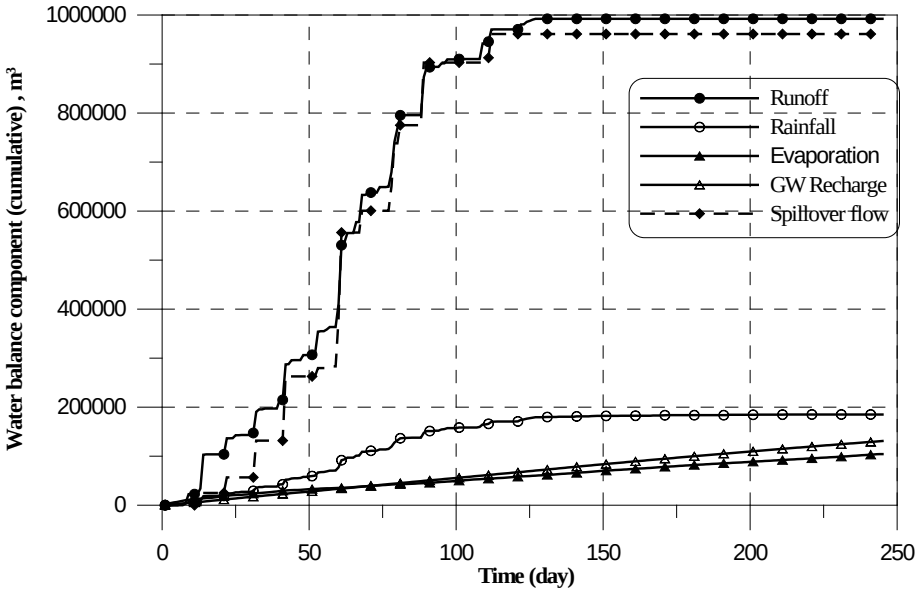

Figure 6-11: Plots of cumulative values of inflow, $Q_i(t)$, flow from direct rainfall over the lake, Ri(t), evaporation from the lake water surface, $E_{vp}(t)$, groundwater recharge from lake, $Q_{gw}(t)$ and spill over flow from the lake, $Q_o(t)$

Table 6-2: Computed cumulative figure of water balance components of the Telibandha Lake for 245 days (1st June, 2013 - 31st January, 2014)

Inflow, Qi (m^3)	Direct rainfall, Ri (m^3)	Evaporation, Evp (m^3)	GW Recharge, Q_{gw}(m^3)	Spillover flow, Q_o(m^3)
992,290	185,062	104,388	130,908	961,150

6.4 Conclusions

The analyzed data helped in identifying the potential of the sites for implementing MAR-ASR-ASTR schemes. Generally, both, the Telibandha Lake and the Telibandha area, have a high potential of surface runoff generation from rainfall occurring in their respective catchments. The average annual rainfall of the Raipur city area was found to be about 1206 mm, of which 85% is received during monsoon months (June-September).

The geological setup of the Telibandha Lake is dominated by massive stromatolitic limestone and ferruginous shales. Formations below 5 m are damp limestone of 15 to 20 m thickness and below there is a dry limestone formation up to 90 m depth. In the Telibandha area, the geological formations are comprised of a thick laterite layer followed by a thin layer of shale and below a massive layer of limestone formation. The geological formations at both the sites pose constraints for MAR proposition because of the limited self-purification potential of the thick limestone formations.

The lake water quality indicated a contamination by bacteriological parameters (viz. faecal coliforms and total coliforms), turbidity and COD, which exceed the permissible limits of drinking water standards prescribed by the BIS (10500:2012). All other constituents satisfy the limits prescribed by the BIS.

6.4.1 MAR at the Telibandha Lake

The cumulative quantity of water balance components of the lake show that during monsoon months the lake receives a high amount of surface runoff, a large quantity of which spills over from the lake without being used. Retaining monsoon surface runoff for self-purification (by dilution) of the contaminated lake water, and recharge of diluted lake water to the underneath aquifer could thus help conserving surface runoff and augmenting groundwater resources for subsequent recovery.

On the contrary, the geological strata of the aquifer, being dominated by limestone formation, which has limited infiltration and self-purification capacity, inhibits the suitability for implementing a MAR scheme at the Telibandha Lake area. In addition, there is no specific guideline in place in India regulating the use of treated/partially treated contaminated water for the replenishment of aquifers.

6.4.2 MAR in Telibandha Area

For the Telibandha area, as the proposed scheme is based on surface runoff conservation having no risk of mixing with domestic sewer systems, the implementation of MAR-ASR is recommended.

Both identified catchments and proposed sites have a good potential of surface runoff generation. By constructing suitable conservation structures, such as check dams, surface runoff can be stored. The infiltration of the ponded water can be facilitated by providing few recharge shafts connecting the recharge pond to the underlying limestone formation. However, maximum precautions would be necessary in order to avoid mixing of domestic sewer drains to the recharge pond water.

6.4.3 Artificial Recharge in the New Raipur area

For New Raipur that is coming up in the east of the Raipur city, artificial recharge is proposed to be implemented before water quality problems arise. An area around Sunita Park was proposed by CGWB. A more favourable site has been proposed by NGRI as a result of this study along the weak structure zone (may be paleochannel or fracture) along the station 8 i.e. in Kachna Village (Figure 6-12).

In general, the extent of pollution in more or less all *talabs* and streams restricts any additional artificial recharge unless the pollution in the *talabs* is completely removed. Fortunately, the underlying thick shale with a very low vertical hydraulic conductivity currently limits the infiltration of the polluted water into the aquifer.

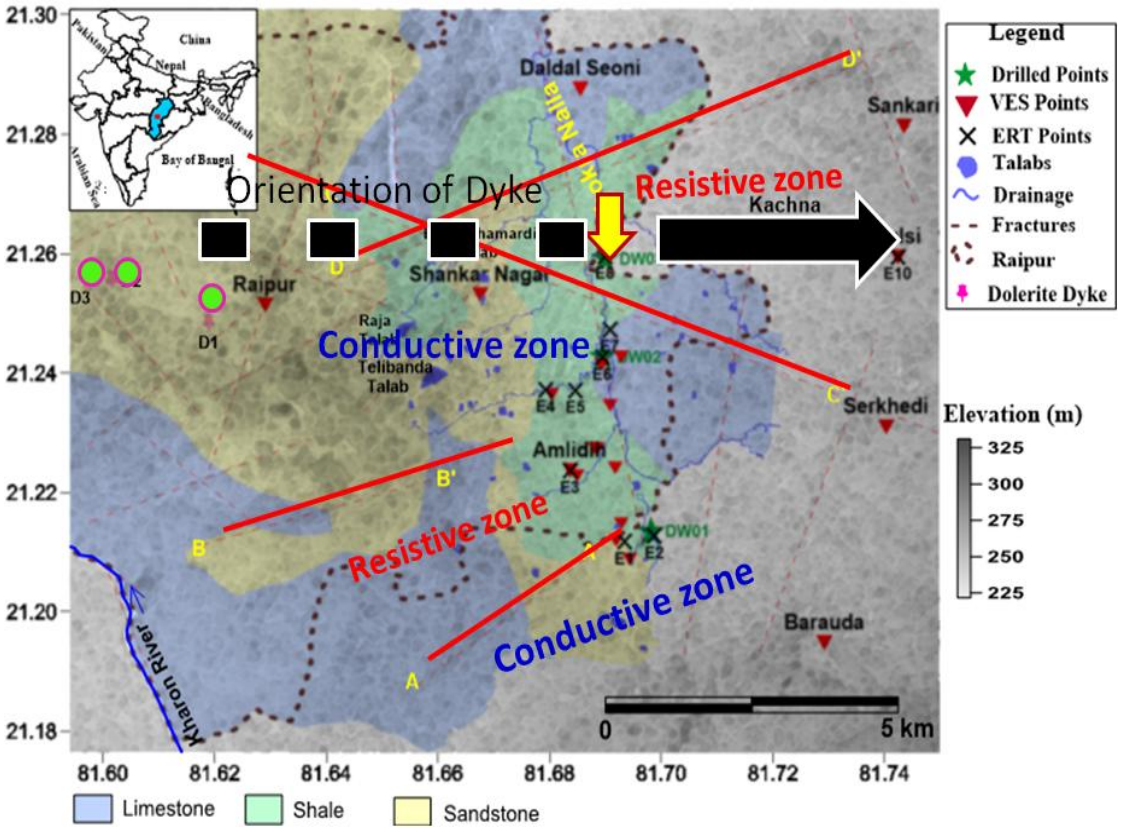

Figure 6-12: Results of Surface Electrical Structure mapping of the area suggesting the favourable zones for MAR

6.5 References

Arora, T, Gaur,T, GautamRekha, ChabbraKapil, Mundari Jai Prakash , Ahmed, S (2013). Geo-electrical investigations in Raipur Urban Area, - A report prepared under the 'SAPH PANI (EU Grant Agreement no. 282911). CSIR-NGRI, Hyderabad.

Bodhankar, N, Chatterjee, B (1994). Pollution of limestone aquifer due to urban waste disposal around Raipur, Madhya Pradesh, India. Environmental Geology 23: 209-213

Boisson, A., Sprenger, C., Lakshmanan, E., Picot-Colbeaux, G., Ghosh, N.C., Ahmed, S., Kumar, S., Singh, S., Thirunavukkarasu, 2013. Documentation of acquired data and conceptual model of MAR impact as input for WP5 modelling, p. 117.

CGWB, (2007) Central Ground Water Board Central Ground Water Board North Central Chhattisgarh Region.www.cgwb.gov.in/NCCR/index.html, data retrieved 08.09.2014

Hantush, M S, (1967) Growth and decay of groundwater mounds in response to uniform percolation. Water Resour. Res. 3, 227-234.

Loke, M.H., Barker, (1996) Practical Techniques For 3 D Resistivity Survey And Data Inversion, Geophysical Prospecting, 44, 499-523

Mukherjee, R, Sahoo, M, Naik, K C, (2011). Raipur city, Chhattisgarh. In: Groundwater scenario in major cities of India. Report of Central ground water board: 188-195.

Annex 1: Field methods

Table A- 1: List of field investigations applied at MAR case studies.

Field Method	Brief description (or reference)	Objective	Raipur Teliabanda Lake	Raipur Teliabanda Area	Chennai Check Dam	Chennai Pilot Recharge Pond	Chennai Temple Tanks	Maheshwaram Percolation Pond	NGRI Campus Dug Wells
Geophysical									
Electrical Resistivity Tomography	Three dimensional mapping of the lithology of the area	To capture the subsurface lithological and hydrogeological information		X	X			X	X
Geomagnetic Survey	Depth of penetration- max 10 m from surface	To capture the subsurface lithological and hydrogeological information		X	X				

Water sampling and on-site measurements									
Groundwater or surface water grab sampling	A bucket or bailer is lowered into a well (usually dug-well) or surface water body and sampled water is poured into sampling bottles (previously cleaned and rinsed thoroughly with well water), acidification of cation sample, filtration (45 µm)	To obtain water samples for determining ground- or surface water quality	X		X	X		X	X
Groundwater sampling by submersible or suction pump	Submersible pump is placed in the borehole at selected depth. Pumping for 30 min (purging) and sampling	Chemical and isotopic sampling of the aquifer water			X	X		X	
Water level measurement	Measure depth of water table beneath levelled reference point with dip-meter	Determine water level of ground- or surface water for water balance or hydraulic interpretation	X	X	X	X		X	X
On-site measurements	Measurement of pH-values, temperature, Eh, EC, Oxygen with probes either in bucket or flow-through cell	Determine hydrochemical parameters that may change during transport to the laboratory			X	X		X	X
Special sampling (e.g. microbiology, tracers)	Kept in Ice box at the time of collection, Analysed immediately after transporting to the lab	To understand the microbiological load reduction by check dam recharge			X	X			

Multi- parameter logging	Logging at different dates with multi parameter probe (Temperature, Electrical conductivity, pH)	Spatial and temporal evolution monitoring of the complete water column; Indication on recharge processes (structure and temporal evolution)						X	
Multi- parameter record	Measurement of temperature and EC with probes and data logger at small time step	Temporal evolution of the physico-chemical parameters						X	X
Drilling and sediment sampling									
Hand auger	Hand augering is made use to understand the lithology of the area and to collect soil samples at different depths	To understand the lithology of the area		X		X		X	
Rotary drilling	Collection of soil samples from different (greater) depths	To understand the lithology of the area						X	
Pumping tests									
Slug and bail	Slug injected in the borehole	Estimation of transmissivity (local scale)			X			X	
Step pumping	Sequence of constant-rate steps to determine well performance characteristics	Determination of well loss and well efficiency						X	
Long-/ short term pumping	Maintain pumping at the well at a constant rate	Estimation of transmissivity and other aquifer properties						X	

Infiltration tests (ring infiltrometer, open-end)	Ring infiltrometer is used near the check dam on Arani river	To understand the recharge at the check dam	X	X	X				X
Surveying and mapping									
Levelling of boreholes								X	
Hydrogeological mapping				X				X	X
GPS Survey	Tracking of tank contours using manual GPS	Monitoring of tank area evolution		X	X			X	X
DGPS Survey	Differential GPS (high accuracy)	Obtaining accurate topography of the area			X			X	X
Heat Pulse Flow Meter measurements	Logging of boreholes under ambient flow and pumping	Identify the main productive zones/fractures and quantify their transmissivity						X	
Tank water level measurements	Manual (through scale reading) and automatic tank water level measurements	Monitoring of tank water level evolution						X	
Automatic groundwater level monitoring	Automatic monitoring using CTD Divers (temperature, conductivity, water level)	Monitoring at high frequency the evolution of water levels						X	

Annex 2: Results of water sampling in Raipur

Table A- 2: Results of water quality constituents for the samples collected from different sources in the Raipur city area (highlighted values indicate exceed BIS standards).

Sr. No	Parameters	Units	Samples ID										
			DW1	DW2	DW3	DW4	DW5	DW6	TW	HP	TL	TL*	KR
1	Temperature	^{0} C	26	24	25	24	25	25	29.8	30	25	-	25
2	pH		6.95	7.36	7.69	7.08	7.26	7.12	7.25	7.93	7.57	7.11	8.08
3	EC	uS/cm	275	968	515	385	615	802	882	875	424	690	169
4	TDS	mg/L	176	620	330	246	393	513	565	560	271	398	108
5	Turbidity	NTU	3.03	2.2	4.12	130	2.5	1.19	0.78	1.21	17	12	21
6	Total Hardness	mg/L as $CaCO_3$	110	292	222	152	228	254	326	212	112	117	86
7	Calcium	mg/L	31	71	70	45	66	80	98	58	26	35	25
8	Magnesium	mg/L	8	28	12	10	16	13	20	17	13	7	6
9	Sodium	mg/L	30	119	74	42	74	96	114	102	96	85	18
10	Potassium	mg/L	8	85	6.5	11	9	54	7	2.5	32	25	4
11	Iron	mg/L	0.08	0.12	0.22	0.15	0.23	0.05	0.02	0.04	0.06	0.015	0.13
12	Manganese	mg/L	0.4	1.3	0.1	0.1	0.2	0.2	0.5	0.1	0	0.017	0

13	Bicarbonate	mg/L	165	587	289	189	302	378	390	332	220	174	126
14	Chloride	mg/L	25	88	89	60	88	137	115	84	106	110	15
15	Sulfate	mg/L	6.6	20	28	15	28	20	43	34	26	32.7	2
16	Nitrate	mg/L	14.5	6.6	11.4	11	9	18	9	70	7	1.98	4
17	Phosphate	mg/L	0.4	1.2	0.2	0.8	0.2	0.3	0.21	0.3	0.5	SNA	0.23
18	Fluoride	mg/L	0	0.5	0.3	0.2	0.33	0.33	0.22	0.17	0.1	SNA	0.1
19	DO	mg/L	7.2	2	8	6.1	4.9	5.1	5.4	3.8	7.2	SNA	6
20	COD	mg/L	14	21	12	13.71	6.86	27	6.86	13.71	13.71	28.7	27.42
21	BOD	mg/L	1	4.1	0.8	1.7	0.5	1	1.7	0.5	2.1	4.8	1.3
22	Fecal Coliform	MPN/100 ml	4	4	SNA	9	15	7	4	SNA	21	SNA	9
23	Total Coliform	MPN/100 ml	21	93	SNA	93	150	93	43	SNA	240	SNA	23

SNA – Sample not available; TL* - pre-monsoon results, TL – post-monsoon results .

Annex 3: Geochemistry Maheshwaram

Sampling and analyses

Water samples were collected in clean and three times rinsed polyethylene bottles. Raw water was sampled for isotopes and HCO_3^- analyses. Water for anions analyses was filtrated (0.45µm) in situ. Water for cations analyses was filtrated (0.45µm) and acidified (HNO3 acid, 1M) in situ. Bottled were completely filled, limiting air contact.

Cl^-, NO_3^-, SO_4^{2-} and F^- were analysed by ionic chromatography (Dionex) according to the NF ISO 10304 method. HCO_3^- contents were determined using the NF ISO 9963-1 method based on potentiometric analysis. Ca^{2+}, K^+, Na^+, Mg^{2+} were analysed by ICP-emission spectrometry according to the NF ISO 11885 method. Stable isotopes ratios ($\delta^{18}O$, δ^2H) were measured by mass spectrometry.

Major ions results

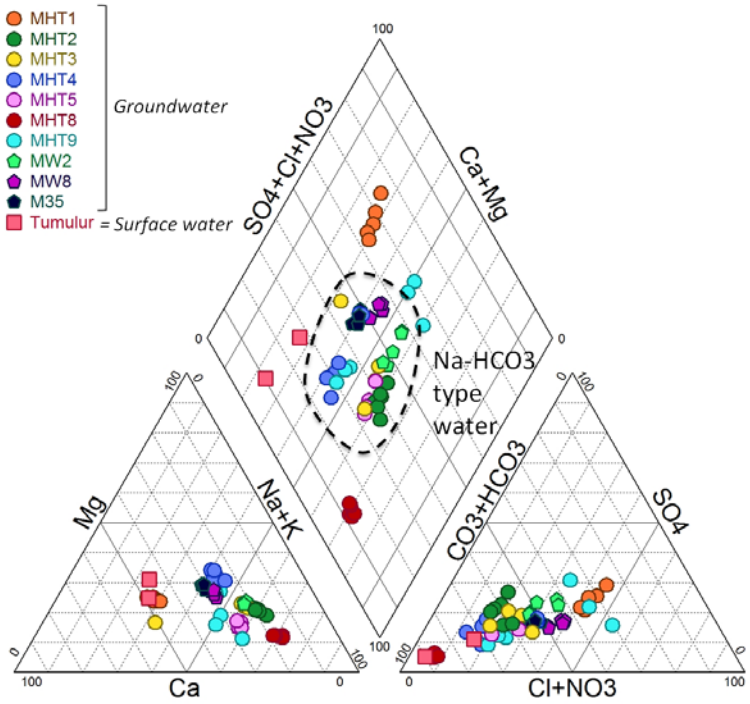

Figure A- 1: Piper diagram for groundwater (10 wells) and Tumulur tank surface water for the 2013-2014 sampling campaign.

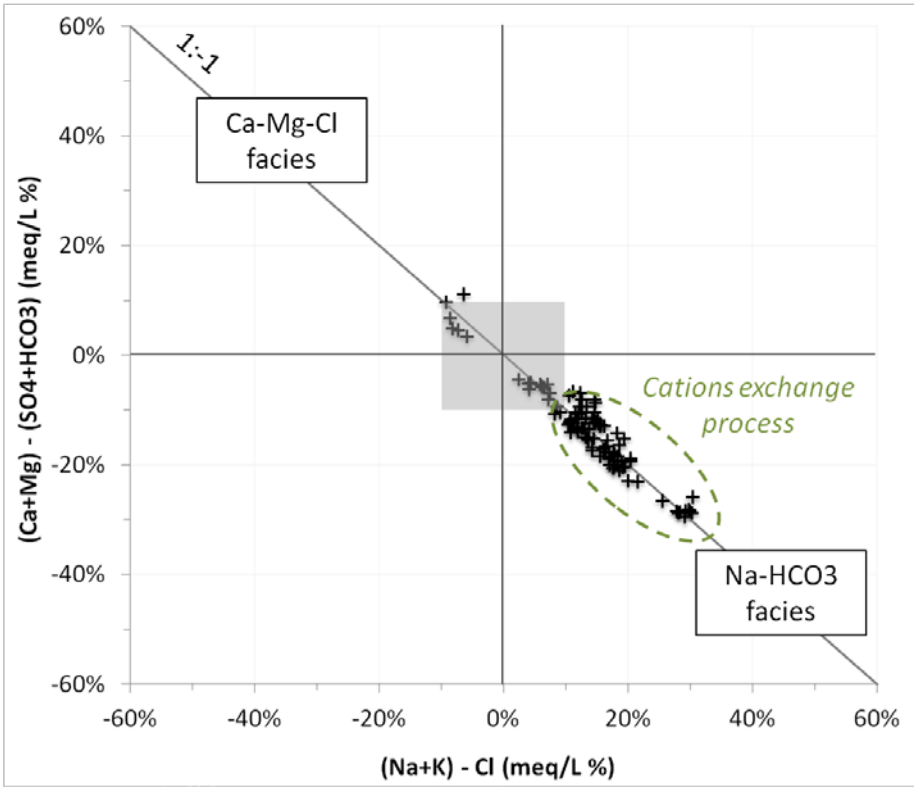

Figure A- 2: (Na+K)-Cl vs. (Ca+Mg)-(SO4+HCO3) plot for Tummulur site groundwater (7 scientific bore wells and 3 farm bore wells) for the 2013-2014 sampling campaigns. NB: the ±10 % area (grey area) does not allow to account for ion exchange processes.

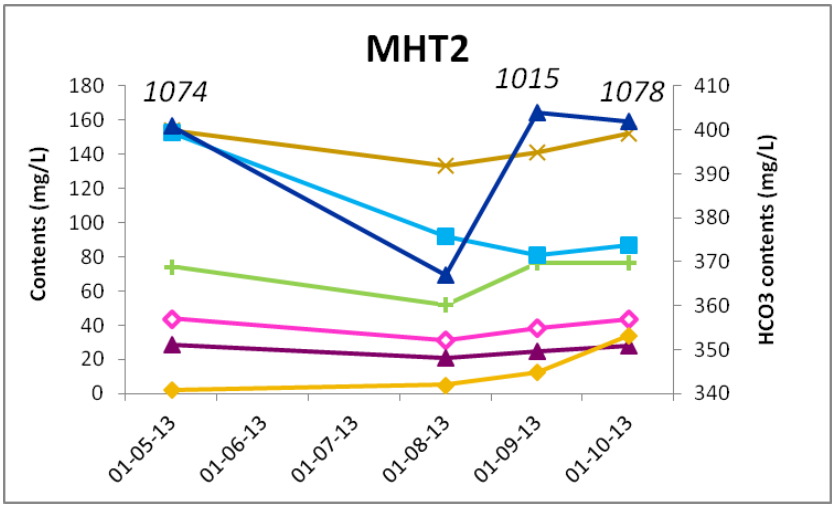
MHT2
1074
1015
1078
Contents (mg/L)
HCO3 contents (mg/L)
180
160
140
120
100
80
60
40
20
0
410
400
390
380
370
360
350
340
01-05-13
01-06-13
01-07-13
01-08-13
01-09-13
01-10-13

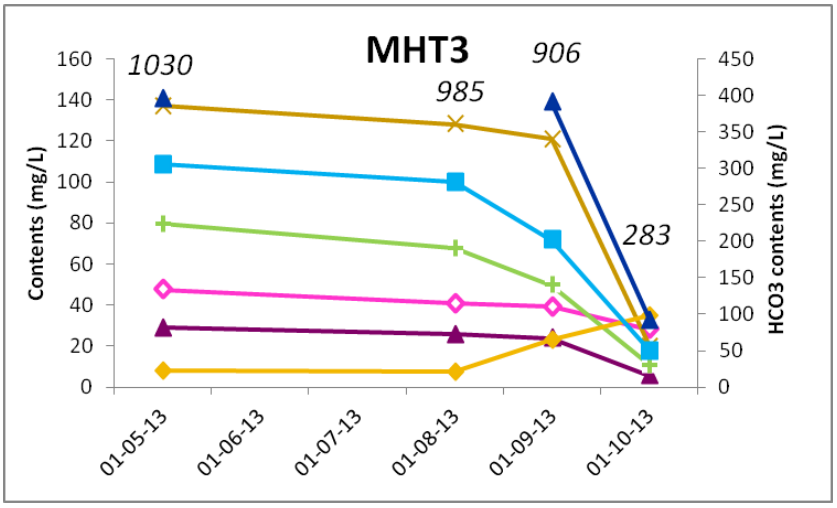
MHT3
1030
985
906
283
Contents (mg/L)
HCO3 contents (mg/L)
160
140
120
100
80
60
40
20
0
450
400
350
300
250
200
150
100
50
0
01-05-13
01-06-13
01-07-13
01-08-13
01-09-13
01-10-13

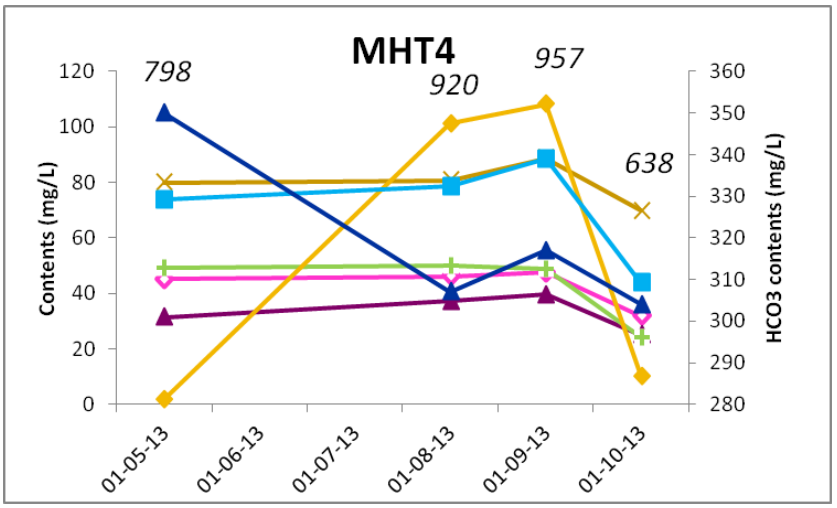
MHT4
798
920
957
638
Contents (mg/L)
HCO3 contents (mg/L)
120
100
80
60
40
20
0
360
350
340
330
320
310
300
290
280
01-05-13
01-06-13
01-07-13
01-08-13
01-09-13
01-10-13

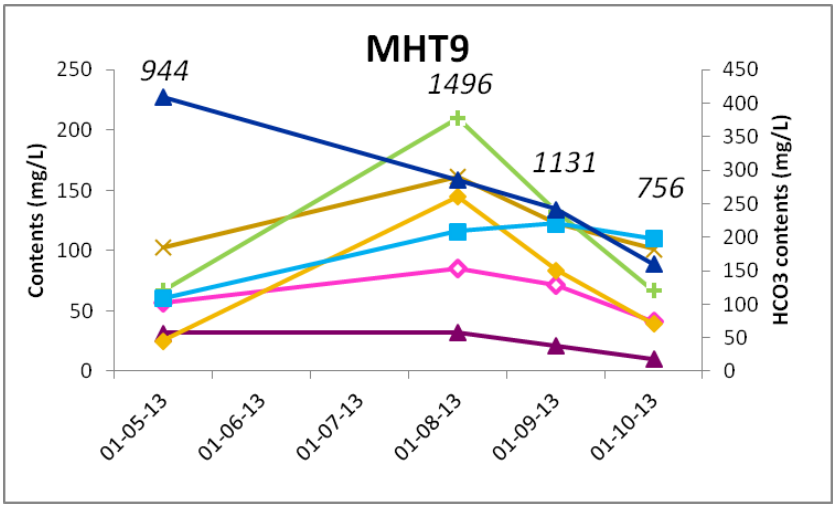

Figure A- 3: Evolution of Ca^{2+}, Mg^{2+}, Na^{+}, Cl^{-}, NO_3^{-}, SO_4^{2-} and HCO_3^{-} contents (mg/L) for the campaigns of May (i.e. before monsoon), August, September (i.e. early stages of the monsoon), and October 2013 (i.e. late stage of the monsoon) with the corresponding electrical conductivity.